Vol. 296, No. 3, October 20, 1994
Completing Volume 296

ISSN 0003-2670

ANALYTICA CHIMICA ACTA

An international journal devoted to all branches of analytical chemistry

ELSEVIER

ANALYTICA CHIMICA ACTA

Scope. *Analytica Chimica Acta* publishes original papers, rapid publication letters and reviews dealing with every aspect of modern analytical chemistry. Reviews are normally written by invitation of the editors, who welcome suggestions for subjects. Letters can be published within **four months** of submission. For information on the Letters section, see inside back cover.

Submission of Papers

Americas

Prof. Harry L. Pardue
Department of Chemistry
1393 BRWN Bldg, Purdue University
West Lafayette, IN 47907–1393
USA

Tel:(+1-317) 494 5320
Fax:(+1-317) 496 1200

Computer Techniques

Prof. J.T. Clerc
Universität Bern
Pharmazeutisches Institut
Baltzerstrasse 5, CH-3012 Bern
Switzerland

Tel:(+41-31) 6314191
Fax:(+41-31) 6314198

Prof. Sarah C. Rutan
Department of Chemistry
Virginia Commonwealth University
P.O. Box 2006
Richmond, VA 23284-2006
USA
Tel:(+1-804) 367 7517
Fax:(+1-804) 367 8599

Other Papers

Prof. Alan Townshend
Department of Chemistry
The University
Hull HU6 7RX
Great Britain

Tel:(+44-482) 465027
Fax:(+44-482) 466410

Prof. Willem E. van der Linden
Laboratory for Chemical Analysis
Department of Chemical Technology
Twente University of Technology
P.O. Box 217, 7500 AE Enschede
The Netherlands
Tel:(+31-53) 892629
Fax:(+31-53) 356024

Prof. Paul Worsfold
Dept. of Environmental Sciences
University of Plymouth
Plymouth PL4 8AA
Great Britain

Tel:(+44-752) 233006
Fax:(+44-752) 233009

Submission of an article is understood to imply that the article is original and unpublished and is not being considered for publication elsewhere. *Anal. Chim. Acta* accepts papers in English only. There are no page charges. Manuscripts should conform in layout and style to the papers published in this issue. See inside back cover for "Information for Authors".

Publication. *Analytica Chimica Acta* appears in 16 volumes in 1994 (Vols. 281–296). *Vibrational Spectroscopy* appears in 2 volumes in 1994 (Vols. 6 and 7). Subscriptions are accepted on a prepaid basis only, unless different terms have been previously agreed upon. It is possible to order a combined subscription (*Anal. Chim. Acta* **and** *Vib. Spectrosc.*).
Our p.p.h. (postage, packing and handling) charge includes surface delivery of all issues, except to subscribers in the U.S.A., Canada, Australia, New Zealand, China, India, Israel, South Africa, Malaysia, Thailand, Singapore, South Korea, Taiwan, Pakistan, Hong Kong, Brazil, Argentina and Mexico, who receive all issues by air delivery (S.A.L.–Surface Air Lifted) at no extra cost. For Japan, air delivery requires 25% additional charge of the normal postage and handling charge; for all other countries airmail and S.A.L. charges are available upon request.

Subscription orders. Subscription prices are available upon request from the publisher. Subscription orders can be entered only by calendar year and should be sent to: Elsevier Science B.V., Journals Department, P.O. Box 211, 1000 AE Amsterdam, The Netherlands. Tel: (+31-20) 5803 642, Telex: 18582, Telefax: (+31-20) 5803598, to which requests for sample copies can also be sent. Claims for issues not received should be made within six months of publication of the issues. If not they cannot be honoured free of charge. Readers in the U.S.A. and Canada can contact the following address: Elsevier Science Inc., Journal Information Center, 655 Avenue of the Americas, New York, NY 10010, U.S.A. Tel: (+1-212) 633 3750, Telefax: (+1-212) 633 3990, for further information, or a free sample copy of this or any other Elsevier Science journal.
Advertisements. Advertisement rates are available from the publisher on request.

US mailing notice – Analytica Chimica Acta (ISSN 0003-2670) is published 3 times a month (total 48 issues) by Elsevier Science B.V. (Molenwerf 1, Postbus 211, 1000 AE Amsterdam). Annual subscription price in the USA US$ 3035.75 (valid in North, Central and South America), including air speed delivery. Second class postage paid at Jamaica, NY 11431. *USA Postmasters*: Send address changes to Anal. Chim. Acta, Publications Expediting, Inc., 200 Meacham Av., Elmont, NY 11003. Airfreight and mailing in the USA by Publication Expediting.

ANALYTICA CHIMICA ACTA

An international journal devoted to all branches of analytical chemistry

(Full texts are incorporated in CJELSEVIER, a file in the Chemical Journals Online database available on STN International; Abstracted, indexed in: Aluminum Abstracts; Anal. Abstr.; Biol. Abstr.; BIOSIS; Chem. Abstr.; Curr. Contents Phys. Chem. Earth Sci.; Engineered Materials Abstracts; Excerpta Medica; Index Med.; Life Sci.; Mass Spectrom. Bull.; Material Business Alerts; Metals Abstracts; Sci. Citation Index)

VOL. 296 NO. 3 CONTENTS OCTOBER 20, 1994

(Continued overleaf)

Contents (continued)

ELSEVIER

Analytica Chimica Acta 296 (1994) 223–234

ANALYTICA CHIMICA ACTA

Validation of an automated precolumn exchange system (PROSPEKT) coupled to liquid chromatography with diode array detection. Application to the determination of pesticides in natural waters

Silvia Lacorte, Damià Barceló *

Department of Environmental Chemistry, CID-CSIC, C / Jordi Girona 18–26, 08034 Barcelona, Catalonia, Spain

Received 18 January 1994; revised manuscript received 2 May 1994

Abstract

An automated precolumn exchange system (PROSPEKT) coupled to liquid chromatography with diode array detection (LC-DAD) has been used for the determination of trace pesticides in natural (drinking and ground) waters. Relevant parameters such as pH and type of precolumn (C_{18} and PLRP-s) were optimized for a variety of organophosphorus pesticides, herbicides and pesticide transformation products. Calibration graphs at low levels of determination (0.1–1.5 μg/l) were constructed. The validation of the present automated method has been guaranteed by participating in Aquacheck interlaboratory exercises where more conventional gas chromatographic determinations are being used. The overall relative standard deviation between values obtained in our laboratory and the average value obtained by 14–15 other laboratories varied between 1.6 and 36% for most of the studied compounds. Problems encountered in the determination of certain organophosphorus pesticides led to high variations in the mean values and errors of many laboratories. In this sense, problematic compounds like mevinphos, which gave two peaks corresponding to the *cis*- and *trans*-isomers, parathion-methyl and diazinon, which showed coelution problems, or malathion, which presented poor quantitation due to low absorption in the UV range. In addition, fenthion, which was not determined, gave 3–4 compounds, corresponding to various degradation products. Confirmation of the different pesticides exhibiting an UV maximum > 220 nm was feasible due to their characteristic UV spectra and satisfactory levels of 0.02 μg/l were found when preconcentrating 150 ml of ground water sample.

Keywords: Liquid chromatography; Automated precolumn exchange system (PROSPEKT); Pesticides; Waters

1. Introduction

The maximum allowable concentration established by the Commission of the European Communities-Drinking Water Directive (CEC-DWD) for pesticides and their transformation products (TPs) is 0.1 μg/l [1]. The TPs are formed both by hydrolysis or photolysis in water under laboratory conditions [2–4] and by microbial degradation in soils and hydrolysis in natural waters [4,5]. It is thus hardly surprising that the National Pesticide

* Corresponding author.

SSDI 0003-2670(94)00222-8

Survey (NPS), in a joint project between EPA's Office of Drinking Water and the Office of Pesticide Programs has included many of these pesticides and TPs in their monitoring programs [6–8].

On-line systems [solid-phase extraction (SPE) coupled on-line with liquid chromatography (LC)], either automated (e.g., PROSPEKT) or fully automated (control of SPE, gradient elution and DAD with unique software) [9,10] have been developed from SPE methods using precolumns with a C_8 or C_{18} bonded silica phase or styrene–divinylbenzene polymer phases (PRP-1 or PLRP-s) [9,11–15]. Another alternative is trace enrichment using membrane extraction disks (containing C_8, C_{18} or styrene–divinylbenzene polymer phases) coupled on-line [16–19] with LC.

The aim of this work was to validate an automated on-line SPE method using C_{18} precolumns to determine various pesticides and their polar TPs at 0.1 μg/l level in natural waters. Development of methods for pesticide TPs was encouraged in a recent report from the CEC [1]. The different compounds were determined by liquid chromatography with diode array detection (LC-DAD), so confirmation was always possible. The compound selection was based on their use in our area of interest (the Ebre delta area); it was particularly based on organophosphorus pesticides and various herbicides of different chemical nature. The monitoring program for organophosphorus pesticides in natural waters is a matter of controversy [8] since in the NPS-US EPA, many of the pesticides such as azinphos-methyl, demeton, diazinon, ethyl parathion, fenitrothion, fenthion, malathion and methyl parathion were withdrawn for monitoring purposes due to their instability in biologically inhibited water solutions stored at 4°C [8]. However, in Europe such compounds are of interest, and a proof of that interest is their inclusion in the 76/464/EEC list of pesticides to be monitored in the aquatic environment [8] and also the interest of Europe to supervise them through different interlaboratory exercises, e.g., Aquacheck, which includes a long list of organophosphorus pesticides. In addition, organophosphorus pesticides such as fenitrothion, pyridafenthion and others have been detected by our group in various natural waters of the Ebre delta area (Tarragona, Catalonia) [20,21].

2. Experimental

2.1. Equipment

The LC analyses were performed with a Waters 600-MS solvent delivery unit with a 20-μl injection loop and equipped with a Waters 996 photodiode array detector (Waters, Millipore, MA). A 25 cm × 4.6 mm i.d. analytical column packed with 5-μm octadecylsilica (Toyo Soda Manufacturing) was used. The automated SPE devise (PROSPEKT) used in this work consists of a cartridge exchange module, a pump (or solvent delivery unit, SDU) and an electrically operated low-pressure six-port valve, which is connected to the gradient pumps. Samples were preconcentrated on 10 mm × 2 mm i.d. disposable precolumns of PROSPEKT (Spark, Emmen, Netherlands) prepacked with 40-μm C_{18} (Baker, Deventer, Netherlands) and precolumns containing 15–25 μm styrene–divinylbenzene copolymer, PLRP-s (Polymer Labs., Church Stretton, UK). The precolumns were conditioned via a solvent-delivery unit from Spark. Prior to LC analysis, surface water was filtered through 0.45-μm filters (Millipore, Bedford, MA) to remove suspended particles.

2.2. Chemicals and reagents

HPLC-grade acetonitrile and methanol were obtained from Merck (Darmstadt). LC-grade water was prepared by purifying demineralized water in a Milli-Q filtration system (Millipore). Pesticides were obtained from Promochem (Wesel, Germany) except vamidothion and vamidothion sulfone that were a gift of Rhône Poulenc (Lyon), atrazine, simazine, bensulfuron-methyl and bensulfuron-methyl metabolite from Du Pont de Nemours and cyanazine and cyanazine acid from Riedel-de Haën (Seelze-Hannover).

Two stock solutions were prepared in methanol, the first one containing six pesticides: vamidothion sulfone, vamidothion, fenamiphos,

pyridafenthion, fenitrothion and temephos and the second solution containing six herbicides: cyanazine acid, benfulfuron metabolite, simazine, cyanazine, atrazine and bensulfuron-methyl. These stock solutions were used to spike Milli-Q water and finished drinking water at the ng/l level. Spiked waters never contained more than 0.5% of methanol.

2.3. Procedures

Breakthrough volumes

Breakthrough volumes of each analyte were determined by percolating 20, 40, 60, 100 and 200 ml of Milli-Q water spiked with a decreasing concentration of the analytes so that the amount injected was always 100 ng. For the pesticide solution, breakthrough curves were studied by percolating the water sample acidified (pH 3) with perchloric acid or not (pH 7) through C_{18} precolumns. For the herbicides, breakthrough volumes were calculated with C_{18} and PLRP-s precolumns with and without acidifying the water.

The experimental set up was as follows: (a) conditioning of the precolumn was done with 10 ml of acetonitrile, 10 ml of methanol and 10 ml of Milli-Q water at 2 ml/min, (b) percolation of the water sample through the precolumn at a flow rate of 2 ml/min, (c) desorption was carried out by coupling the precolumn on-line with the analytical column and starting the gradient, and (d) cleaning of the precolumn was performed with 4 ml of methanol plus 4 ml of acetonitrile in order to grant its reutilization (at least two times with drinking water).

The gradient conditions were carried out with acetonitrile–water (adjusted to pH 3 with perchloric acid) as mobile phase to avoid ionization of the transformation products. Perchloric acid was used since it does not absorb at low wavelengths and allows a reliable identification of the compound through spectral analysis.

For the pesticide solution, the gradient started with 10% acetonitrile and 90% water, linearly to 15% acetonitrile and 85% water in 5 min, to 55% acetonitrile and 45% water in 7 min, to 70% acetonitrile and 30% water in 12 min, and linearly to 100% acetonitrile with an analysis duration of 35 min. For the herbicides, the gradient starts at 0 min with 5% acetonitrile in water, to 10% acetonitrile and 90% water in 5 min, to 35% acetonitrile in water in 3.5 min, which is kept isocratic for 14.5 min, and increases linearly to 70% acetonitrile in water in 12 min, at a flow rate of 1 ml/min.

Table 1
Breakthrough volumes of herbicides and organophosphorus pesticides calculated in Milli-Q water spiked from 0.5 to 5 μg/l using C_{18} and PLRP-s precolumns and at pH 7 and 3

Compound	Breakthrough volume				Wavelength (nm)
	C_{18}		PLRP-s		
	pH 3	pH 7	pH 3	pH 7	
Cyanazine acid	< 50	n.d	n.d	n.d	205
Bensulfuron-methyl metabolite	100	n.d	< 70	< 40	220
Simazine	80	50	100	> 150	220
Cyanazine	100	60	100	> 150	220
Atrazine	100	60	100	> 150	220
Bensulfuron-methyl	100	80	> 200	> 150	220
Vamidothion sulfone	< 50	n.d	n.d	n.d	205
Vamidothion	< 50	n.d	n.d	n.d	254
Fenamiphos	> 200	n.d	n.d	n.d	220
Pyridafenthion	> 200	n.d	n.d	n.d	220
Fenitrothion	> 200	n.d	n.d	n.d	254
Temephos	> 200	n.d	n.d	n.d	254

n.d. = not determined.

Calibration graphs

Calibration graphs were constructed for all the compounds analyzed over a concentration range of 0.1 to 1.5 μg/l. A sample volume of 150 ml of finished drinking water acidified with perchloric acid at pH 3 was percolated through C_{18} precolumns. Analytical conditions were as described above.

Further quantitation studies were performed with the external standard calibration method using UV absorption at the wavelength which gave the best correlation coefficient values (indicated in Table 2).

Validation of the system

Validation of the system was carried out by participating in an interlaboratory calibration study for organophosphorus compounds and atrazine organized by Aquacheck (WRC, Medmenham, UK). A certified standard solution containing an unknown concentration of pesticides (azinphos-ethyl and methyl, dichlorvos, fenitrothion, malathion, mevinphos, chlorfenvinphos, diazinon, fenthion, parathion-ethyl and methyl, and atrazine) and a 2-l bottle of ground water was provided by the organization. The aim was to spike the ground water with the solution provided in order to determine the levels of these pesticides in water using the method that has been developed in our laboratory. Preconcentration of 150 ml of sample was carried out immediately after spiking using C_{18} precolumns and analytical separation was performed with a C_{18} precolumn of 15 × 3.9 mm i.d. (Waters, Millipore) using solvent A, acetonitrile–methanol (70:30), and solvent B, Milli-Q water, with the following gradient elution program: from 4% A and 96% B to 10% A and 90% B in 10 min, to 45% A and 55% B in 11 min, isocratic until 40 min, and from these conditions to 90% A and 10% B in 30 min, at a flow rate of 1 ml/min. Detection was realized at 254 and 230 nm and quantitation was done by external standard calibration.

Moreover, repeatability studies were performed both by percolating 50 ml of Milli-Q water spiked with 0.5 μg/l of the herbicide solution through C_{18} precolumns and by loop injection of the same solution.

3. Results and discussion

3.1. Breakthrough volumes

Table 1 shows the breakthrough values obtained for organophosphorus pesticides and herbicides. Breakthrough values for fenamiphos, pyridafenthion, fenitrothion and temephos surpass 200 ml. These values indicate that 100% recoveries of these analytes are achieved by preconcentrating a volume of 200 ml spiked at a concentration of 0.5 μg/l through C_{18} precolumns. These results are consistent with those reported in [22], which gives a 100% recovery for

Table 2
Calibration data for apolar pollutants and their degradation products (0.1–1.5 μg/l) after preconcentration of 150 ml of finished drinking water through C_{18} precolumns

Compound	Calibration equation	Linear range	r^2
Cyanazine acid	$Y = -640 + 9913X$	0.5–1.5	0.9963
Bensulfuron metabolite	$Y = -7395 + 25146X$	0.5–1.5	0.9768
Simazine	$Y = -265 + 88938X$	0.1–1.5	0.9977
Cyanazine	$Y = -1537 + 81043X$	0.1–1.5	0.9946
Atrazine	$Y = 1063 + 106709X$	0.1–1.5	0.9984
Bensulfuron-methyl	$Y = -1339 + 20006X$	0.1–1.5	0.9957
Vamidothion sulfone	$Y = 2589 + 4085X$	0.1–0.7	0.9846
Vamidothion	$Y = 1381 + 940X$	0.5–1.5	0.9395
Fenamiphos	$Y = -1015 + 8299X$	0.1–1.5	0.9467
Pyridafenthion	$Y = -2478 + 56322X$	0.1–1.5	0.9971
Fenitrothion	$Y = 210 + 17397X$	0.1–1.5	0.9948
Temephos	$Y = 970 + 1866X$	0.1–1.5	0.9864

fenitrothion when percolating 300 ml of Milli-Q water through C_{18} precolumns, indicating that breakthrough has not yet occurred.

For vamidothion and vamidothion sulfone, which have a high water solubility (4 kg/l), lower breakthrough volumes are achieved due to little retention on C_{18} precolumns.

Breakthrough values for herbicides were determined using precolumns of C_{18} and PLRP-s and at pH 3 and 7 in order to discern the maximum breakthrough volumes that could be gathered for the compounds studied, paying special attention to the more polar compounds. The values thus obtained are also indicated in Table 1.

Breakthrough volumes of the herbicides obtained by percolating Milli-Q water acidified at pH 3 through C_{18} precolumns gave higher values compared to non-acidified samples; in particular, cyanazine acid and bensulfuron-methyl metabolite, which are not retained on the precolumn in ionized form. In contrast to that, when PLRP-s precolums were used, higher breakthrough volumes of the apolar herbicides were obtained at pH 7. In general, for the parental herbicides, PLRP-s gave higher breakthrough volumes than C_{18} precolumns. Problems arise from the organic material found in natural waters, which is released as interfering matrix (mainly composed of humic and fulvic substances) and elute at some point during the analytical run, depending on the gradient. This matrix interferes with the more polar compounds, thus camouflaging the detection of these analytes, as observed by other authors who employed on-line SPE methods either using the PROSPEKT or other systems [9,10,19, 23]. This is the case for cyanazine acid and bensulfuron-methyl metabolite, the former being only detected when C_{18} precolumns are used and the water sample is acidified at pH 3 (Fig. 1). The interferences of humic substances in preconcentrating river water samples is a partly known problem which has not yet been solved.

The breakthrough values reported in Table 1 are calculated at spiking levels from 0.5 μg/l to 5 μg/l, preconcentrating different water volumes in such a way that the amount loaded onto the precolumn was always 100 ng. It has been reported [18] that breakthrough volumes increase

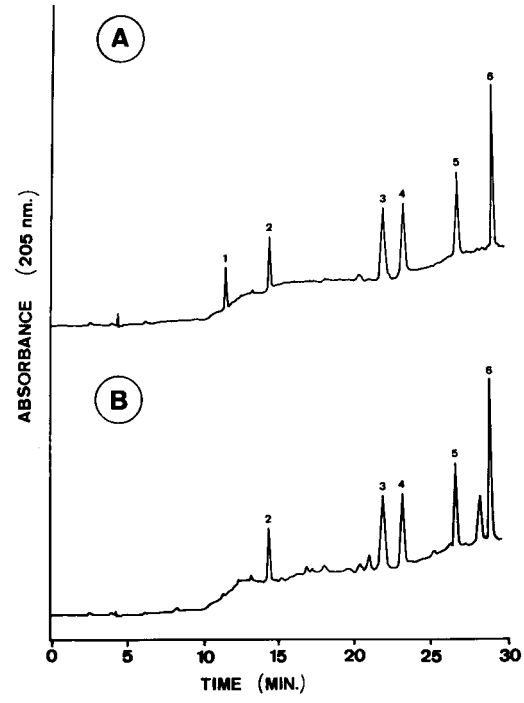

Fig. 1. LC-DAD chromatograms obtained after preconcentration of 40 ml of finished drinking water spiked with a mixture of herbicides through (A) C_{18} precolumns and (B) PLRP-s precolumns. Amount injected of each herbicide: 100 ng. Peaks: 1 = cyanazine acid, 2 = bensulfuron-methyl metabolite, 3 = simazine, 4 = cyanazine, 5 = atrazine and 6 = bensulfuron-methyl. LC gradient elution program: 0 min with 5% acetonitrile in water, to 10% acetonitrile and 90% of water in 5 min, to 35% acetonitrile in water in 3.5 min, which is kept isocratic for 14.5 min, and increases linearly to 70% acetonitrile in water in 12 min, at a flow rate of 1 ml/min. Stationary phase: a 25 cm × 4.6 mm i.d. analytical column packed with 5-μm octadecylsilica (Toyo Soda).

by a factor of 7 when the concentration decreases by a factor of 25, although the loading capacity of the sorbent decreased by a factor of 3. Since the reported values in Table 1 are calculated at a spiking level of 0.5 μg/l (200 ml) to 5 μg/l (20 ml) we will analyze water solutions at 0.1 μg/l. It is expected that for compounds showing breakthrough volumes < 50 ml (using a solution of 2 μg/l), the breakthrough volume will be increased by a factor of 4–5 for compounds at the 0.1 μg/l level, and consequently, breakthrough will not occur when preconcentrating 150 ml of water. Moreover, breakthrough volumes using various

types of water (drinking, surface and Milli-Q) will not offer high variations, as reported by several authors [13,14,23].

Since breakthrough values for the polar compounds were higher with acidified water samples and with C_{18} precolumns than with PLRP-s, while the breakthrough volumes of the more apolar compounds did not differ significantly between the two phases, further studies of preconcentration of pollutants from finished drinking water were carried out with C_{18} precolumns.

3.2. Calibration plots

Table 2 shows the calibration equations for the pesticides under study. The optimum wavelength (indicated in Table 1) has been obtained through the different calibration plots obtained for each compound. It is advisable to obtain a limit of detection (LOD) following this procedure since the maximum wavelength will be adapted to the compound and to matrix interferences, when present. The correlation coefficients of all parent pesticides in finished drinking water are over 0.99, and a lineal range from 0.1 to 1.5 μg/l is achieved. The only exceptions are fenamiphos, vamidothion and vamidothion sulfone, which can be easily degraded in solution, as reported in previous experiments from our group [2]. In addition, fenamiphos and their transformation products were analyzed in interlaboratory exercises using finished drinking water spiked at levels much higher than in the present work, e.g., generally between 30 and 300 μg/l, using Method 4 of the EPA National Pesticide Survey [24]. The different laboratories that analyzed these compounds lost more than 30% of their data points as outliers, exceeding the 2/9 rule recommended by the AOAC. This fact indicates that some of these compounds are difficult to analyze and to carry out collaborative studies between laboratories. This is most probably due to their instability in water solutions.

The low correlation coefficients observed for bensulfuron-methyl metabolite may be due both to its low breakthrough values and to matrix interferences, and therefore, presented difficulties in quantification at low spiking level.

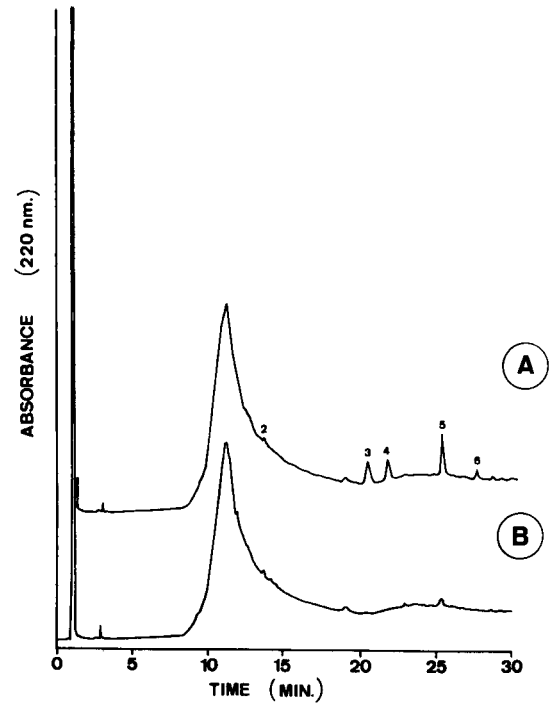

Fig. 2. LC-DAD chromatogram obtained after preconcentration of 150 ml of finished drinking water spiked at 0.3 μg/l with a mixture of herbicides through a C_{18} precolumn. Peak numbers and analytical conditions as in Fig. 1.

These compounds are of concern since their lineal range is narrower than for the rest of the compounds and minimum quantitation should be done at the 0.3–0.5 μg/l level, higher than the limits imposed by the EEC. These limits can be lowered by percolating a sample volume close to the breakthrough volume, and thus working within the limits where 100% recovery is obtained. The LOD of the pesticides were in the range of 30 to 50 ng/l, with a signal-to-noise ratio of 3, except for cyanazine acid, bensulfuron-methyl metabolite and vamidothion, which could be detected at a level of 0.5 μg/l due to matrix interferences (see Fig. 2). These LODs refer to extraction of 150 ml of finished drinking water spiked at a level of 0.3 μg/l. Such values will be increased when essaying river waters, due to enhanced interferences.

3.3. Precision and accuracy

Milli-Q water was spiked at a level of 0.5 μg/l of a solution containing four herbicides, and the analytical procedure was repeated 5 times in order to study the precision and accuracy of the method. The relative standard deviations (R.S.D.) of the peak areas were < 10%. The values obtained for atrazine and simazine are similar to those reported by Pichon and Hennion [23] and Lintelmann et al. [25] and confirm that good precision can be attained while using coupled-mode analysis. Also, these are acceptable values according to the US E.P.A regulations and prove the repeatability of the method. An R.S.D. of around 5% was observed when direct loop injection was carried out. The differences between the two different procedures confirm the theory that quantitation can never be performed in comparison to loop-injection [23].

3.4. Validation of the system

The automated on-line solid phase precolumn exchange system (PROSPEKT) was validated by participating in the Aquacheck interlaboratory comparison study organized by the WRC, at Medmenhem, UK. The reason to participate in such interlaboratory comparison is quite obvious. The increasing requirements to demonstrate comparability of analytical data in environmental monitoring demands some external assessment of the quality of the results provided by individual laboratories. One way of doing this is by assessment of performance in interlaboratory comparisons using centrally distributed samples [26]. In the case of organophosphorus and atrazine analysis most of the laboratories involved use gas chromatographic techniques. In addition, and according to our knowledge, the automated on-line solid phase extraction system has not been previously validated in interlaboratory exercises. This will be very useful since such automated or fully automated systems are being implemented in the environmental monitoring of pesticides in the Rhine basin program [9,10].

Fig. 3 shows the two chromatograms obtained at 254 and 230 nm for one of the mixtures of intercalibration after the determination using the PROSPEKT. Table 3 shows the results obtained by our laboratory and the %error regarding the mean obtained from analyses by different laboratories. For quantitation, single point calibration was used.

Table 3
Mean concentration (ng/l) and % of mean difference in relation to reference values of organophosphorus and triazine compounds obtained from the two intercalibration studies carried out in July and November 1993. Results are obtained from spiking well water with the certified material from Aquacheck

Compound	June 1993		November 1993	
	Mean conc. (ng/l)	%Mean difference	Mean conc. (ng/l)	%Mean difference
Azinphos-methyl	98.3	23	24.4	32
Dichlorvos	46.0	−36	63.9	21
Fenitrothion	34.0	17	23.4	9
Malathion	154.4	89	24.9	55
cis-Mevinphos	n.d	n.d	46.5	27.4
trans-Mevinphos	n.d	n.d	64.6	0.9
Chlorfenvinphos	47.7	36	37.0	−11
Azinphos-ethyl	95.2	12	41.9	−24
Parathion-E + diazinon [a]	n.d	n.d	111.2	3.7
Parathion-methyl	26.0	22	97.4	15
Atrazine	n.d	n.d	198.6	1.6

n.d. = not determined.
[a] The percentage of error was calculated by summing the concentration of each coeluted compound.

If we look at the compounds of Tables 2 and 3, it can be noticed that in the Aquacheck interlaboratory exercise there are many organophosphorus compounds that were not present in the calibration data previously performed by our laboratory. As can be seen in Table 2, most of the organophosphorus compounds showed good linearity and consequently quantitation from 0.1 to 1.5 μg/l should not a be a problem. The organophosphorus compounds used in Tables 2 and 3 are considered to be hydrophobic since log P_{OW} (partition coefficient of octanol–water) is higher than 2 and varies from 2.6 to 3.9 [27]. Therefore, separation using C_{18} materials is preferred and consequently no problems regarding breakthrough volumes will be observed. Aquacheck analyses show that ground water samples offer less interferences (see Fig. 3) than drinking water samples (Fig. 2). Therefore, no problems with the first eluting organophosphorus pesticides are noticed. Considering all these questions, we can assume a similar linearity for organophosphorus compounds as reported in Table 2.

Another remark concerns the evaluation of results from analyses carried out using Aquacheck. The results are evaluated indicating the error threshold values. If such values are below 17%, they are acceptable. Flagged and double flagged results are also indicated in the final Aquacheck report for results exceeding the maximum acceptable error or twice the allowable error, respectively. When looking at the values of Table 3, we can observe that 11 are below 23% error, 4 values exhibit errors between 24–36% and the other errors are higher than 50% or not determined. When looking at previous collaborative studies using dichloromethane extraction and LC analysis for a variety of pesticides spiked at higher levels usually varying from 1–100 μg/l (Method 4, NPS-EPA), it has been shown that the overall R.S.D. varied from 5.5–38.6% [23]. Since the method used in this paper has not been sufficiently tested in collaborative studies, we can assume that the results obtained are quite satisfactory and we should also consider that the spiking level is much lower than the NPS collaborative study (by a factor of 1000).

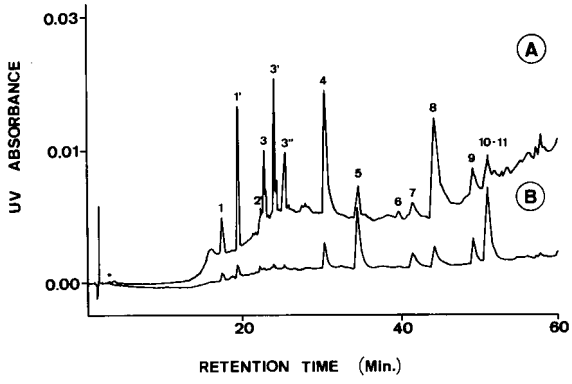

Fig. 3. LC-DAD chromatogram obtained at (A) 230 nm and (B) 254 nm of 150 ml of well water spiked with a certified solution containing a mixture of 11 pesticides (from Aquacheck). Peaks: 1 = *cis*-mevinphos, 1′ = *trans*-mevinphos, 2 = dichlorvos, 3 = fenthion, 3′ and 3″ = fenthion TPs, 4 = azinphos-methyl, 5 = parathion, 6 = malathion, 7 = fenitrothion, 8 = azinphos-ethyl, 9 = chlorfenvinphos, 10 = parathion-ethyl and 11 = diazinon. The concentration levels of the pollutants detected are summarized in Table 3.

Fig. 3 shows a chromatogram of the Aquacheck certified material where the major compounds that give problems are: mevinphos, parathion-ethyl and diazinon, malathion and fenthion. These compounds, with the exception of mevinphos, have been reported as unstable in biologically inhibited water, stored at 4°C and at pH 3 during 14 days. The NPS-US EPA has therefore decided not to include them in their monitoring programs [7,8]. Problems arise for malathion, which has an UV absorbance at < 205 nm. Even though it is possible to characterize their spectrum by subtracting the background noise (Fig. 4), quantification at a low ng/l level may cause a high inaccuracy due to matrix interferences. Quantification of mevinphos appeared to be another source of error since this compound is rapidly degraded and is supplied as a mixture of two isomers. Quantification was done considering both of them. Each isomer could be characterized and Fig. 3 shows their spectra. The second eluting isomer was identified as *trans*-mevinphos, due to a higher spectral maximum and a more intense absorption. Those results are consistent with results presented by DiCorcia and Marchetti [28].

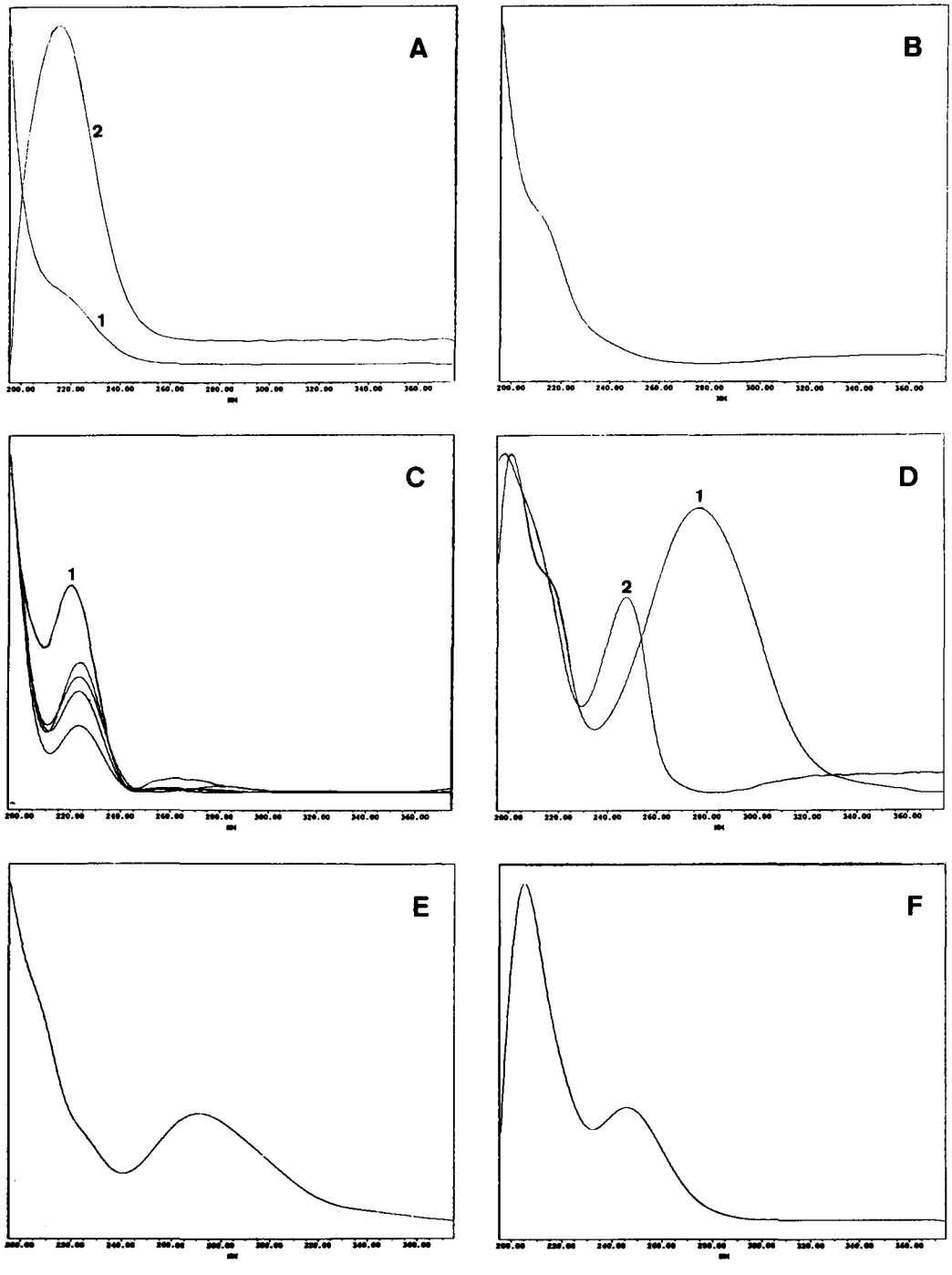

Fig. 4. UV absorbance spectra of (A) *cis*- (1) and *trans*-mevinphos (2), (B) malathion, (C) fenthion and its transformation products, (D) parathion-ethyl (1) and diazinon (2), (E) fenitrothion and (F) chlorfenvinphos, all obtained from the chromatogram in Fig. 3.

They describe the presence of the two isomers. Similarly to these workers, we have also found that *trans*-mevinphos is present at a 3–4 times higher level than *cis*-mevinphos. Quantification of both isomers was carried out by calculating the relationship between *trans*- and *cis*-mevinphos in several standards, using preconcentration. The results obtained indicate that *trans*-mevinphos is on the average 2.3 times more abundant than *cis*-mevinphos. This value was used to correct the amount of each preconcentrated isomer, and recalculation of each isomer from the Aquacheck samples was carried out. Results thus encountered were 46.5 and 64.6 μg/l for *cis*- and *trans*-mevinphos, respectively. Results for *trans*-mevinphos match exactly with reference values of Aquacheck. The presence of these two peaks it is not a problem of instability of mevinphos in water solution, since the National Pesticide Survey-EPA has included this compound in its list which means that at least it is stable for 14 days at 4°C using biologically inhibited well water at pH 3 [7,8]. The problems analysing mevinphos have also been reflected in the results of the Aquacheck interlaboratory studies. We have participated up till now in two interlaboratory exercises together with 22 and 25 other laboratories in the first (June 1993) and second (November 1993) exercise, respectively. For mevinphos only 12 of 22 laboratories and 17 out of 25 laboratories gave results and from that value only 7 and 8 laboratories, respectively, gave acceptable results, which are the lowest acceptable values (together with those of fenthion).

For fenthion, the time needed for the on-line preconcentration, ca. 75 min, was sufficient to produce the degradation of fenthion in water, and it appears in the chromatogram (Fig. 3) as multiple peaks corresponding to its metabolites (fenthion-*O*-analogue, fenthion sulfoxide and sulfone). The spectra corresponding to each of these are shown in Fig. 4.

An obvious error for parathion-ethyl was generated by coelution of this compound with diazinon. The peak was quantified as parathion-ethyl but after further investigation it was possible to discern both compounds (Fig. 4).

As can be seen in Fig. 3, both azinphos-methyl and ethyl presented some tailing, and this can be the source of error presented in Table 3.

3.5. Confirmation of compounds

The analytical method used in this paper permitted also the confirmation of pesticides at levels as low as 0.02–0.03 μg/l (such as for fenitrothion and chlorfenvinphos (Fig. 4)). This indicates a superior confirmation of the present system used compared to previous reports where confirmation in natural waters was only feasible at 0.5–1 μg/l [9] for monolinuron and 0.2 μg/l [23] for atrazine. In all these cases compounds exhibiting UV spectra above 220 nm have been confirmed. Problems arise when compounds such as malathion (Fig. 4) need to be confirmed at the 0.025 μg/l level. It is hardly possible to confirm such compounds although at a 10 times higher level there is no problem in confirmation. This is probably due to the use of different diode array systems. In our case, the optical slit of the diode was set at 2.4 nm, and the system was operated at one spectrum per second. This combination permitted to acquire good spectral resolution, which is essential for the characterization of compounds at a low ng/l level. The Milenium software permits to operate at a resolution of 1.2 nm and spectra can be recorded 10 times per second.

4. Conclusions

The validation of an automated precolumn exchange system (PROSPEKT) followed by liquid chromatography with diode array detection has been described. Calibration graphs were plotted at a quantitation level of 0.1 μg/l using natural waters. By participation in Aquacheck interlaboratory exercise it was possible to determine 11 pesticides in ground water samples at levels varying from 0.02–0.2 μg/l. A relative standard deviation from the mean values varied from 1.6–36% for 7 of the 11 pesticides analyzed. This is an acceptable value and comparable to other errors detected when analyzing pesticides in drinking water samples at higher spiking levels (30–300 μg/l using established methods of analysis, such

as Method 4 of the NPS-US EPA). The difficulties in the analysis of organophosphorus pesticides have been detected due to instability in water (fenthion), thus giving degradation products during the period of analysis, caused by poor absorption in the UV range (malathion), coelution problems (diazinon-parathion ethyl) and presence of two isomers (*cis* and *trans*) in the sample, which could be separated by SPE-LC-DAD, whereas the results indicated by Aquacheck report only one value. The difficulties encountered in the interlaboratory comparison of the various organophosphorus pesticides in ground water samples distributed by Aquacheck have been pointed out in the number of acceptable results reported by the different laboratories (with an error below 17%) being in many cases below 50% (for four compounds). In other cases, only 7 and 9 of a total of 22 and 25 laboratories gave acceptable results for mevinphos and fenthion, respectively. The results reported in the interlaboratory exercise suggest that the use of PROSPEKT apparatus is a robust method – and this is proved by the fact that the lowest error detected was for atrazine (1.6%) – and that the problems encountered are general problems in the determination of organophosphorus pesticides in water samples but not of the technique in use. This is clear since many of the laboratories that gave flagged or double flagged results were using gas chromatographic techniques with selective detectors which in principle give better detection limits when compared to the system used in this paper. They have also been widely tested, and have therefore been included in official methods of analysis.

Confirmation of certain pesticides at the 0.02 μg/l level was feasible although certain compounds with absorption maxima < 210 nm still cannot be unequivocally confirmed. The use of on-line solid-phase extraction and thermospray mass spectrometry has partly solved this problem by showing a linearity range of 0.02–1.5 μg/l [29,30], although in this case other problem may arise such as difficulties in the ionization for certain compounds and in the linearity range due to change of temperatures of the interface as a result of the gradient elution system used. On-line SPE-LC-DAD-MS will probably give the best solution to all the problems although at much higher costs, which may be a problem for many laboratories involved in the surveillance of organic pollutans in water samples.

Acknowledgments

This work was supported by the Environment Research and Development Program 1991–1994 (Commission of the European Communities), contract No. EV5V-CT93-0245 and PLANICYT (AMB94-0950-CE). S.L. gratefully acknowledges financial support from CICYT (Grant AMB92-0218).

References

[1] M. Fielding, D. Barceló, A. Helweg, S. Galassi, L. Torstensson, P. Van Zoonen, R. Wolter and G. Angeletti. Pesticides in Ground and Drinking Water. Water Pollution Research Report 27, Commission of the European Communities, Brussels, 1992, pp. 1–136.
[2] D. Barceló, G. Durand and N. de Bertrand, Toxicol. Environ. Chem., 38 (1993) 183.
[3] N. De Bertrand and D. Barceló, Anal. Chim. Acta, 254 (1991) 235.
[4] J. Abian, G. Durand and D. Barceló, J. Agric. Food Chem., 41 (1993) 1264.
[5] G. Durand and D. Barceló. Toxicol. Environ. Chem., 36 (1992) 225.
[6] D.J. Munch, R.L. Graves, R.A. Maxey and T.M. Engel, Environ. Sci. Technol., 24 (1990) 1446.
[7] D.J. Munch and Ch.P. Frebis, Environ. Sci. Technol., 26 (1992) 921.
[8] D. Barceló, J. Chromatogr., 643 (1993) 117.
[9] J. Slobodnik, E.R. Brouwer, R.B. Geerdink, W.H. Mulder, H. Lingeman and U.A.Th. Brinkman, Anal. Chim. Acta, 268 (1992) 55.
[10] J. Slobodnik, M.G.M. Groenwegen, E.R. Brouwer, H. Lingeman and U.A.Th. Brinkman, J. Chromatogr. 643 (1993) 359.
[11] M.W.F. Nielen, R.W. Frei and U.A.Th. Brinkman, in R.W. Frei and K. Zech (Eds.), Selective Sample Handling and Detection in HPLC, Part A, Elsevier, Amsterdam, 1988, Chap. 1.
[12] V. Coquart and M.C. Hennion, J. Chromatogr., 553 (1991) 329.
[13] E.R. Brouwer, I. Liska, R.B. Geerdink, P.C.M. Frintrop, W.H. Mulder, H. Lingeman and U.A.Th. Brinkman, Chromatographia, 32 (1991) 445.

[14] I. Liska, E.R. Brouwer, A.G.L. Ostheimer, H. Lingeman, U.A.Th. Brinkman, R.B. Geerdink and W.H. Mulder, Int. J. Environ. Anal. Chem., 47 (1992) 267.
[15] R. Reupert, I. Zube and E. Plöger, LC–GC, 5 (1992) 43.
[16] E.R. Brouwer, H. Lingeman and U.A.Th. Brinkman, Chromatographia, 29 (1990) 415.
[17] E.R. Brouwer, D.J. Van Iperen, I. Liska, H. Lingeman and U.A.Th. Brinkman, Int. J. Environ. Anal. Chem., 47 (1992) 257.
[18] S. Chiron and D. Barceló, J. Chromatogr., 645 (1993) 125.
[19] S. Chiron, A. Fernandez-Alba and D. Barceló, Environ. Sci. Technol., 27 (1993) 2352.
[20] D. Barceló, M. Solé, G. Durand and J. Albaigés, Fresenius' J. Anal. Chem., 339 (1991) 676.
[21] S. Lacorte, C. Molina and D. Barceló, Anal. Chim. Acta, 281 (1993) 71.
[22] M.R. Driss, M.C. Hennion and M.L. Bouguerra, J. Chromatogr., 639 (1993) 352.
[23] V. Pichon and M.C. Hennion, J. Chromatogr., 665 (1994) 269.
[24] K.W. Edgell, E.J. Erb, J.E. Longbottom and V. Lopez-Avila, J. Assoc. Off. Anal. Chem., 75 (1992) 858.
[25] J. Lintelmann, C. Mengel and A. Kettrup, Fresenius' J. Anal. Chem., 346 (1993) 752.
[26] R.J. Mesley, W.D. Pocklington and R.F. Walker, Analyst, 116 (1991) 975.
[27] A. Noble, J. Chromatogr., 642 (1993) 3.
[28] A. DiCorcia and M. Marchetti, Environ. Sci. Technol., 26 (1992) 66.
[29] S. Chiron, E. Martinez and D. Barceló, J. Chromatogr., 665 (1994) 283.
[30] S. Chiron, S. Dupas, P. Scribe and D. Barceló, J. Chromatogr., 665 (1994) 295.

ELSEVIER

Analytica Chimica Acta 296 (1994) 235–241

ANALYTICA CHIMICA ACTA

Comparison of reversed-phase chromatographic systems with principal component and cluster analysis

Esther Forgács

Central Research Institute for Chemistry, Hungarian Academy of Sciences, P.O. Box 17, 1525 Budapest, Hungary

Received 3 March 1994; revised manuscript received 21 April 1994

Abstract

The separation of ethoxylated 1,1,3,3-tetramethylphenyl surfactants was investigated by reversed-phase liquid chromatography (RP-LC) using various supports (C_1, C_2, C_6, C_8, C_{18}, polyethylene-coated silica, and polyethylene-coated alumina) and with reversed-phase thin-layer chromatography (RP-TLC) using impregnated silica and alumina supports. The retention data matrix was evaluated both by principal component analysis and cluster analysis. The retention characteristics of both polyethylene-coated supports were similar to those of C_1, and the retention capacity of RP columns for surfactants increased with the increasing length of the covalently bonded hydrocarbon chain. Both multivariate mathematical statistical methods gave similar results and adequate separation was performed with the RP-LC and RP-TLC systems.

Keywords: Chromatography; Principal component analysis; Cluster analysis ; Non-ionic surfactants

1. Introduction

The majority of separations in liquid chromatography (LC) is carried out in the reversed-phase separation mode. Many reversed-phase chromatographic supports have been developed with a hydrophobic ligand covalently bonded to the polar silica surface [1,2]. However, the retention characteristics of reversed-phase supports depend on the physicochemical parameters of the support. The retention of solutes may depend on the length of the alkyl chain [3] or it can be independent of the length of the alkyl chain [4]. This discrepancy can be explained by the different types of solutes used for the evaluation of the reversed-phase column. However, the silanol groups not covered by the hydrophobic ligand may influence the retention of polar solutes resulting in a retention order different from that predicted according to the molecular lipophilicity [5,6]. The influence of free silanol groups on the retention was defined as the silanophil effect [7]. When the density of covalently bonded alkyl chains increases, the silanophil effect becomes low or negligible [8,9].

Much effort has been devoted for the development of reversed-phase supports without the silanophil side effect. It has been observed that the silanophil effect is absent on polystyrene coated silica [10]. Not only polystyrene but also other polymers such as octadecyl poly(vinyl alcohol) copolymers [11], polytrifluorostyrene [12] and polyethylene [13] have been tested as coating agents of silica for the preparation of reversed-

SSDI 0003-2670(94)00213-6

phase supports. It has been established that polymer coated supports show excellent mechanical and pH stability [14]. Multivariate mathematical–statistical methods such as factor analysis [15], correspondence factor analysis [16], principal component analysis [17], canonical correlation analysis [18] and cluster analysis [19] have been extensively used for the elucidation of the similarities and dissimilarities between various reversed-phase systems. These methods are suitable for the evaluation of retention data matrices of considerable dimensions [20].

The retention behaviour of non-ionic surfactants in various reversed-phase thin-layer chromatographic (TLC) systems has been extensively investigated [21,22] and it was established that they cannot be separated according to the length of ethylene oxide chain under reversed-phase conditions.

The objectives of the present work were the determination of the retention behaviour of some non-ionic surfactants under various reversed-phase LC and TLC conditions and to find the similarities and dissimilarities between the retention characteristics of reversed-phase chromatographic systems by using multivariate mathematical–statistical methods such as principal component analysis (PCA) and cluster analysis (CA).

2. Experimental

The non-ionic surfactants were the ethoxylated derivatives of 1,1,3,3-tetramethylbutylphenol containing in average 5 (compound I), 7.5 (II), 10.5 (III), 11.5 (IV), 16 (V) and 30 (VI) ethylene oxide groups per molecule.

2.1. RP-TLC

DC-Alufolien silica gel 60 and aluminium oxide 60 F_{254} plates (Merck, Darmstadt) were impregnated by overnight predevelopment in *n*-hexane–paraffin oil (95:5, v/v). The non-ionic surfactants were separately dissolved in methanol to give a concentration of 5 mg/ml, and 2 μl of solution were spotted onto the plates. The development was carried out in sandwich chambers ($22 \times 22 \times 3$ cm) at room temperature, and the running distance was ca. 15 cm. The chambers were not presaturated. The eluent contained 35–80 and 50–95 vol.% methanol in steps of 5 vol.% for impregnated alumina and silica layers, respectively. The use of different concentration ranges for the different impregnated plates was motivated by the fact that the surfactants showed higher mobility on impregnated alumina than on impregnated silica layers. After development the plates were dried at 105°C, and the spots were detected with modified Burger reagent [23]. Each determination was performed in quadruplicate.

2.2. Mathematical–statistical evaluation of RP-TLC data

The R_M values were calculated for each surfactant–eluent combination from $R_M = \log(1/R_F - 1)$. The R_M values were separately extrapolated to zero methanol concentration:

$$R_M = R_{M0} + bC \quad (1)$$

where C is the concentration of methanol in the eluent (%, v/v) and R_M is the actual R_M value of the surfactant determined at this methanol concentration. R_{M0} (intercept) and b (slope) values from Eq. 1 were considered as the best means of estimating the lipophilicity (R_{M0}) [24] and specific hydrophobic surface area (b) [25] of the surfactants. The data were omitted from the calculations when the coefficient of variation between the parallel determinations was $> 6\%$.

To check the validity of the hypothesis that in the case of homologous series of solutes the intercept and slope values of Eq. 1 are strongly intercorrelated [26,27], linear correlations between the corresponding parameters were calculated separately for impregnated alumina and silica supports:

$$R_{M0} = a_1 + B_1 b \quad (2)$$

To elucidate the influence of unimpregnated supports on the reversed-phase retention behaviour of surfactants, linear relationships were

calculated between the R_{M0} and b values of Eq. 1 determined on impregnated alumina and silica:

$$R_{M0(silica)} = a_2 + B_2 R_{MO(alumina)} \quad (3)$$

$$b_{(silica)} = a_3 + B_3 b_{(alumina)} \quad (4)$$

As the surfactants differ only in the length of the ethylene oxide chain, and this substructure probably influences their retention, linear correlations were also calculated between the length of ethylene oxide chain (n_e) and the specific hydrophobic surface area (b in Eq. 1) of the surfactants:

$$b_{(silica)} = a_4 + B_4 n_e \quad (5)$$

$$b_{(alumina)} = a_5 + B_5 n_e \quad (6)$$

All B terms are constants.

2.3. RP-LC

The LC equipment consisted of a Liquopump Type 312 (Labor MIM, Budapest), a Cecil CE-212 spectrophotometer (Cambridge) used as the detector, a Valco 20-μl injector (Houston, TX), and a Waters 740 integrator (Milford, MA). The flow-rate was 0.5 ml/min and the detection wavelength was 235 nm. The eluent was methanol–water (80:20, v/v). Columns of 25 cm × 4 mm i.d. were used in each experiment. They were filled with silica based C_1 (column A), C_2 (B), C_6 (C), C_8 (D), C_{18} (E) reversed-phase supports as well as with polyethylene coated silica (column F) and alumina (column G). The polyethylene-coated supports were prepared in our laboratory and the retention characteristics of polyethylene-coated silica have been reported elsewhere [13]. The surfactants were dissolved in the eluent at a concentration of 0.05 mg ml^{-1}. The retention time of each compound was determined by three consecutive determinations. The capacity factor and the coefficient of variation of the capacity factor were calculated for each compound on each column.

2.4. Multivariate methods for the comparison of the RP-TLC and RP-LC systems

To find the similarities and dissimilarities between the retention behaviour of surfactants and reversed-phase chromatographic systems principal component analysis (PCA) was applied [28]. The surfactants were the variables and the parameters of Eq. 1 (both for impregnated alumina and silica) as well as the capacity factors of the surfactants on the 7 columns were the observed parameters. The same data matrix was also evaluated by cluster analysis [29].

3. Results and discussion

3.1. RP-TLC

The parameters of Eq. 1 are compiled in Table 1. The equation fits the experimental data well, the significance levels in each instance being over 99% (see calculated r values) indicating that the ratios of variance explained (change in the R_M values) by the independent variable (change in methanol concentration) are high. The R_M values decrease in each instance with increase in methanol concentration, i.e., these compounds do not show any anomalous retention behavior in this concentration range that would invalidate the evaluation using Eq. 1.

Table 1
Relationship between the R_M value of non-ionic surfactants and the concentration of methanol (C) in the eluent. Numbers refer to the surfactants specified in the Experimental section

Surfactant	$R_M = R_{M0} + bC$			
	R_{M0}	$-b \times 10^{-2}$	$s_b \times 10^{-3}$	$r_{calc.}$
Impregnated silica				
I	4.23	5.66	2.59	0.9897
II	3.85	5.06	2.29	0.9905
III	3.69	4.86	2.10	0.9908
IV	3.56	4.61	1.85	0.9920
V	3.81	4.79	1.73	0.9935
VI	2.98	3.34	2.35	0.9761
Impregnated alumina				
I	3.35	4.92	1.76	0.9937
II	3.02	4.59	1.83	0.9922
III	2.92	4.63	0.91	0.9981
IV	2.93	4.72	1.76	0.9931
V	3.00	4.88	1.22	0.9969
VI	3.21	5.52	2.08	0.9930

Significant linear correlation was found between the lipophilicity (R_{M0}) and the specific hydrophobic surface area (b) of surfactants determined on impregnated silica:

$$R_{M0(silica)} = 1.18 + (0.53 \pm 0.04) b_{(silica)} \quad (7)$$

$r_{calc.} = 0.9882$, $r_{99.9\%} = 0.9741$

This finding indicates that the non-ionic surfactants behave as a homologous series of solutes on impregnated silica. However, the two molecular parameters were not correlated on impregnated alumina. This result supports the hypothesis that the supports retain their original retention even after impregnation; that is the impregnation agent does not cover each adsorption center on the support surface.

Neither the lipophilicity nor the specific hydrophobic surface area values determined on impregnated alumina and silica showed significant correlation. This finding lends support to the hypothesis outlined above that the adsorption by supports prevails even after impregnation. Significant relationships were found between the specific hydrophobic surface area of surfactants and the number of ethylene oxide groups per molecule. However, the character of the correlation strongly depended on the nature of the support (Fig. 1). The specific hydrophobic surface area decreased on impregnated silica with increasing number of ethylene oxide groups per molecule, and it increased on impregnated alumina. This result may be due to the fact that the ethylene oxide oligomers are weak Lewis acids. They are repelled by the acidic adsorption centers on the silica surface not covered by the impregnating agent resulting in lower contact surface with the increasing length of ethylene oxide chain. Conversely, the polar (acidic) ethylene oxide chain readily interacts with the basic adsorption centers on the surface of the alumina support resulting in an enhanced contact surface in case of longer ethylene oxide chains.

3.2. RP-LC

The log k' values and the coefficients of variation are listed in Table 2. The coefficients of variation in each instance were fairly small (in most cases $< 0.5\%$) indicating the good reproducibility of the measurements. Small differences

Table 2
Capacity factor (log k') and the coefficient of variation (C.V.%) of the capacity factor of surfactants measured on various reversed-phase columns. Letters and roman numbers refer to RP-LC columns and surfactants specified in the Experimental section, respectively

Column	Surfactant					
	I		II		III	
	log k'	C.V.%	log k'	C.V.%	log k'	C.V.%
A	−0.131	0.36	−0.090	0.43	−0.110	0.19
B	0.113	0.24	0.120	0.61	0.119	0.57
C	0.314	0.18	0.347	0.54	0.290	0.35
D	0.310	0.44	0.305	0.37	0.313	0.22
E	0.594	0.31	0.639	0.23	0.627	0.46
F	−0.404	1.14	−0.231	0.87	−0.310	0.68
G	−0.364	0.73	−0.437	0.91	−0.402	0.64
	IV		V		VI	
A	−0.090	0.23	−0.081	0.37	−0.063	0.52
B	0.116	0.36	0.129	0.19	0.101	0.49
C	0.355	0.21	0.319	0.34	0.315	0.57
D	0.313	0.49	0.299	0.63	0.266	0.25
E	0.601	0.38	0.675	0.22	0.682	0.29
F	−0.272	0.96	−0.165	0.81	0.007	0.77
G	−0.408	0.92	−0.447	0.63	−0.640	1.31

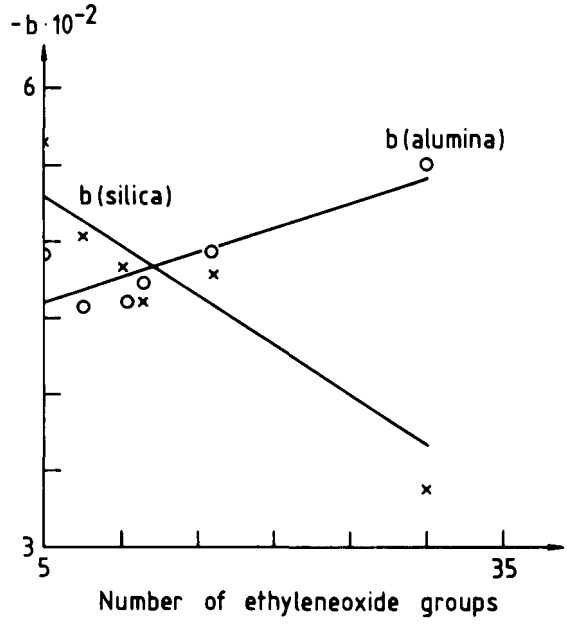

Fig. 1. Relationship between the number of ethylene oxide groups per molecule (n_e) and the specific hydrophobic surface area of surfactants determined on impregnated alumina (b_{Alu}) and silica (b_{Sil}) supports. $b_{Alu} = 4.44 + 3.26 \times 10^{-2} n_e$, $r_{calc.} = 0.8532$; $b_{Sil} = 5.82 - 8.21 \times 10^{-2} n_e$, $r_{calc.} = 0.9571$.

were found between the capacity factors of surfactants on each RP-LC column proving again that reversed-phase chromatography is unsuitable for the separation of surfactants according to the length of the ethylene oxide chain. However, considerable differences were observed between the retention capacity of columns. The retention capacities of polyethylene-coated silica and alumina columns as well as the C_1 column were the lowest. The capacity increased with increasing length of the apolar hydrocarbon chain covalently bonded to the silica surface. The similarity between the retention capacity of polymer-coated and C_1 columns can be tentatively explained by the supposition that the polyethylene coating probably lies parallel with the support surface, the end groups being in close contact with the adsorption centers of the support. Only the surface of the polyethylene coating exposed to the eluent is available for the solutes. It is a hydrophobic layer similar to that of the C_1 coating in thickness and it differs considerably from the "brush-like" coatings where the alkyl chains more or less penetrate the mobile phase and more than one CH_2 group can interact with the hydrophobic substructure of the solute. Significant linear relationships were found between the log k' values of the surfactants and the number of ethylene oxide groups per molecule (n_e) indicating that polyethylene coated supports behave as real reversed-phase supports.

Impregnated silica:

$$\log k' = -0.40 + (11.6 \pm 2.36) n_e$$

$$r_{calc.} = 0.9263, \; r_{99\%} = 0.9172$$

Impregnated alumina:

$$\log k' = -0.33 - (0.85 \pm 1.08) n_e$$

$$r_{calc.} = 0.9687, \; r_{99\%} = 0.9172$$

3.3. Comparison of RP-TLC and RP-LC systems

In principal component analysis the first principal component explained the overwhelming majority of the variance (98.66%), indicating that the retention behaviour of each surfactant is similar in each reversed-phase chromatographic system and it can be described by one background variable. Unfortunately, PCA does not define this background variable as a concrete physicochemical entity but only indicates its mathematical possibility. As each chromatographic system was reversed-phase it is assumed that the first background variable corresponds to the molecular hydrophobicity, which governs the retention of sur-

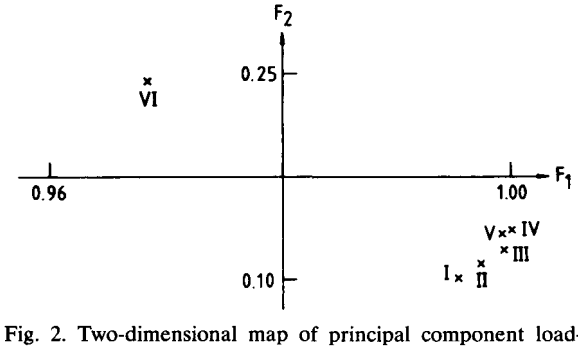

Fig. 2. Two-dimensional map of principal component loadings. Numbers refer to the surfactants specified in the Experimental section.

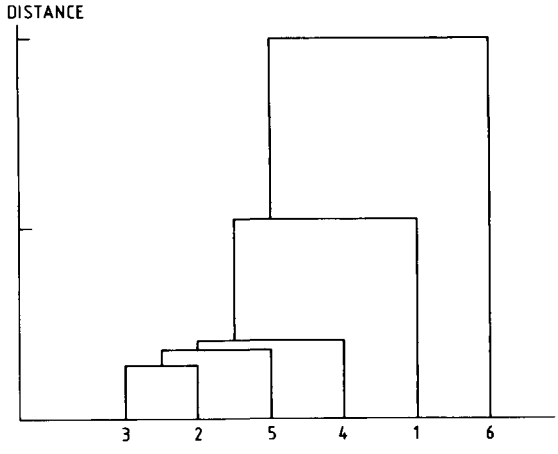

Fig. 3. Cluster dendrogram of surfactants. Numbers refer to the surfactants specified in the Experimental section.

factants in each system. The two-dimensional map of PC loadings and the cluster dendrogram of surfactants taking into consideration simultaneously their retention in each reversed-phase chromatographic system are shown in Fig. 2 and Fig. 3, respectively. The information content of both calculation methods is similar: surfactant VI with the longest ethylene oxide chain is situated far from the other surfactants on both maps, whereas the differences between the retention behaviour of the other surfactants is fairly small.

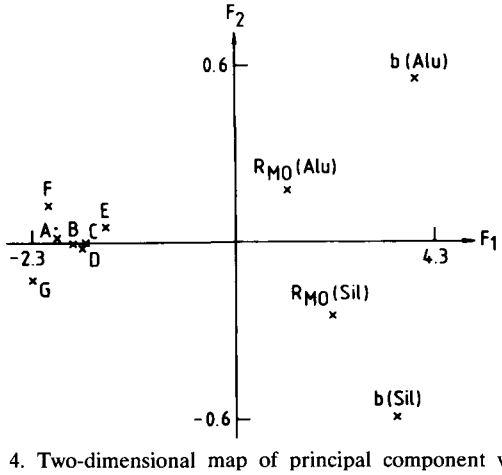

Fig. 4. Two-dimensional map of principal component variables (reversed-phase chromatographic systems). Letters refer to reversed-phase LC columns mentioned in the Experimental section.

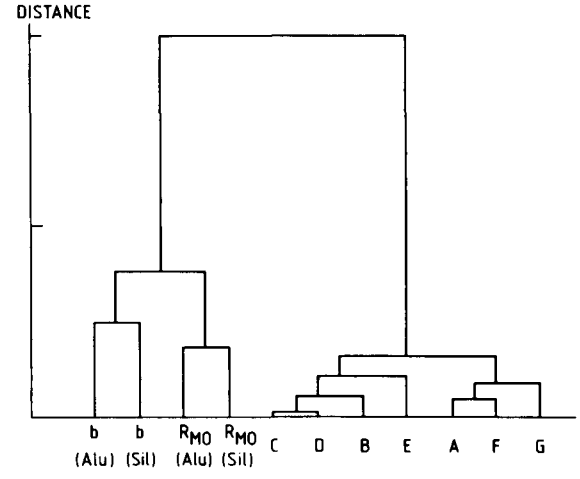

Fig. 5. Cluster dendrogram of reversed-phase chromatographic systems. Letters refer to the reversed-phase LC columns mentioned in the Experimental section.

The two-dimensional map of principal component variables and the cluster dendrogram of the reversed-phase systems are shown in Fig. 4 and Fig. 5, respectively. RP-TLC parameters form a separate cluster on both maps indicating the different retention characteristics of RP-TLC. This finding proves again the similar information content of the multivariate methods. Polyethylene-coated supports are very near to C_1, supporting our previous conclusions about the character of the polymer coating.

It can be concluded from the data that both principal component analysis and cluster analysis are suitable for the correct classification of reversed-phase chromatographic systems. It must be emphasized that the conclusions discussed above are based on calculations carried out on one special data matrix and are not the results of theoretical considerations. Therefore they have to be applied to different data matrices with extreme caution.

Acknowledgments

This work was supported by a grant for Cooperation in Science and Technology with Central and Eastern European Countries: "Enhanced re-

moval and prevention of environmental pollution by attachment and immobilization of bacteria at surfaces".

References

[1] J.J. Kirkland, C.H. Dilks and J.E. Henderson, LC·GC, 6 (1993) 436.
[2] H.A. Claessens, E.A. Vermeer and C.A. Cramers, LC·GC, 6 (1993) 692.
[3] H. Engelhardt, H. Löw and W. Götzinger, J. Chromatogr., 544 (1991) 371.
[4] B.S. Ludolf, C.-Y. Jeng, A.H.T. Chu and S.H. Langer, J. Chromatogr. A., 660 (1994) 3.
[5] B. Buszewski, J. Schmid, K. Albert and E. Bayer, J. Chromatogr., 552 (1991) 415.
[6] B. Buszewski, Z. Suprynowicz, P. Staszcuk, K. Albert, B. Pfleiderer and E. Bayer, J. Chromatogr., 499 (1990) 385.
[7] K.E. Bij. C. Horvath, W.R. Melander and A. Nahum, J. Chromatogr., 203 (1981) 65.
[8] B. Buszewski and Z. Suprynowicz, Anal. Chim. Acta, 208 (1988) 263.
[9] B. Buszewski, J. Chromatogr., 538 (1991) 293.
[10] A. Kurganov, O. Kuzmenko, V.A. Davankov, B. Eray, K.K. Unger and U. Trübinger, J. Chromatogr., 506 (1990) 391.
[11] P. Vallat, W. Fan, N. El Tayar, P.-A. Carrupt and B. Testa, J. Liquid Chromatogr., 15 (1992) 2133.
[12] A.D. Kataev, V.V. Saburov, O.A. Reznikova, D.V. Kapustin and V.P. Zubov, J. Chromatogr. A., 660 (1994) 131.
[13] E. Forgács, J. Liquid Chromatogr., 16 (1993) 3757.
[14] A. Kurganov, V. Davankov, T. Isajeva, K. Unger and F. Eisenbeis, J. Chromatogr. A., 660 (1994) 97.
[15] S.J. Schmitz, H. Zwanziger and H. Engelhardt, J. Chromatogr., 544 (1991) 381.
[16] M. Righezza and J.R. Chretien, J. Chromatogr., 544 (1991) 393.
[17] E. Forgács and T. Cserháti, J. Chromatogr., 600 (1992) 43.
[18] E. Forgács, T. Cserháti and B. Bordás, Chromatographia, 36 (1993) 19.
[19] E. Forgács, T. Cserháti and B. Bordás, Anal. Chim. Acta, 279 (1993) 115.
[20] T. Cserháti and K. Magyar, J. Biochem. Biophys. Meth., 24 (1992) 249.
[21] M. Szögyi and T. Cserháti, J. Planar Chromatogr. 5 (1992) 267.
[22] T. Cserháti, J. Biochem. Biophys. Meth., 27 (1993) 133.
[23] G.F. Longman, The Analysis of Detergents and Detergent Products, Wiley, London, 1977, p. 517.
[24] J. Gasparic, in J.C. Giddings, E. Grushka and P.R. Brown (Eds.), Advances in Chromatography, Vol. 31, Marcel Dekker, New York, 1992, pp. 153.
[25] C. Horváth, W. Melander and I. Molnár, J. Chromatogr., 125 (1976) 129.
[26] T. Cserháti, Chromatographia, 18 (1984) 318.
[27] K. Valkó, J. Liquid Chromatogr., 7 (1984) 1405.
[28] K.V. Mardia, J.T. Kent and J.M. Bibby, Multivariate Analysis, Academic Press, London, 1979, p. 213.
[29] P. Willett, Similarity and Clustering in Chemical Information System, Research Studies Press, New York, 1987.

ELSEVIER

Analytica Chimica Acta 296 (1994) 243–247

ANALYTICA CHIMICA ACTA

A simple and reliable method to extract and measure iodine in soils

A.A. Marchetti *, L. Rose, T. Straume

University of California, Lawrence Livermore National Laboratory, P.O. Box 808, Livermore, CA 94551-0808, USA

Received 22 March 1994

Abstract

A procedure was developed for the extraction of iodine from soil samples by alkaline ashing. After the extraction, the iodine was measured using gas chromatography. The method was validated using NIST Standard Reference Materials: San Joaquin Soil (SRM 2709), Montana Soil (SRM 2711) and Buffalo River Sediment (SRM 2704). The method gave consistently reproducible results that are in good agreement with the noncertified iodine concentrations reported by NIST, which were measured using neutron activation analysis. The method presented here requires relatively low cost equipment and can be performed in most environmental measurement laboratories. Also, since it has been demonstrated to be reliable for soils, it may help in the development of NIST certified soil standards for iodine.

Keywords: Gas chromatography; Iodine in soil samples; Environmental samples; Chemical extraction; Accelerator mass spectrometry (AMS)

1. Introduction

Since the development of accelerator mass spectrometry (AMS) to measure long-lived radioisotopes, there has been considerable interest in the use of ^{129}I (half life 1.6 10^7 years) as a geological and environmental tracer. The AMS technique allows the determination of as little as ca. 10^6 atoms of ^{129}I in mg-size samples [1] and is therefore ideal for measurement of the very low $^{129}I/^{127}I$ ratios observed in environmental samples (ratios in common soils are in the 10^{-9} range).

For many important environmental evaluations, e.g., reconstruction of radioiodine deposition patterns from large-scale releases of fission products [2], it is necessary to know the amount of ^{129}I present in the sample. However, in order to determine the total amount of ^{129}I in the sample, both the $^{129}I/^{127}I$ ratio *and* the total amount of iodine must be measured. As stated above, the $^{129}I/^{127}I$ ratio can be measured accurately using AMS. However, measurement of the total amount of iodine in the sample requires a reliable and efficient method to extract iodine from the environmental medium of interest, in this case, soil.

Evaluation of several methods available in the published literature demonstrated the need for development of an efficient method to extract iodine from soils and other environmental samples. A simple and reliable preparation method is required when dealing with the large number of samples usually involved in environmental studies.

Ashing or fusion with an alkaline aid can be used to extract iodine from a given matrix. However, a literature search of available ashing techniques for iodine determination reveals numerous contradictions. For example, a handbook reviewing several decomposition

* Corresponding author.

Elsevier Science B.V.
SSDI 0003-2670(94)00238-H

methods in analytical chemistry [3] states that iodine is quite certainly lost at an ashing temperature of 600°C and that the temperature should be kept as low as possible. On the other hand, ref. [4] claims that various environmental samples have been successfully ashed at 650°C for iodine determination. Significant losses of iodine have been reported using sodium compounds as ashing aids [3,5] but another work indicates that sodium hydroxide can be used successfully [6]. Overall, it should be kept in mind that the procedures and type of samples change among authors and this could explain at least in part these different claims.

There are other methods to extract iodine. Some that are based on acid digestion have shown wide variations in the recovery of iodine [5,7]. The procedures in which the acid digestion is followed by distillation of iodine [8,9] seem to give good recoveries but they are labour intensive and can generate large amounts of hazardous acid waste. Other methods rely on the combustion of the sample in a stream of oxygen [10–12]. In this case, the iodine in the sample should be transformed to I_2 and carried by the gas stream to an absorber. In principle, it would be expected that combustion should minimize any matrix effect in the recovery of iodine. However, lack of reproducibility has been reported in the determination of iodine in citrus leaves [12].

Here, a simple ashing method is presented that yielded highly reproducible results for the iodine concentration in different soils. The iodine extracted from the soil samples was measured using a relatively simple technique. Briefly, iodine reacts in acid solution with a ketone forming an iodo derivative which is extracted in hexane and then measured using gas chromatography (GC) with an electron-capture detector [13,14]. The ashing method was tested using three NIST Standard Reference Materials (SRM): San Joaquin Soil (SRM 2709); Montana Soil (SRM 2711); and Buffalo River Sediment (SRM 2704). The concentrations of iodine in these SRMs are not certified values. They therefore do not have associated uncertainties, but do provide a means for comparison. In addition to the NIST standards, a sample of top soil from the Lawrence Livermore National Laboratory (LLNL) grounds was also tested (note that LLNL is only about 30 km west of the San Joaquin valley in central California).

2. Experimental

2.1. Instrumentation

The determinations were performed using a Hewlett Packard 5880A gas chromatograph with a J&W capillary column DB-624 and a ^{63}Ni electron-capture detector. A Hewlett Packard 3396A integrator was used to determine peak areas. The samples were injected automatically with a Hewlett Packard 7673 Sampler using the splitless technique. For each run, the initial temperature of the column oven was set at 50°C for 1 min following injection. Then the temperature was raised at 10°C/min to a final value of 150°C where it remained for one more minute. The injector and detector temperatures were 150°C and 300°C, respectively.

2.2. Reagents

All chemicals were analytical-grade reagents unless otherwise stated. All solutions were prepared using deionized water. Baxter B&J High Purity Solvent Hexane UV was used in the extractions and EM Science technical-grade 3-pentanone was used to prepare the derivative.

2.3. Sample preparation

For the ashing procedure, 2.00 g of soil sample were placed in a 100-ml zirconium crucible and mixed with 2 ml of absolute ethanol, 4 ml of 4 M KOH and 2 ml of 20% KNO_3. The mixture was then thoroughly dried on a hot plate (ca. 100°C) and placed in a muffle. The crucible was covered with a watch glass and heated at 4°C/min to 400°C overnight. The next day, the crucible was removed from the muffle and allowed to cool down. Then, 0.1 g of Na_2SO_3 and 0.5 g of sulfamic acid were dissolved in 30 ml of deionized water and added to the crucible. The mixture was carefully stirred using a glass rod. After this, 1 ml of a saturated solution of $CaCl_2$ was added and the mixture was brought to a gentle boil for about 5 min. Finally, the mixture was filtered using a 0.45-μm pore size filter and the liquid brought to 50 ml with deionized water.

To prepare the iodo derivative, a 25-ml aliquot was placed in a 100-ml separatory funnel followed by 1 ml of 4% 3-pentanone, 1 ml of 5 M H_2SO_4 and 1 ml of 30% H_2O_2. After about 10 min, 10 ml of hexane were

added to extract the iodo derivative. The mixture was vigorously shaken for about 2 min. Then, the aqueous phase was separated and discarded. Approximately a 2-μl volume of the hexane phase was injected by the automatic sampler into the chromatograph. The standards were prepared by dilution of a KI solution containing 1000 μg/g of iodide. Known amounts of iodide were taken to 25 ml with deionized water and then the iodo derivative was prepared and extracted as indicated for the samples. The calibration curve was constructed by plotting the peak area as a function of the total amount of iodine present in the 25-ml aliquot. A total of 10 points were measured between 0.1 and 9.0 μg of iodine and each point was measured 5 times.

3. Results and discussion

3.1. Calibration

A retention time of about 9.4 min was measured for the iodo derivative. The response was linear in the range studied: $A = 1.0449I + 0.126$, where A is the peak area and I is the amount of iodide in μg. The standard deviation of the slope and intercept were 0.0049 and 0.020, respectively. The coefficient of correlation was 0.9995. About a ten-fold improvement in precision was introduced by the use of the automatic sampler as compared to previous trials using manual injection. The relative error in the peak area was less than 1.0%. Reagent blanks did not show any measurable amount of iodine. This procedure was able to clearly detect as little as 0.05 μg of iodine in a 25-ml aliquot.

3.2. Analysis of soils

Before developing the ashing technique, attempts were made to adapt other sample preparation procedures described in the literature to the GC determination of iodine in soils. For example, the distillation method described in Ref. [8] for the determination of iodine in milk was applied to soil but did not result in any measurable iodine in the trapping solution. Another separation method described in Ref. [15] that utilizes an ion-exchange resin resulted in a relatively low recovery of iodine as compared to the results obtained later using the ashing technique. However, it should be noted that these were only preliminary tests and were not confirmed by replication. The determination of iodine using GC has been applied to the analysis of foods [16,17]. The ashing procedure as described in ref. [17] was not successful when applied to soil samples. Furthermore, the results corresponding to the analysis of NIST Nonfat Milk Powder (SRM 1549) as presented in Ref. [17] could not be reproduced here. However, this ashing procedure was adopted as a starting point and then modified by trial and error to maximize the recovery of iodine in soil samples.

At first, the ash extracts would turn into gel when they were neutralized. The reason was the presence of silica in the samples. Silica becomes soluble during the alkaline ashing and then precipitates as the strongly basic ash extract is neutralized. This problem was prevented by the addition $CaCl_2$ as a flocculating agent during the extraction step. Most of the silica would then remain with the insoluble ash residue. Ashing tests conducted at temperatures of 550°C and 500°C resulted in little or no iodine detected. The temperature was then lowered to 400°C, allowing the ashing to occur overnight. Using this temperature, iodine was detected at about the expected levels (a few μg/g). However, the reproducibility of the measurements was very poor even between aliquots of the same extract. Soon, it became clear that the time between the preparations of the ash extract and of the derivative was very critical to the recovery of iodine. For example, two aliquots of the same solution analyzed a day apart resulted in iodine contents of 3.1 and 0.8 μg/g, respectively. In another case, the aliquots were analyzed a day apart but were not neutralized until the derivative was prepared resulting in values of 4.4 and 4.0 μg/g, respectively.

Neutralizing the basic ash solution produced a rapid loss of iodine possibly evaporated as molecular I_2. Iodide can be oxidized by nitrite that could be formed from using KNO_3 as an ashing aid. An attempt to ash using only KOH resulted in low recovery relative to the samples in which KNO_3 was also used. From this experience, it was decided to use a solution of sulfamic acid and Na_2SO_3 instead of only deionized water to prepare the ash extract. The sulfamic acid would eliminate nitrites as nitrogen and the sulfite would keep the iodine as iodide. Also, the neutralization step was omitted from the procedure, since it was found that the acid added to prepare the derivative was enough to make the extract acidic and catalyze the iodination of 3-pentanone. Another modification was the use of hydrogen

Table 1
Iodine concentrations (μg/g) measured in different soils [a]

LLNL top soil	San Joaquin Soil SRM 2709 [b]	Montana Soil SRM 2711 [c]	Buffalo River Sediment SRM 2704 [d]
5.26	4.35	2.97	1.86
5.77	4.45	3.05	1.90
5.16	4.50	2.90	1.81
5.08	4.49	3.04	1.98
5.42	4.40	2.95	1.95
5.34 ± 0.27	4.44 ± 0.06	2.98 ± 0.06	1.90 ± 0.07

[a] Results of five consecutive and independent determinations for each sample.
[b] NIST noncertified value, 5 μg/g.
[c] NIST noncertified value, 3 μg/g.
[d] NIST noncertified value, 2 μg/g.

peroxide instead of a potassium dichromate solution to oxidize the iodide to iodine. In several tests, it was observed that slightly higher recoveries of iodine were obtained using hydrogen peroxide.

With the modified ashing procedure, a series of determinations were performed on samples of LLNL top soil resulting in reproducible values. Subsequently, the method was tested using three NIST Standard Reference Materials. These were San Joaquin Soil (SRM 2709), Montana Soil (SRM 2711) and Buffalo River Sediment (SRM 2704). The concentration of iodine is not a NIST certified value in any of these standards. In fact, there is no certified standard for iodine in soil because it is difficult to obtain reliable iodine measurements in these matrices. The results of five consecutive and independent determinations of iodine are presented in Table 1 for all the samples tested here. The last row of Table 1 shows the average and standard deviation of these results. These are 5.34 ± 0.27, 4.44 ± 0.06, 2.98 ± 0.06, and 1.90 ± 0.07 μg/g for LLNL top soil, SRM 2709, SRM 2711, and SRM 2704, respectively. The noncertified NIST values for the iodine concentrations of SRM 2709, SRM 2711, and SRM 2704 are 5, 3, and 2 μg/g, respectively, which are in good agreement with those measured here. According to NIST Certificates of Analysis, the weight losses due to moisture are about 1.8 to 2.5% for SRM 2709, 1.7 to 2.3% for SRM 2711, and 0.8% for SRM 2704. Thus, corrections for water content would slightly improve the agreement between these values but they are within the statistical uncertainty of our measurements. As seen in Table 1, the standard deviation of the LLNL soil samples is much higher than those corresponding to NIST Standard Reference Materials. This could be due to inhomogeneities in the sample, as the LLNL soil sample was not processed to ensure complete mixing.

In summary, the method presented here to determine iodine in soils provides reproducible results and has shown good agreement with the noncertified values reported in three different NIST standards. It is important to note that, as indicated in their certificates, these standards have been analyzed at NIST using a different technique (i.e., neutron activation analysis). Therefore, the method described here could be applied in principle as an independent technique to measure concentration of iodine in those reference materials and could thus contribute to the development of certified soil standards for iodine. Also, the simplicity of this method and the general availability of gas chromatographs makes this approach cost effective and easy to implement in most laboratories.

Acknowledgements

The authors would like to thank Dr. L.R. Anspaugh for helpful discussions, and Marina Jovanovich and Roger Martinelli for setting up the gas chromatograph. This work was performed under the auspices of the U.S. Department of Energy by the Lawrence Livermore National Laboratory under contract number W-7405-Eng-48 with support from LLNL/LDRD project 93-DE-043.

References

[1] D. Elmore and F.M. Phillips, Science, 236 (1987) 543.
[2] T. Straume, Lawrence Livermore National Laboratory Report, UCRL 53689-93 (1994) 154.
[3] R. Bock, A Handbook of Decomposition Methods in Analytical Chemistry, Wiley, New York, 1979, p. 141.
[4] Y. Muramatsu, Y. Ohmomo and D. Christoffers, J. Radional. Nucl. Chem., 83 (1984) 353.
[5] F. Sun and K. Julshamn, Spectrochim. Acta, 42B (1987) 889.
[6] A. Wifladt and W. Lund, Talanta, 36 (1989) 395.
[7] G.B. Jones, G.B. Belling and R.A. Buckley, Analyst, 104 (1979) 469.
[8] M.M. Joerin, Analyst, 100 (1975) 7.
[9] W. Holak, Anal. Chem., 59 (1987) 2218.
[10] Y. Muramatsu, S. Uchida, M. Sumiya and Y. Ohmomo, J. Radioanal. Nucl. Chem. Lett., 94 (1985) 329.
[11] R.M. Lindstrom, G.J. Lutz and B.R. Norman, J. Trace Microprobe Tech., 9 (1991) 21.
[12] B.R. Norman and G.V. Iyengar, Fresenius' J. Anal. Chem., submitted for publication.
[13] R.A. Hasty, Mikrochim. Acta, (1971) 348.
[14] R.A. Hasty, Mikrochim. Acta, (1973) 621.
[15] B.T. Wilkins and S.P. Stewart, Int. J. Appl. Radiat. Isot., 33 (1982) 1385.
[16] S. Grys, J. Chromatogr., 100 (1974) 43.
[17] T. Mitsuhashi and Y. Kaneda, J. Assoc. Off. Anal. Chem., 73 (1990) 790.

ELSEVIER

Analytica Chimica Acta 296 (1994) 249–253

ANALYTICA CHIMICA ACTA

Determination of taurine in biological samples by reversed-phase liquid chromatography with precolumn derivatization with dinitrofluorobenzene

Zilin Chen *, Gang Xu, Karl Specht, Rongjian Yang, Shiwang She

Sino-German Joint Research Institute, Nanchang 330047, China

Received 1 November 1993

Abstract

A rapid and sensitive method for the determination of taurine in human milk and urine by reversed-phase liquid chromatography (LC) has been developed. It involves precolumn derivatization with dinitrofluorobenzene in $NaHCO_3$ buffer (pH 9.0), catalysed by dimethyl sulphoxide, separation by LC on a μBondapak Phenyl column at 40°C with acetonitrile–water (1 : 1) and 0.01 mol l^{-1} phosphate buffer (pH 5.5) as mobile phase and UV absorbance detection at 360 nm. The peak area is proportional to the concentration of taurine in the range 10–80 μg ml^{-1}, the correlation coefficient being 0.9997. The detection limit in standard solutions is 0.1 μg ml^{-1} (signal-to-noise ratio = 3). The relative standard deviations ($n = 6$) of retention time and peak area are 0.45% and 2.29%, respectively. The average recovery for human milk and urine are 95.8% and 101.0%, respectively.

Keywords: Liquid chromatography; Biological samples; Milk; Taurine; Urine

1. Introduction

Taurine (2-aminoethanesulphonic acid) is a free, non-protein, β-amino acid occurring in many biological materials. It has been shown that taurine has wide physiological functions [1] and a close relationship with many diseases [2,3]. In recent years, it has been reported that taurine also has much nutritive value such as in adjusting the metabolism of trace elements, improving the synthesis of DNA, RNA and proteins in the brain and acting as a regulator in human cell proliferation [4,5]. Therefore, some researchers have suggested that taurine should be considered as a conditionally essential nutrient of the human body [6,7]. In the food industry, more attention is being paid to the use of taurine as a food additive.

Taurine is found in biological materials, occurring widely in muscle tissue, milk and urine. Many factors interfere with the assay of taurine. For these reasons, it is important to develop a rapid and sensitive method for determining taurine in biological samples.

The common method of determining taurine is by thin-layer chromatography [8]. Spectrophotometric methods have also been described [9,10].

* Corresponding author.

SSDI 0003-2670(94)00206-2

Okazaki [11] studied the determination of taurine in biological samples by gas chromatography with spectrophotometric detection [11]. Another general method is with the use of an amino acid analyser [12–14]. Many papers have described the use of liquid chromatography (LC) [15–17]. Examples are a rapid assay of taurine in brain by LC with electrochemical detection [18] and a LC determination of taurine in biological fluids by postcolumn fluorescence reaction with thiamine [19].

The derivatization reaction with dinitrofluorobenzene (DNFB) is a common reaction used for amino acid analysis [20,21]. In this work, this reaction, catalysed by dimethyl sulphoxide (DMSO), was used for the rapid assay of taurine in biological samples by LC with UV absorbance detection. Both the accuracy and precision of the assay of human milk and urine are satisfactory.

2. Experimental

2.1. Chemicals

Taurine stock solution of concentration 1.0 mg ml^{-1} was prepared. Taurine (biochemical reagent) and DNFB (chemically pure) were obtained from Shanghai Chemicals and acetonitrile (HPLC grade) from Shanghai Wujin Chemical Factory. All other reagents were of analytical-reagent grade and were used as received. All aqueous solutions were prepared using water purified with a Elgastat UHQ-2 system.

2.2. Apparatus

The analytical LC column was a μBondapak Phenyl column (30 cm × 3.9 mm i.d.) from Waters (Millipore, Milford, MA). The LC system consisted of two pumps (Model 510, Millipore), a universal liquid chromatography injector (Model U6K, Millipore) with a 100-μl loop, a Lambda-Max Model 481 LC spectrophotometer (Millipore) and a Baseline 820 chromatography workstation (data acquisition and processing chromatography software, the hardware involved a System Interface Module, an AST 386SX/20 computer and an NEC P6200 pinwriter). A Philips PU-8740 UV–visible scanning spectrophotometer and a Beckman XL-80 ultracentrifuge were used.

2.3. Liquid chromatographic conditions

The column temperature was 40°C. The mobile phase components were (B) acetonitrile–water (1 : 1, v/v) and (A) 0.01 mol l^{-1} phosphate buffer [accurately adjusted to pH 5.50 (pH meter)]. For binary gradient elution, the programme was from A–B (80 : 20) at 0 min, to A–B (2 : 98) at 30 min. The flow-rate was 1.0 ml min^{-1}. The detector settings were 360 nm and 0.05 absorbance full-scale. The mobile phase solutions were filtered through a 0.45-μm membrane filter and degassed by ultrasonication before use. A 5-μl portion of sample was injected each time.

2.4. Acquisition and preparation of samples

Human milk

Breast milk samples were obtained from healthy, well nourished mothers at the Jiangxi Gynaecology and Obstetrics Hospital. The samples (each about 15 ml) were stored below −40°C.

After the milk samples had been thawed, they were delipidated by centrifugation at 2000 *g* and 20°C for 20 min. A 3.0-ml volume of delipidated milk was mixed with 3.0 ml of 3.0% sulphosalicylic acid (SSA) solution. Samples were allowed to stand for 20 min at 20°C. The samples were deproteinized by centrifugation (20 min, 10 000 *g*, 4°C) and 1.0 ml of the supernatant was removed for the derivatization reaction.

Urine

After obtaining samples, they were diluted (1 : 1) with water and filtered through a Sep-Pak C_{18} cartridge (Waters). Deproteination was carried out in the same way as with the milk samples.

2.5. Precolumn derivatization procedure

A 1.0-ml volume of a prepared sample or of a taurine standard solution used for calibration was transferred into a 10-ml flask. A 2.0-ml volume of

0.01 mol l^{-1} $NaHCO_3$ (pH 9.0), two drops of pure DNFB and 0.5 ml of DMSO were added. After shaking on a vortex mixer for a moment, it was heated for 10 min in a 40°C water-bath, then removed and diluted to 10 ml with phosphate buffer (pH 7.0). A 5.0-μl portion of this solution was injected for LC separation.

3. Results and discussion

3.1. Spectral properties of DNP–taurine derivative

Taurine was converted into its DNP derivative by reaction with DNFB catalysed by DMSO in a weakly-alkaline buffer. UV–visible scanning spectrophotometry indicated that maximum absorption of the DNP–taurine derivative was at 360 nm. The DNP–taurine derivative is stable for several days.

3.2. Optimization of derivatization conditions

Without catalysis, the derivatization reaction takes more than 1 h at 40°C, and is therefore not suitable for the rapid assay of large numbers of samples. With catalysis by DMSO, the reaction is complete in 10 min at 40°C.

Table 1 shows that the optimum amount of DMSO was 0.5 ml. It was shown that DMSO did not affect the LC separation of DNP–taurine.

Heating increases the rate of derivatization. For a 10-min reaction time, the optimum temperature was 40°C.

As shown in Table 2, the optimum pH was 9.0.

As the solubility of DNFB in aqueous solution is not great, shaking is necessary. As shown in Table 3, shaking for 30 s on a vortex mixer was sufficient.

A 0.05-ml volume (about two drops) of DNFB was sufficient to achieve complete derivatization under the above conditions.

Table 1
Effect of amount of DMSO on absorbance

DMSO (ml)	0.0	0.25	0.50	0.75	1.00
Absorbance	0.109	0.228	0.324	0.308	0.227

Table 2
Optimization of pH for derivatization

pH	6.0	7.0	8.0	9.0	10.0
Absorbance	0.114	0.480	0.517	0.546	0.529

3.3. Chromatographic investigation

Experiments were carried out by using a solution of A (water of pH 5.5 adjusted with acetic acid, pH 5.5 phosphate buffer, pH 6.5 NaOAc–HOAc buffer, pH 7.0 phosphate buffer or pH 9.0 $NaHCO_3$ buffer) and B (1:1 methanol–water or acetonitrile–water). The best chromatographic performance was obtained when pH 5.5 phosphate buffer and acetonitrile–water (1:1) were used as mobile phases with gradient elution.

Many gradient programmes were tried. The best chromatographic performance was obtained by the use of a mixture of A (pH 5.5 phosphate buffer) and B [acetonitrile–water (1:1)], initially 80:20 and changing linearly to 2:98 at 30 min.

To remove all DNP-amino acids from the column, a 30-min elution time was required. The best chromatographic performance was achieved when the column temperature was kept at 40°C.

3.4. Calibration

Volumes of 10, 20, 40, 60 and 80 μg ml^{-1} standard taurine solution were used to provide calibration results according to the above procedure. The chromatographic peak response (area) was linearly related to the concentration of taurine in the range 10–80 μg ml^{-1}. The correlation coefficient was 0.9997.

3.5. Precision

Six replicates of 40 μg ml^{-1} taurine gave a relative standard deviation of peak area of 2.3%

Table 3
Effect of shaking time

Time (s)	0	30	60	90
Absorbance	0.266	0.556	0.558	0.559

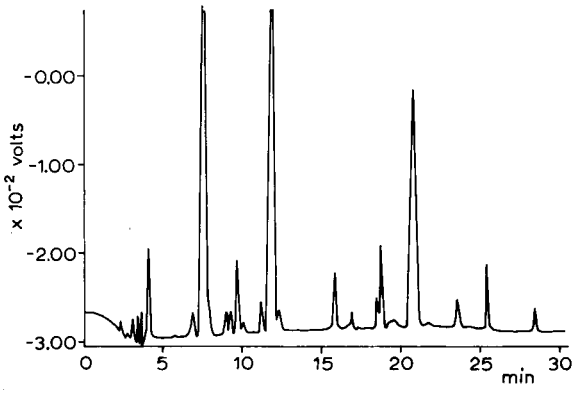

Fig. 1. Chromatogram of human milk sample.

and of retention time of 0.45%. The mean retention time was 9.735 min.

3.6. Standard addition

Different concentrations (20–40 μg ml^{-1} in the final sample) of standard taurine were added to human milk and urine samples to determine recovery. The average recoveries for human milk and urine were 95.8% and 101.0% ($n = 4$), respectively.

3.7. Detection limit

The detection limit for a standard taurine solution was < 0.10 μg ml^{-1} (signal-to-noise ratio = 3).

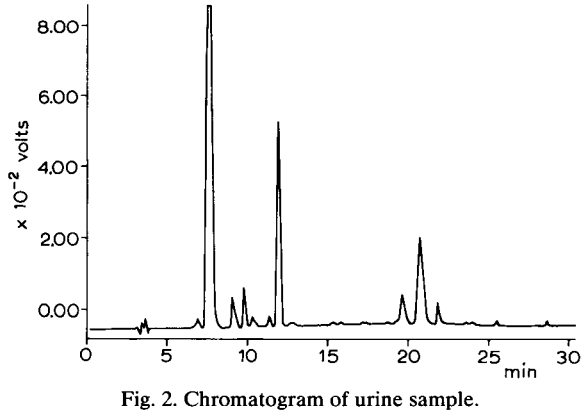

Fig. 2. Chromatogram of urine sample.

3.8. Application to the determination of taurine in human milk and urine

The chromatograms for human milk and urine are shown in Figs. 1 and 2, respectively. The results for the taurine content of 20 mothers' colostral milk in Nanchang City were 41.60 ± 17.13 μg ml^{-1} (mean ± S.D.) and those for 6 mens' urine samples from the same city were 97.48 ± 8.89 μg ml^{-1}.

4. Conclusions

A rapid and sensitive procedure was developed for determining taurine in biological samples. The procedure uses DNFB as the derivatization reagent with catalysis by DMSO and effects separation by reversed-phase LC with UV detection at 360 nm where the baseline does not easily drift. The analytical time is shorter than in previous work [20,21]. This method is suitable for the rapid assay of large numbers of samples. By optimization of the derivative reaction conditions and chromatographic conditions, the method has been demonstrated to be precise and capable of accurately determining taurine concentrations in milk and urine over a wide linear range (10–80 μg/ml). The detection limit is lower than 0.1 μg ml^{-1} (signal-to-noise ratio = 3). The relative standard deviation ($n = 6$) of retention time and peak area are 0.45% and 2.29%, respectively. The average recoveries in human milk and urine are 95.8% and 101.2%, respectively.

References

[1] E. Gerald and M.D. Gall, Pediatrics, 83 (1989) 433.
[2] L.R. Jiang, Amino Acids, 20 (1983) 34.
[3] H.L. Zhang, Amino Acids, 56 (1992) 31.
[4] X.B. Han, Acta Nutr. Sin., 11 (1989) 319.
[5] X.H. Zhao, Shengli Kexue Jinzhan (Prog. Physiol. Sci.) 18 (1987) 34.
[6] W.B. Rowe, et al., J. Am. Coll. Nutr., 5 (1986) 2.
[7] J.X. Chipponi, Am. J. Clin. Nutr., 35 (1982) 1112.
[8] Hangzhou University, Handbook of Analytical Chemistry, Vol. 2, Chemical Industry Publication, 1982, p. 839.
[9] D.N. Lau and S.F. Luk, Analyst, 115 (1990) 653.
[10] J. Charles and J. Parker, Anal. Biochem., 108 (1980) 305.
[11] T. Okazaki, Bunseki Kagaku, 38 (1989) 401.

[12] C.De. Maro, Anal. Biochem., 48 (1972) 346.
[13] J. Rosmns et al., J. Chromatogr., 70 (1972) 241.
[14] C.L. Long, Anal. Biochem., 29 (1969) 265.
[15] P.C. Hopkins, Neurochem. Int., 15 (1989) 429.
[16] G.M. Anderson, J. Chromatogr., 431 (1988) 400.
[17] E.C. Nicolas, J. Assoc. Off. Anal. Chem., 73 (1990) 627.
[18] S. Marai, J. Pharmacol. Methods, 23 (1990) 195.
[19] Yokoyama, J. Chromatogr., 568 (1991) 212.
[20] X.L. Liu, Chin. J. Pharmacol. Anal., 5 (1985) 282.
[21] Y.L. Chen, Chin. J. Pharmacol. Anal., 10 (1990) 149.

ELSEVIER

Analytica Chimica Acta 296 (1994) 255–261

ANALYTICA CHIMICA ACTA

Fluorescence studies on the reduction of quinone by cyanide in aqueous 2-hydroxypropyl-β-cyclodextrin solutions

C.A. Groom, J.H.T. Luong *

Biotechnology Research Institute, National Research Council Canada, Montreal, Québec H4P 2R2, Canada

Received 18 January 1994; revised manuscript received 11 May 1994

Abstract

Water-soluble 2-hydroxypropyl-β-cyclodextrin was used to enclose 1,4-dibenzoquinone, 1,4-naphthoquinone, and 9,10-anthraquinone to form inclusion complexes. The inclusion complex of 1,4-dibenzoquinone was the most reactive of the three complexes in the presence of cyanide anion. The 1,4-dibenzoquinone inclusion complex reacted with cyanide anion to form a fluorescent product with stable excitation and emission maxima at 410 and 480 nm, respectively. Assuming one to one stoichiometry the formation constant for 2-hydroxypropyl-β-cyclodextrin and 1,4-dibenzoquinone was estimated to be 4 M^{-1}. Formation of the inclusion complex did not enhance fluorescence yield but increased the rate of product formation in aqueous solutions. In the presence of excess cyanide the limit of detection for 1,4-dibenzoquinone was 0.006 mM with a linear range of 0.01 to 0.04 mM. For cyanide detection the linear range of the assay was 2 to 10 mM with a detection limit of 0.041 mM. Rate assays for cyanide possessed linear ranges from 0.041 to 12 mM. The reaction was used to detect cyanide in beverages, acetaminophen preparations and brass plating solutions.

Keywords: Fluorimetry; 2-Hydroxypropyl-β-cyclodextrin; 1,4-Dibenzoquinone; Inclusion complex; Cyanide

1. Introduction

Cyclodextrins are a class of toroidally shaped cycloamyloses with hydrophilic edges and an electron rich hydrophobic cavity. The most common cyclodextrins are α, β, and γ-cyclodextrins with 6, 7, or 8 glucopyranose units, respectively linked by α-1–4 bonds to form a rigid structure capable of forming inclusion complexes with various hydrophobic compounds. This property has led to a plethora of practical applications related to the solvation of hydrophobic chemicals and pharmaceutical products in aqueous media. Reviews for this class of compounds are produced by Szejtli [1], Clarke et al. [2], Thoma and Stewart [3], and Saenger [4].

For certain cases the changes in fluorescence property including quantum yield, fluorescent spectrum and decay time often associated with the solution of compounds in organic solvents are also observed in structured media such as the cyclodextrins [5]. For instance, 1-anilinonaphthalene-8-sulfonate which is strongly fluorescent in organic solvents, but shows only negligible fluorescence in water, becomes significantly fluorescent in aqueous cyclodextrin solutions [6]. Fluorescent enhancement is also dependent on the cavity size of cyclodextrins as α-cyclodextrin increases the fluorescence of the aqueous solution about 2-fold, whereas β-cyclodextrin has a nearly 10-fold effect. In addition, inclusion of the analyte molecule inside the cyclodex-

* Corresponding author.

SSDI 0003-2670(94)00241-D

trin cavity is also known to afford protection from quenchers.

The acute toxicity of cyanide in foodstuffs is well documented [7] and various amperometric [8], colorimetric, argentometric, polarographic and potentiometric methods are employed for its detection [9]. Still the best analytical procedure for the fluorometric assay of cyanide is that described by Guilbault and Kramer [10]. Addition of as little as 0.2 μg of CN^- to *p*-benzoquinone results in an intense green fluorescence (λ_{ex} 440, λ_{em} 500 nm) and the reaction is normally done in organic media to generate fluorescent cyanohydroquinone products. The reaction was reported to be rapid, sensitive and highly specific as sulfide, thiosulfate, thiocyanate, ferrocyanide, and 26 other anions tested exhibited no interference.

In this study, 2-hydroxypropyl-β-cyclodextrin (hp-β-cyclodextrin) was used to solubilize 1,4-benzoquinone to form a water-soluble inclusion complex. The reduction of 1,4-benzoquinone by cyanide anion in aqueous cyclodextrin solutions was then performed to investigate a feasible development of in situ fluorometric assays for the determination of cyanide.

2. Experimental

2.1. Apparatus and reagents

1,4-Dibenzoquinone, 1,4-naphthoquinone and 9,10-anthraquinone, 2-hydroxypropyl-β-cyclodextrin (hp-β-cyclodextrin) were purchased from Aldrich (Milwaukee, WI). All other chemicals were obtained from Anachemia (Montreal). Plating solutions were obtained from a local plating company (L and G Plating Ltd, Montreal, PQ) and beverage samples were obtained from local markets.

2.2. Quinone solutions

2-Hydroxypropyl-β-cyclodextrin solutions were prepared by adding powdered cyclodextrin to distilled water and agitating to produce a 50% by weight stock solution. The stock was then diluted to desired concentrations with distilled water. Solutions of 1,4-dibenzoquinone (Q), 1,4-naphthoquinone (NQ), and 9,10-anthraquinone (AQ) were prepared by adding an excess of solid compound to an aqueous solution of defined hp-β-cyclodextrin content and stirring overnight. Remaining solid material was removed by centrifugation at 12.1×10^3 g for 10 min (Beckman J2-21M centrifuge, JA 20 rotor) with subsequent filtration of supernatant through 0.2 μm Acrodisc (Gelman Sciences, Ann Arbor, MI) polysulfone filters. Dissolved quinone concentrations were estimated using absorbances obtained with a Beckman DU 640 spectrophotometer. The absorbency coefficients for Q (435 nm), NQ (341.5 nm), and AQ (327 nm) are 18.18 M^{-1} cm^{-1}, 2750 M^{-1} cm^{-1}, and 4600 M^{-1} cm^{-1}, respectively [11]. The three quinone compounds were also dissolved in water and ethanol using the above procedure. Solutions were subsequently stored in the absence and presence of light at 4 and 25°C.

2.3. Fluorometry

Fluorescence measurements were conducted using in a Gilford Fluoro IV spectrofluorometer equipped with a 150 W high-pressure xenon light source and an R446 photomultiplier (range 200–800 nm) detector. The excitation and emission concave holographic diffraction gratings (1200 line/mm) were blazed at 250 nm and 450 nm, respectively. The determination of cyanide using fluorescence was completed as follows. Standard curves were prepared by mixing required volumes of aqueous 100 mM KCN solution with 250 mM hp-β-cyclodextrin containing 0.3 mM quinone and monitoring the resultant fluorescence (λ_{ex} 410 nm, λ_{em} 480 nm). A similar method was used for the detection of cyanide in samples. Samples were contained in 3 ml, 1×1 cm, quartz cuvettes.

2.4. Amperometry

The formation constant for the complexation of quinone and hp-β-cyclodextrin was estimated amperometrically using a CV-1B voltammograph with cell stand and *X–Y* recorder (Bioanalytical Systems, West Lafayette, IN). Using known total quinone and cyclodextrin concentrations, the concentration of non-complexed quinone was determined by its reduction at the surface of a glassy carbon amperometric electrode. The working electrode operating potential was set at -0.4 V with respect to an Ag/AgCl reference electrode and a platinum counter electrode was employed. A standard

curve relating nA to quinone concentration was constructed prior to measurements with cyclodextrin. Reduction of the quinone–hp-β-cyclodextrin complex was prevented by covering the working electrode with a 1000 MWCO Spectro/Por cellulose dialysis membrane (Spectrum, Houston, TX). The predetermined total quinone and cyclodextrin concentrations were established by the addition of stock solutions and the free quinone concentration was then determined using a standard curve of quinone versus current. The total quinone concentration ranged from 0.01 to 1.2 mM while the total hp-β-cyclodextrin concentration was varied from 0.5 to 25 mM. The difference between the free quinone concentration and the total quinone concentration was taken to be the complexed quinone concentration. Assuming a 1 to 1 stoichiometry of complexation, the concentration of complexed hp-β-cyclodextrin was therefore determined. The concentration of free hp-β-cyclodextrin was established by subtraction of the complex concentration from the total hp-β-cyclodextrin concentration. The above information was then used to calculate the formation constant $K = [QCD]/[Q][CD]$.

2.5. Cyanide detection

The detection of cyanide was performed by fluorometry and using a pyridine barbituric acid colorimetric reference method [9]. In some cases samples were pretreated by acid distillation as outlined by Franson [9]. Brass rinse solutions were determined directly for cyanide content by adding concentrated hp-β-cyclodextrin with quinone to samples. For the determination of cyanide in beverage samples, known volumes of 1 M KCN (aq.) were added to 25 ml volumes of beverage. The samples were then diluted 500-fold for detection using fluorometry and for the pyridine barbiturate reference method. Samples of acetaminophen containing cyanide were prepared by adding 1 M KCN to 25 ml solutions of acetaminophen in ethanol.

3. Results and discussion

3.1. Characterization of quinone–cyclodextrin inclusion complexes

The respective solubilities of quinone, naphthoquinone and anthraquinone with respect to cyclodextrin

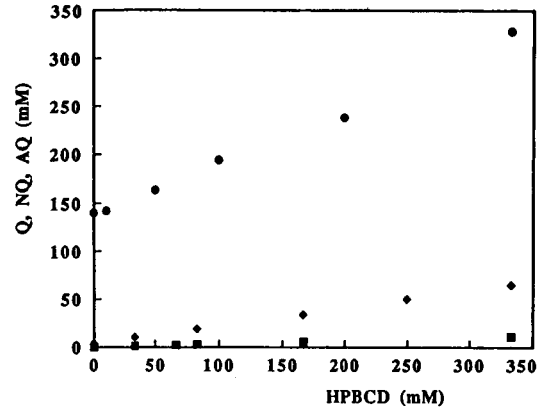

Fig. 1. Solubility of (●) 1,4-dibenzoquinone (Q), (♦) 1,4-naphthoquinone (NQ) and (■) 9,10-anthraquinone (AQ) in aqueous solutions of 2-hydroxypropyl-β-cyclodextrin of varied concentration.

are shown in Fig. 1. While the mechanism of inclusion, a combination of chemical and steric factors, remains to be investigated, it is obvious that molecular proportion and hydrophobic interaction play an important role in the inclusion process. The hp-β-cyclodextrin cavity has a diameter of 0.64 nm and a depth of 0.8 nm, and can therefore easily accommodate 1,4-benzoquinone on a 1 to 1 basis but is unable to completely include naphthoquinone or anthraquinone. The polarity of the cyclodextrin cavity is heterogenous, varying along the axis of the cavity with proximity to the respective C(3)–H hydrogens, glycosidic oxygens and C(5)–H hydrogens. The overall polarity of the cavity was reported to be comparable to that of *p*-dioxane [12] and the solubilities of naphthoquinone and anthraquinone in the two solvents reflect this phenomenon. The dynamic behaviour of the inclusion phenomenon must also be considered, particularly in the case of 1,4-benzoquinone as it is soluble in water to an extent of 140 mM. Changes in the optical property of the included compound are often used to measure the extent of complexation using the Benesi-Hildebrande equation and its derivatives [1]. The method is based on the assumption that almost all of the optically active compound is occluded by a large excess of cyclodextrin. As the relatively low absorbency coefficient of quinone ($E_{435} = 18.18\ M^{-1}$) and its high solubility in water relative to hp-β-cyclodextrin precluded the use of this method, an amperometric procedure was used to calculate an estimate of the formation constant for 1,4-dibenzoquinone and hp-β-cyclodextrin. The value is

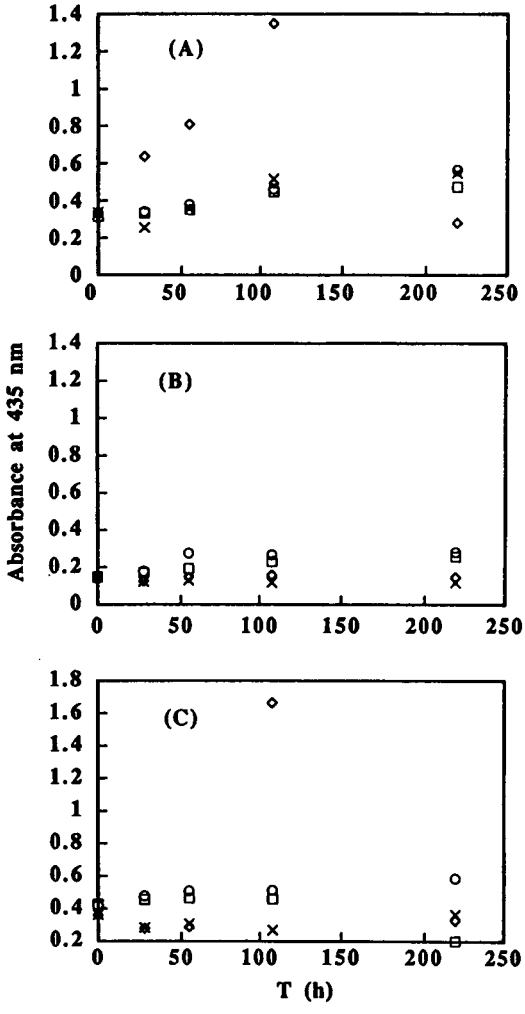

Fig. 2. Stability of 1,4-dibenzoquinone in solutions of (A) 2-hydroxypropyl-β-cyclodextrin (B) deionized water and (C) ethanol: (○) 25°C, stored under light, (□) 25°C stored in dark, (◇) 4°C, stored under light, (×) 4°C, stored in dark.

presented with caution as hp-β-cyclodextrin can physically affect the transport of free quinone across the dialysis membrane without complexation. For this reason the hp-β-cyclodextrin concentration was maintained at or below 25 mM. The resulting formation constant $K = [QCD]/[Q][CD]$ was calculated to be 4 M^{-1}, a value in reasonable agreement with the findings of Kuroda et al. [13], who measured the quenching effect of benzoquinone on the fluorescence of cyclodextrin-sandwiched porphyrin complexes. An equilibrium constant for benzoquinone in α-cyclodextrin of 6.8 M^{-1} was reported by Yan-Ching and Ache [14], who credited the relatively low amount of complexation to the small size of benzoquinone in relation to the cyclodextrin cavity. 1,4-benzoquinone was reported to form aggregates in aqueous solution [15] and this property is evident in viewing the stability of this compound in hp-β-cyclodextrin under various conditions (Fig. 2). A tendency to rapidly polymerize and precipitate in the presence of light at 4°C is evident. When containers were covered with foil and stored at room temperature, the quinone cyclodextrin reagent had a shelf life of 1 week.

3.2. Characteristics of quinone–cyanide reactions

When the quinone cyanide reaction was carried out in hp-β-cyclodextrin, the reaction products fluoresced with stable excitation and emission maxima at 410 nm and 480 nm, respectively (figure not shown). The fluorescent wavelength maxima were thus equivalent to values reported by Guilbault and Kramer [10] for products of the reaction in DMSO. The lack of a shift to shorter wavelength maxima would indicate that the excited state of the reaction product can undergo relaxation despite the stearic limitations and relative rigidity of the of hp-β-cyclodextrin cavity. A comparison of the excitation and emission spectra for hp-β-cyclodextrin and DMSO did not reveal an increase in spectral bandwidth, indicating an insignificant heteromicroenvironmental effect. The solution cyclodextrin concentration did not significantly increase the fluorescence yield of reaction product, or of preparations of com-

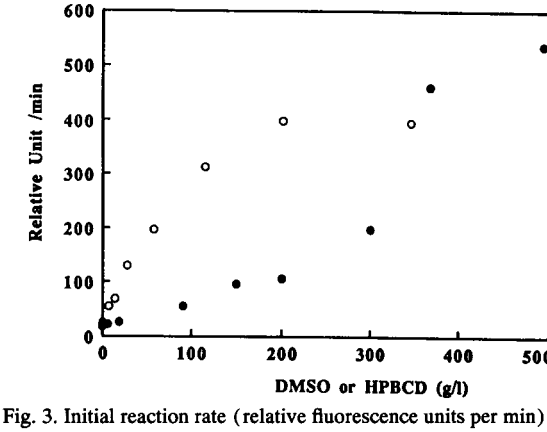

Fig. 3. Initial reaction rate (relative fluorescence units per min) for 0.3 mM 1,4-dibenzoquinone and 1.2 mM potassium cyanide in varying concentrations (g/l) of (●) dimethylsulfoxide (DMSO) and (○) 2-hydroxypropyl-β-cyclodextrin.

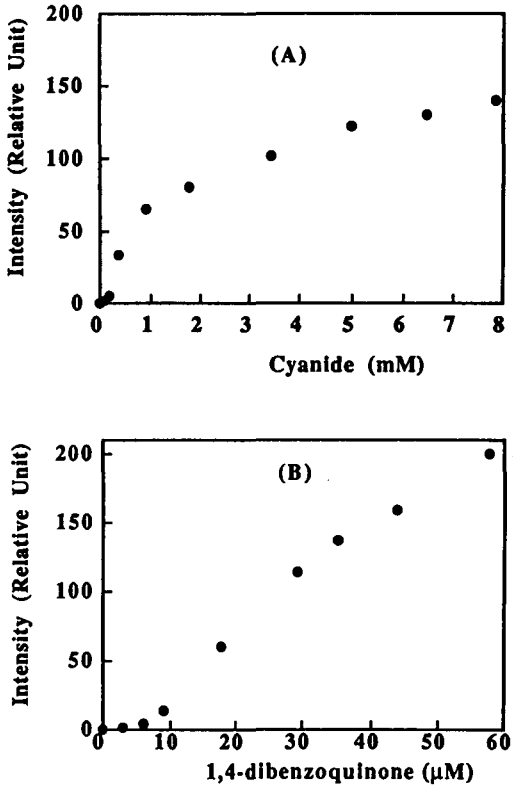

Fig. 4. (A) Fluorescence intensity as a function of cyanide concentration for a 0.3 mM solution of 1,4-dibenzoquinone in 200 mM in aqueous 2-hydroxypropyl-β-cyclodextrin. (B) Fluorescence intensity as a function of 1,4-dibenzoquinone in 200 mM aqueous 2-hydroxypropyl-β-cyclodextrin (cyanide concentration = 50 mM).

mercially available 2,3-dicyanohydroquinone, but exhibited a positive effect on initial reaction rate (Fig. 3). The increase in rate was presumably a result of the occlusion of water from the reaction complex by hp-β-cyclodextrin. The concentrations of hp-β-cyclodextrin and DMSO are expressed as g/l to compensate for the large difference in molecular weight of the two compounds. At concentrations below 150 g/l the inclusion effect of cyclodextrin provides for microenvironment with lower water content that cannot be achieved using DMSO. Above 300 g/l the performance of the two solvents are comparable, but the water content of the DMSO solvents become less than 60% by weight.

Standard curves illustrating the linear ranges and detection limits with respect to cyanide and benzoquinone are shown as Fig. 4 (A and B). The optimal benzoquinone concentration for the determination of cyanide in 250 mM hp-β-cyclodextrin was found to be 0.3 mM, but the result may be a function of fluorometer geometry as inner filter effects are evident at higher quinone concentrations. Using the above conditions a sampling time of 20 min was required to reach maximum fluorescence. The rate of reaction as a function of cyanide concentration was linear between 0 and 12 mM and rate dependent assays for cyanide were conducted with a sampling time of 4 min. The absolute detection limit for cyanide was 41 μM, which was about threefold less sensitive to the value determined for preparations using DMSO as solvent (14 μM). The lowest detectable benzoquinone concentrations were 6 μM and 3 μM, respectively for hp-β-cyclodextrin and DMSO. The use of hp-β-cyclodextrin at concentrations greater than 250 mM resulted in viscous preparations that were difficult to handle and which decreased precision because of dispersion of light in the cuvettes.

The product fluorescence was affected by pH, being inhibited below 6 and exhibiting a sharp peak around 7 (Fig. 5). This phenomenon makes the control of sample pH a significant parameter in the determination of cyanide for real samples. According to Brown and Porter [16] the anionic primary reaction product (2,3-dicyanohydroquinone) is protonated at pH below 5.9 to produce a compound that displays excitation and emission maxima at 350 and 450 nm, respectively. At pH below 6 the products of the reaction in hp-β-cyclodextrin displayed excitation and emission maxima at the above stated wavelengths. For quinones in general the oxidizing environment encountered at low pH reduces fluorescence by coordinate linkage to electrons in the lowest available occupied non bonding oxygen

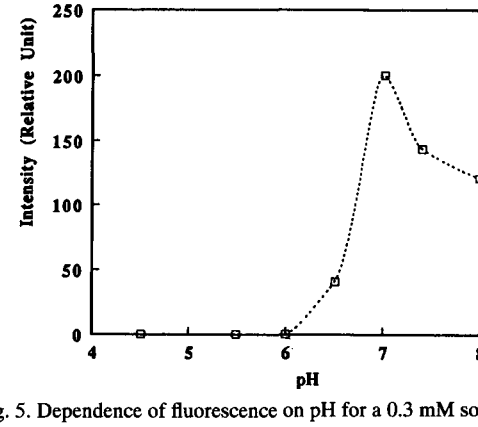

Fig. 5. Dependence of fluorescence on pH for a 0.3 mM solution of 1,4-dibenzoquinone in 200 mM in aqueous 2-hydroxypropyl-β-cyclodextrin (cyanide concentration = 10 mM).

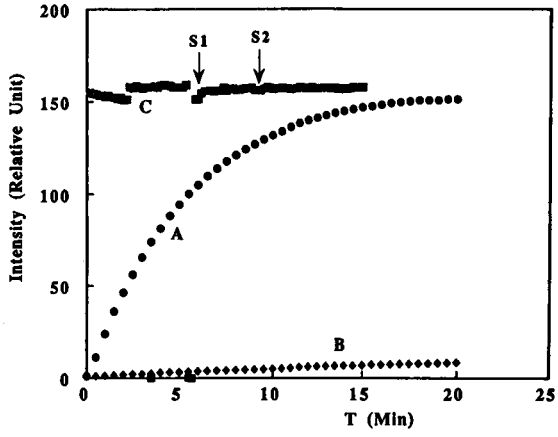

Fig. 6. Effect of sodium sulphite addition on time course for the reaction of 0.3 mM solution of 1,4-dibenzoquinone in 200 mM in aqueous 2-hydroxypropyl-β-cyclodextrin (cyanide concentration = 1.2 mM). (A) No additions. (B) Addition of Na_2SO_3 (final concentration = 11 mM prior to the initiation of the reaction with cyanide. (C) Additions of Na_2SO_3 (S1 final concentration = 100 mM, S2 final concentration = 200 mM) following reaction.

orbitals [17]. While the presence of anions at less than 3 mM appeared not to significantly inhibit the reaction, higher ionic strengths strongly inhibited the rate of fluorophore formation. This phenomenon was best illustrated by the effect of adding sodium sulfite for the scavenging of oxygen before reaction and following completion of reaction (Fig. 6). The presence of sulfite (11 mM) before reaction completion severely inhibits product formation, while the addition of sulfite following reaction has no effect on sample fluorescence. Among various buffers used at a concentration of 100 mM to maintain the system at pH 8, glycine, phosphate and acetate were most applicable and provided up to 95% fluorescence intensity in comparison to distilled water. Imidazole and borate were slightly less effective (88% fluorescence intensity) while tris only provided 80% fluorescence intensity (data not shown).

3.3. Determination of cyanide in samples

The results of cyanide determinations for real samples are listed as Table 1 (value = mean $\pm$ 95% confidence interval, student t distribution, $n = 3$). To avoid reaction inhibition the samples in question (juice, wine, beer, brass plating solutions) were diluted 500-fold before reliable determinations of cyanide were obtained. For plating solutions it was apparent that the high ionic strength of the samples inhibited fluorophore formation. For juice samples, the addition of undiluted sample (0.03 ml added to a 30 ml reaction volume) to fluorescent dicyanohydroquinone solutions resulted in quenching. Acetaminophen preparations did not interfere with product formation and therefore sample dilution was not necessary. A cyanide detection limit of 10 ppb was reported by Zhang and Zhang [18], for a dequenching method in which the complexation of cuprous ion with cyanide releases cuprous ion from the fluorophore calcein. The reaction is vulnerable, however, to interferences produced by other metal ions capable of forming complex cyanides. A fluorometric stop time flow injection method [19] using pyridoxal and pyridoxal phosphate achieved a detection limit of 3 μM, but required lengthy sampling times. A chemiluminescent flow injection method [20] produced

Table 1
Comparison of samples measured using fluorometric and pyridine–barbituric acid reference methods

	Fluorometric (mM)	Reference (mM)	%Difference
Apple juice[a]	29.5 $\pm$ 1.00	33 $\pm$ 1.65	10.6
Orange juice[a]	32.5 $\pm$ 1.15	35.5 $\pm$ 1.8	8.45
Beer[a]	31.5 $\pm$ 1.05	34.5 $\pm$ 1.75	8.69
Acetaminophen[b]	0.098 $\pm$ 0.086	0.108 $\pm$ 0.186	3.7
Brass plate solution[c]	29.59 $\pm$ 0.592	30.63 $\pm$ 1.41	1.4
Brass rinse solution[d]	0.056 $\pm$ 0.0053	0.096 $\pm$ 0.0039	41.6

The numbers (n) of each sample are equal to three.
[a]KCN added to samples to an approximate final concentration of 32.5 mM. Samples were diluted 500-fold.
[b]KCN added to final concentration of 0.1 mM to 1 mM acetaminophen solutions. Samples were assayed undiluted.
[c]Final concentrations shown. Samples diluted 500-fold.
[d]Undiluted samples.

detection limits of the order of 50 μM, but was claimed to require only picogram quantities of cyanide. Cyanide was determined fluorimetrically using taurine and 2,3-naphthalenedialdehyde to a detection limit of 20 μM [21]. In view of this, the assay under current study does not possess a limit of detection lower than other fluorometric cyanide detection methods. However, this method is simple to perform, requires no flow injection equipment, makes use of relatively stable reagents, and can be coupled with biologically active materials such as enzyme, protein, and antigen/antibody.

References

[1] J. Szejtli, Cyclodextrins and Their Inclusion Complexes, Akadémiai Kiadó, Budapest, 1982.

[2] R.J. Clarke, J.H. Coates and S.F. Lincoln, Adv. Carbohydr. Chem. Biochem., 46 (1988) 205.

[3] J.A. Thoma and L. Stewart, in R.L. Whistler, E.F. Paschall, J.N. Bemiller and H.J. Roberts (Eds.), Starch: Chemistry and Technology, Vol. 1, Academic Press, New York, 1965, p. 209.

[4] W. Saenger, in J.L. Atwood J.E.D. Davies and D.D. MacNicol (Eds.), Inclusion Compounds 2: Structural Aspects of Inclusion Compounds Formed by Organic Host Lattices, Academic Press, London, 1984, p. 231.

[5] E.L. Wehry, in G.G. Guilbault (Ed.), Practical Fluorescence, Marcel Dekker, New York, 1990, p. 127.

[6] F. Cramer, W. Saenger and H.C. Spatz, J. Am. Chem. Soc., 89 (1967) 14.

[7] W.R. Jenks, in M. Grayson (Ed.), Encyclopedia of Chemical Technology, Vol. 7, Wiley, New York, 1978, p. 314.

[8] C.A. Groom and J.H.T. Luong, J. Biotechnol., 21 (1991) 161.

[9] M.A. Franson (Ed.), Standard Methods for the Examination of Water and Wastewater, American Public Health Association, American Water Works Association, Water Pollution Control Federation, Washington, DC, 15th edn., 1980, p. 312.

[10] G.G. Guilbault and D.N. Kramer, Anal. Chem., 37 (1965) 1395.

[11] A.I. Scott, Interpretation of the Ultraviolet Spectra of Natural Products, Pergamon, London, 1964.

[12] R.A. Femia, S. Scypinski and L.J. Cline Love, Environ. Sci. Technol., 19 (1985) 155.

[13] Y. Kuroda, M. Ito, T. Sera and H. Ogoshi, J. Am. Chem. Soc., 115 (1993) 7003.

[14] J. Yan-Ching and H.J. Ache, J. Phys. Chem., 81 (1977) 2093.

[15] S. Wada, H. Ichikawa and K. Tatsumi, Biotechnol. Bioeng., 42 (1993) 854.

[16] R.G. Brown and G. Porter, J. Chem. Soc., Faraday Trans., 173 (1977) 1281.

[17] J.R. Poulsen and J.W. Birks, Anal. Chem., 61 (1989) 2267.

[18] Z. Zhang and Y. Zhang, Fenxi Huaxue, 14 (1986) 415 (in Chinese).

[19] P. Linares, M.D. Luque de Castro and M. Valcarcel, Anal. Chim. Acta, 161 (1984) 257.

[20] M. Ishii, M. Yamada and S. Suzuki, Anal. Lett., 19 (1986) 1591.

[21] A. Sano, M. Takezawa and S. Takitani, Talanta, 34 (1985) 743.

ELSEVIER

Analytica Chimica Acta 296 (1994) 263–269

ANALYTICA CHIMICA ACTA

Application of enzyme field-effect transistor sensor arrays as detectors in a flow-injection system for simultaneous monitoring of medium components. Part I. Preparation and calibration.

T. Kullick [a], M. Beyer [a], J. Henning [a], T. Lerch [a], R. Quack [a], A. Zeitz [a], B. Hitzmann [a], T. Scheper [b], K. Schügerl [a,*]

[a] *Institute for Technical Chemistry, University of Hannover, Callinstr. 3, D-30167 Hannover, Germany*
[b] *Institute for Biochemistry, Westfälische Wilhelms-University Münster, Wilhelm-Klemm-Str. 2, D-48149 Münster, Germany*

Received 2 March 1994; revised manuscript received 9 May 1994

Abstract

Enzymes were (co)immobilized on the pH-sensitive gates of an eight-channel field-effect transistor (FET). Glucose was analysed with a glucose dehydrogenase (GDH) FET, maltose with a coimmobilized maltase (MAL)/GDH FET, sucrose with a coimmobilized invertase (INV)/GDH FET, lactose with a β-galactosidase (β-GAL)/galactose dehydrogenase (GALDH)-fusion protein FET and ethanol with a coimmobilized alcohol dehydrogenase (ADH)/aldehyde dehydrogenase (ALDH) FET. These EnFETs were integrated in FIA systems, calibrated and characterized with respect to buffer capacity, pH value, stirrer speed and NAD concentration and cross sensitivity. On account of the pH and buffer capacity sensitivity of the signals of the EnFETs, the pH value was monitored with a pH-FET of the array and the buffer capacity and substrate concentration were calculated from the shape of the signal of the FIA system. The EnFETs were stored at 4°C for many months without activity loss. They have satisfactory activity for performing a large number of analyses.

Keywords: Sensors; Flow injection; Enzymatic methods; Field effect transistors; EnFET

1. Introduction

Since Bergveld [1] reported on the first ion-selective (IS) field-effect transistor (FET) sensor, a large number of papers have been published on ISFET sensors (e.g., [2–6]). By immobilizing enzymes on the pH-sensitive gate of a FET, enzyme-FET (EnFET) sensors were elaborated (e.g., [7–10]).

In our laboratory several EnFETs were developed, integrated in flow-injection analysis (FIA) systems and applied for process monitoring [11–13]. However, the application of a single EnFET as detector in a FIA system is not efficient enough. On account of the high price of the commercial FIA systems, the analysis expenses per analyte component are too high. Therefore, the economy of the FIA systems can be improved

* Corresponding author.

SSDI 0003-2670(94)00224-A

by using sensor-arrays as detectors, which are able to monitor several medium components simultaneously.

The aim of the present investigations was to develop enzyme sensor arrays based on pH-sensitive FETs, integrate them in FIA equipment and use a single multi-enzyme-FET–FIA system for the monitoring of the concentration of several medium components simultaneously.

In this first part the preparation and characterisation of the EnFET sensors are presented.

2. Experimental

2.1. Preparation of the EnFETs

Field Effect Transistor

An n-$Si/SiO_2/Si_3N_4$ field effect transistor (FET) with 55.3 mV/pH-decade steepness in the pH range 1 to 13 (ABC, Puchheim) was applied with an Ag/AgCl reference electrode. The surface area of the gate was 0.25 mm^2. It was operated in constant-charge circuit at a drain-source voltage $U_{DS} = 2$ V and a drain current $I_D = 100$ μA.

Enzymes applied

Glucose dehydrogenase (GDH) (*Bacillus megaterium*, Merck) 4 U/mg lyophilisate, MW = 118 000, $K_M = 4.5$ mM, pH_{opt} 8–9, was used for the analysis of glucose:

$$\beta\text{-D-glucose} + NAD^+ \xrightarrow{GDH} \text{gluconolacton/}$$
$$\text{gluconic acid} + NADH + H^+$$

Invertase (INV) (*Saccharomyces cerevisiae*, Sigma), MW = 100 000, $K_M = 44$ mM, pH_{opt} 3.5–5.5 was used for the conversion of sucrose to fructose and β-D-glucose:

$$\text{sucrose} \xrightarrow{INV} \alpha\text{-D-glucose} + \beta\text{-D-fructose}$$

Maltase (α-glucosidase) (MAL) (*Saccharomyces cerevisiae*, Sigma), MG: 280 000, $K_M = 5.5$ mM, pH_{opt} 4–6 was used to convert maltose to glucose:

$$\text{maltose} \xrightarrow{MAL} \alpha\text{-D-glucose} + \beta\text{-D-glucose}$$

β-Galactosidase (β-GAL) galactosedehydrogenase (GALDH) fusion protein (*Escherichia coli* F11 rec A), MW = 530 000, pH_{opt} 7–8.5: β-GAL was used to convert lactose to galactose and glucose:

$$\text{lactose} \xrightarrow{\beta\text{-GAL}} \beta\text{-D-galactose} + \beta\text{-D-glucose}$$

and GALDH to convert galactose to galactonic acid:

$$\text{galactose} + NAD^+ \xrightarrow{GALDH} \text{galactonic acid}$$
$$+ NADH + H^+$$

Alcoholdehydrogenase (ADH) (*Saccharomyces cerevisiae*, Fluka), MW = 148 000, $K_M = 13$ mM, pH_{opt} 7–8 was used to convert ethanol to acetaldehyde:

$$\text{ethanol} + NAD^+ \xrightleftharpoons{ADH} \text{acetaldehyde}$$
$$+ NADH + H^+$$

Aldehydehydrogenase (ALDH) (*Saccharomyces cerevisiae*, Sigma), MW = 85 000, $K_M = 9.0.10^{-3}$ mM, pH_{opt} 8–9 was used to convert aldehyde to acetate:

$$CH_3CHO + NAD^+ \xrightarrow{ALDH} \text{acetate} + NADH + H^+$$

On account of the reversible reaction between ethanol and acetaldehyde, the conversion of acetaldehyde to acetate is necessary for the quantitative analysis of ethanol. In all of these analyses enzymatic test kits based on NADH determination are used for control measurements.

Enzyme immobilization

Eight-channel FET arrays were applied for the investigations. The gates were covered by different enzymes. Therefore it was important that a method is used, which is suitable for the simultaneous immobilization of the diverse enzymes on the different gates. This was realized by glutaraldehyde enzyme immobilization in the vapour phase by using a closed cell (Fig. 1). The lyophilized enzymes were dissolved in a phosphate buffer (10 mM phosphate, 100 mM KCl, pH 8) and 0.2 μl enzyme solutions were put on

each of the gate surfaces with a micropipette under a microscope in a clean air chamber. The FET array was put in the cell, in which filter paper was immersed into the 25% aqueous glutaraldehyde solution and the enzyme was cross-linked in the glutaraldehyde vapour at 6°C for 15 h [14].

Characterization of the EnFETs

The EnFET and the reference electrode were immersed into the calibration solution which was homogenized with a magnetic stirrer. The concentration of the particular analytes was increased stepwise and the EnFET signal voltage U_i^{FET} after the ith analyte addition and the corresponding pH signal voltage U_i^{pH} were registered. The sensor signal S was defined as:

$$S = \left[\left(U_i^{FET} - U_o^{FET}\right) - \left(U_i^{pH} - U_o^{pH}\right)\right]$$

where U_o^{FET} and U_o^{pH} are the FET and pH signal voltages at a analyte concentration $C_a = 0$.

In the following the EnFET for maltose is described in detail. The same procedure was carried out with all of the five EnFETs.

For the analysis of maltose maltase (MAL) and glucose dehydrogenase (GDH) were coimmobilized. The maximum signal was obtained at a GDH to MAL ratio of 1:3 (Fig. 2).

The buffer capacity and the pH value of the analyte solution have distinct effects on the sensor signal. The higher the buffer capacity the lower the signal. On account of the limited acidity of gluconic acid ($pK_a = 4.7$) and the pH optimum of GDH of 8–9, the signal becomes larger with increasing pH value.

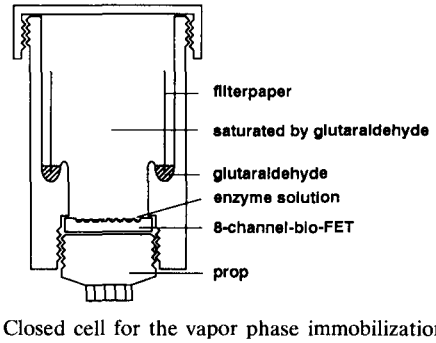

Fig. 1. Closed cell for the vapor phase immobilization of the enzymes on the gate surfaces of the eight-channel FET array.

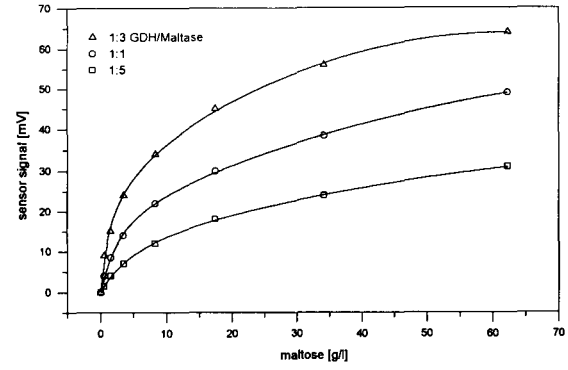

Fig. 2. Influence of the immobilized GDH/MAL ratio on the sensor signal as a function of the maltose concentration at 500 mM KCl, 10 mM KP buffer, 50 mM NAD, pH 8 and 100 rpm.

NAD is the cofactor of the dehydrogenases. 5 mM NAD is needed for the analysis of 5 g/l maltose and 25 mM to that of 20 g/l maltose.

Ionic strenght (up to 1000 mM KCl) and stirrer speed (up to 1000 rpm) effect the analysis of maltose only slightly. With increasing ionic strenght and decreasing stirrer speed the signal height slightly increases. However, this stirrer speed effect is distinct for sucrose analysis. There is a linear relationship between the response time, t_R, and the membrane thickness, d, of the GDH/MAL FET (at $d = 10$ μm, $t_R = 350$ s and at $d = 110$ μm, $t_R = 500$ s).

At 4°C the enzyme-FETs can be stored for months without loss of activity. GDH alone has no cross-sensitivity with regard to maltose and sucrose. However, the MAL/GDH and INV/GDH FETs are sensitive for glucose. Therefore, glucose has to be measured separately in its presence in the sample. The β-GAL/GALDH FET has no glucose sensitivity.

To eliminate the glucose cross-sensitivity of the sucrose analysis, a new EnFET was developed: sucrose was converted to fructose and glucose-1-phosphate with sucrosephosphorylase and

the latter to glucose-6-phosphate with phosphoglucomutase:

$$\text{sucrose} + \text{phosphate ions} \xrightarrow{\text{sucrosephosphorylase}} \text{glucose-1-phosphate} + \text{fructose}$$

$$\text{glucose-1-phosphate} \xrightarrow{\text{phosphoglucomutase}} \text{glucose-6-phosphate}$$

The glucose-6-phosphate was converted to glucose-6-phosphategluconolacton by glucose-6-PDH:

$$\text{glucose-6-phosphate} + \text{NAD} \xrightarrow{\text{glucose-6-PDH}} \text{glucose-6-phosphategluconolacton} + \text{NADH}$$

and finally the latter to 6-phosphogluconic acid:

$$\text{glucose-6-phosphategluconolactone} + H_2O \xrightarrow{\text{gluconolactonase}} \text{6-phosphogluconic acid}$$

By coimmobilisation of these enzymes an EnFET for sucrose analysis was developed, which had a measuring range of 0.025 to 0.6 sucrose g/l, and showed a suitable stability for more than a month. Unfortunately, in the presence of glucose the signal was reduced by reversible glucose inhibition already in presence of 0.2 g/l glucose. Therefore, it can only be applied in absence of glucose.

3. Results and discussion

3.1. Calibration of EnFET–FIA systems

The eight-channel EnFET array was mounted into a flow cell which included the reference electrode (Fig. 3). By the minimal distance and the face-to-face arrangement of the EnFET and reference electrode as well as the cross flow of the carrier buffer the sample segments passed the particular sensors without vortex formation consecutive with very short time difference (0.15 s at 2 ml/min flow rate) (Fig. 4). The pH value was always measured by the first (No. 1) pH-FET in the array. In Fig. 4 the signals of these pH sensors are shown.

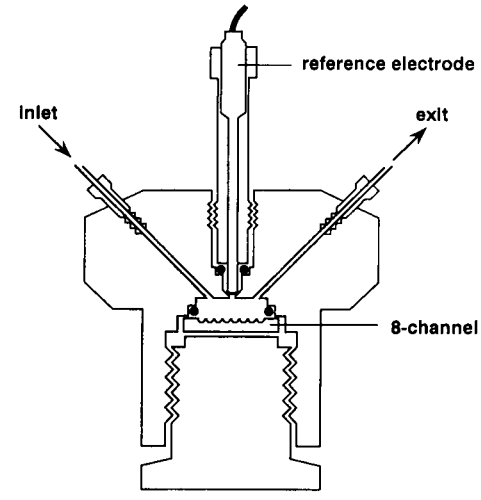

Fig. 3. Flow cell for the eight-channel EnFET with reference electrode.

This multichannel EnFET was mounted into a commercial FIA system (EVA, Eppendorf-Netheler-Hinz, Hamburg) for its calibration.

Fig. 5 shows the calibration of a MAL/GDH FET for maltose in the concentration range between 0.5 and 50 g/l at 2 ml/min 20 mM KP buffer, 50 mM NAD, pH 8 and injection time $t_i = 15$ s.

The EnFET–FIA signals were evaluated by peak height as well as peak integral. The peak

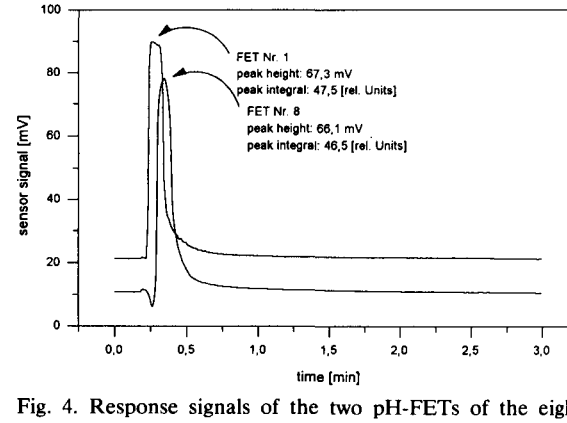

Fig. 4. Response signals of the two pH-FETs of the eight-channel FIA system on a pH pulse.

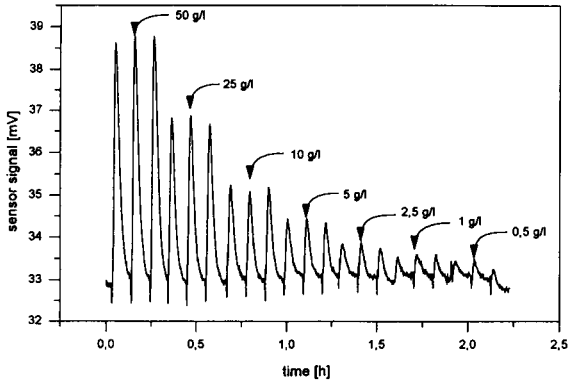

Fig. 5. Calibration of a MAL/GDH FET–FIA system with different maltose concentrations in the range 0.5 and 50 g/l maltose at 20 mM potassium phosphate buffer (KP buffer), 50 mM NAD, pH 8, and with $t_{inj} = 15$ s.

heights gave much lower standard deviation (3–5%) than the integrals (11–12%). Therefore, the peak heights were used for the signal evaluation.

By increasing the injection time (between 10 and 20 s) and the contact time (in the EnFET flow cell) by stopped flow (between 0 and 30 s at constant sample volume) the sensor signals were enlarged, but the calibration curves became non-linear. During the cultivation the substrate and product concentrations changed in a broad range, the measuring ranges of the EnFETs had to be adapted to each of the components and cultivations. Therefore, the analyte concentration was varied in the cultivation medium (e.g., between 2 and 10 g/l glucose) and the calibration was performed with different injection times. The carrier buffer included L-cysteine as antioxidant, ETDA as metal complexing agent and Triton X-100 (Sigma) as surfactant for maintain a bubble free flow in the flow cell.

The long time activity of the GDH FET (Fig. 6) and the MAL/GDH FET (Fig. 7) were satisfactory. The dependence of the MAL/GDH FET on the ionic strenght was negligible (Fig. 8).The same holds true for the β-GAL/GALDH FET as well (Fig. 9). The influence of the stirring rate on the signal height was low for both of them.

The coimmobilized ADH to ALDH ratio was varied (Fig. 10). With the ADH/ALDH (1:2) FET the signal was twice as high as with the

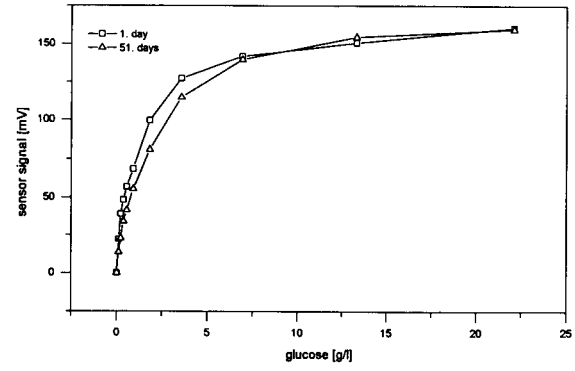

Fig. 6. Long-time stability of the GDH FET: sensor signal as a function of the glucose concentration at 10 mM KP buffer, 100 mM KCl, 50 mM NAD, pH 8 at 25°C after one day and 51 days.

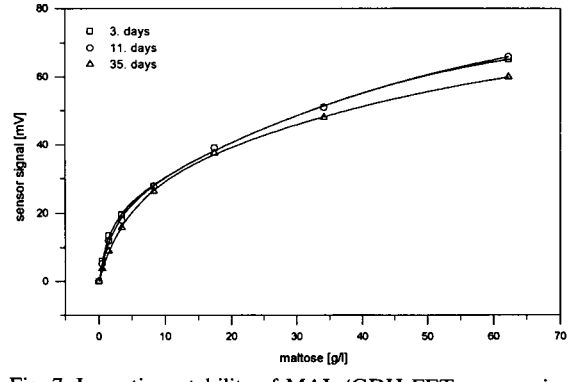

Fig. 7. Long-time stability of MAL/GDH FET: sensor signal as a function of the maltose concentration at 500 mM KCl, 10 mM KP buffer, 50 mM NAD, pH 8 after 3, 11 and 35 days.

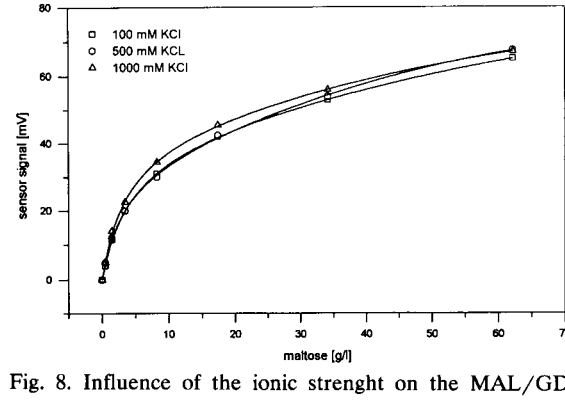

Fig. 8. Influence of the ionic strenght on the MAL/GDH FET sensor signal in the maltose concentration range between 0.5 and 60 g/l at 10 mM KP buffer, 50 mM NAD, pH 8 and 100 rpm.

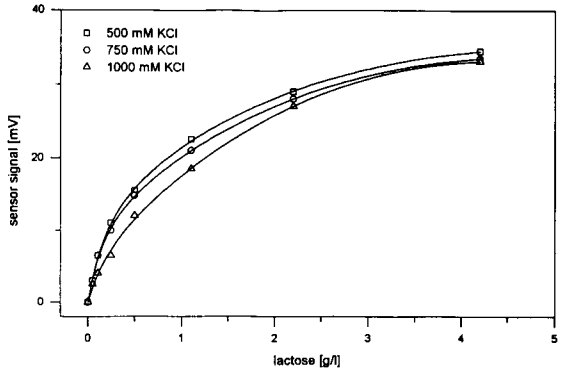

Fig. 9. Influence of the ion strenght on the β-GAL/GALDH FET signal as a function of the lactose concentration at 10 mM KP buffer, 50 mM NAD, pH 8 and 500 rpm.

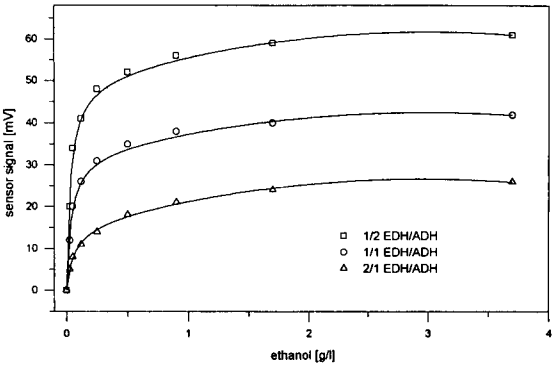

Fig. 10. Influence of the ADH/ALDH ratio in ADH/ALDH FET as a function of the ethanol concentration at 10 mM KP buffer, 100 mM KCl, 50 mM NAD and pH 7.

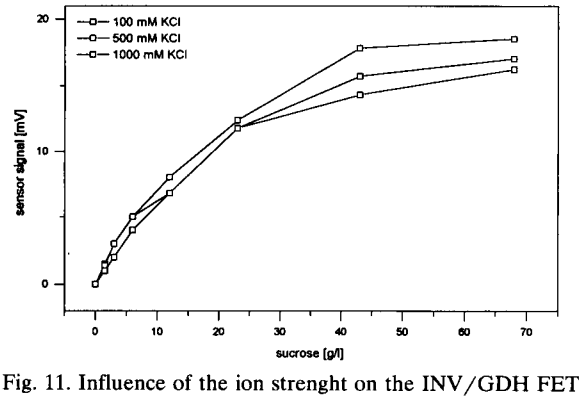

Fig. 11. Influence of the ion strenght on the INV/GDH FET signal as a function of the sucrose concentration at 10 mM KP buffer, 50 mM NAD, pH 7 and 0 rpm.

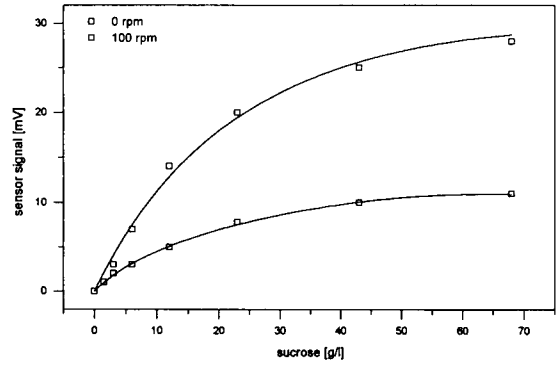

Fig. 12. Influence of the stirrer speed on the INV/GDH FET signal as a function of the sucrose concentration at 10 mM KP buffer, 100 mM KCl, 50 mM NAD and pH 7.

ADH/ALDH (2:1) ratio. With increasing ionic strenght the signal of the ADH/ALDH FET decreases.

The ionic strenght influences the signal of the INV/GDH FET only slightly (Fig. 11), but with increasing stirring rate its signal decreases (Fig. 12). No cross-sensitivity was observed between the INV/GDH FET for sucrose, the MAL/GDH FET for maltose and the β-GAL/GALDH FET for lactose analyses.

The buffer capacity was monitored by means of shape of the EnFET–FIA signal. This procedure is published elsewhere [15].

4. Conclusion

Five EnFETs were developed for the analysis of glucose, maltose, sucrose, lactose and ethanol and were integrated into a commercial FIA system. These EnFET–FIA systems were characterized and calibrated. By means of the carrier buffer, pH, the NAD, injection time and contact time in the flow cell of the EnFETs, the suitable measuring range can be chosen for the monitoring of these medium components.

Acknowledgments

The authors gratefully acknowledge Prof. Bülow, University of Lund for the fusion protein

β-GAL/GALDH and thank the Ministry of Research of Technology of the Federal Republic of Germany, Bonn, for the financial support.

References

[1] P. Bergveld, IEEE Trans. Biomed. Eng., 17 (1970) 70.
[2] K. Tsukuda, M. Sebata, Y. Miyahara and H. Miyaga, Sensors Actuators, 18 (1989) 329.
[3] H. Perrot, N. Jaffrezic-Renault, P. Clehet, W.B. Wlodarski, N.F. de Rooij and H.H. van den Vlekkert, Sensors Actuators, B1 (1990) 380.
[4] H.H. Vlekkert and N.F. de Rooij, Sensors Actuators, B1 (1990) 395.
[5] U. Oesch, S. Caras and J. Janata, Anal. Chem., 53 (1981) 1983.
[6] M. Battilotti, M. Mercuri, G. Mazzamurro, I. Giannini and M. Giongo, Sensors Actuators, B1 (1990) 438.
[7] S.D. Caras and J. Janata, Anal. Chem., 57 (1985) 1917.
[8] E. Tamiya, I. Karube, Y. Kitagawa, M. Ameyawa and K. Nakashima, Anal. Chim. Acta, 207 (1988) 77.
[9] Y. Hanazato, K.-I. Inatomi, M. Nakako, S. Shiono, M. Maeda, Anal. Chim. Acta, 212 (1988) 49.
[10] J. Kimura and T. Kuriyama, J. Biotechnol., 15 (1990) 239.
[11] U. Brand, B. Reinhardt, F. Rüther, T. Scheper and K. Schügerl, Anal. Chim. Acta, 238 (1990) 201
[12] U. Brand, L. Brandes, V. Koch, T. Kullick, B. Reinhardt, F. Rüther, T. Scheper, K. Schügerl, S. Wang, X. Wu, R. Ferretti, S. Prasad and D. Wilhelm, Appl. Microbiol. Biotechnol., 36 (1991) 167.
[13] U. Brand, B. Reinhart, F. Rüther, T. Scheper and K. Schügerl, Sensors Actuators, B4 (1991) 315.
[14] T. Kullick, Dissertation, University of Hannover, 1993.
[15] B. Hitzmann and T. Kullick, in preparation.

ELSEVIER

Analytica Chimica Acta 296 (1994) 271–276

ANALYTICA CHIMICA ACTA

Amperometric flow-injection determination of glucose, urate and cholesterol in blood serum by using some immobilized enzyme reactors and a poly(1,2-diaminobenzene)-coated platinum electrode

Toshio Yao *, Masahiro Satomura, Taketoshi Nakahara

Department of Applied Chemistry, College of Engineering, University of Osaka Prefecture, 1-1 Gakuen-cho, Sakai, Osaka 593, Japan

Received 31 January 1994; revised manuscript received 3 May 1994

Abstract

Glucose, uric acid and cholesterol in blood serum were assayed simultaneously in a flow-injection system by using a 16-way switching valve and a parallel configuration of three immobilized enzyme reactors. A poly(1,2-diaminobenzene)-coated platinum electrode was used to detect selectively hydrogen peroxide generated enzymatically into the enzyme reactors, without any interferences from oxidizable species and proteins present in serum. The precision (coefficient of variation) of the assay was better than 2% for the simultaneous assay of three species in human control serum. The assay speed was up to 38 samples per hour.

Keywords: Amperometry; Flow injection; Enzyme reactor; Polymer-coated electrode; Glucose; Uric acid; Cholesterol

1. Introduction

Amperometric flow-injection analysis (FIA) based on the use of immobilized enzyme reactors has become recognized as a selective, simple, accurate and rapid technique for the determination of a variety of biologically important compounds [1,2]. In such a FIA system, solid electrode-based detectors (e.g., platinum and glassy carbon electrodes) are commonly used for the detection of electroactive products (e.g., H_2O_2 and NADH) generated enzymatically in the enzyme reactor. However, these electrodes are often hampered by a gradual fouling of the electrode surface due to adsorption of large organic molecules such as proteins and also by response to electroactive interferences, especially in the analysis of samples of complex matrices such as blood serum and food.

Recently, many attempts have been made to

* Corresponding author.

SSDI 0003-2670(94)00218-B

achieve higher selectivity and stability for amperometric detection by permselective coatings on the electrode surface [3,4] (based on charge exclusion and/or size exclusion). Sittampalam and Wilson [5] used a cellulose acetate coating to exclude the effects of proteins and also to decrease the effect of interferences due to oxidizable species present in serum. Similarly, perfluorosulfonated Nafion [6] and polyester sulfonic acid [7] were used to prepare polyanionic films on the electrode surface. The membrane has ion-exchange properties that make it permeable to cations and impermeable to anions. These charged film-coated electrodes demonstrated a substantial improvement in differentiation of primary amino (cationic) neurotransmitters from metabolites [8,9]. Furthermore, the coating of a Nafion film over the enzyme layer has found to improve considerably the selectivity of the enzyme electrode [10,11], because the outer Nafion film is able to exclude anionic interferences such as L-ascorbate and urate.

Electropolymerization has also been used as a valuable method for creating size-exclusion films on the electrode surface. The permeability of films could be varied by controlling the amount of charge consumed during the electropolymerization. Thus polyphenol- [12], poly(1,2-diaminobenzene)- [13,14] and poly(*N*,*N*-dimethylaniline) [15] -coated electrodes were used to improve the selectivity of amperometric detection. If such polymer-coated electrodes are used as amperometric detectors in flowing streams, the need for a sample pretreatment may be eliminated. In this paper, a poly(1,2-diaminobenzene)-coated platinum electrode is used as a highly selective detector for hydrogen peroxide generated enzymatically in a multichannel FIA system, which was based on the use of a 16-way switching valve and a parallel configuration of three oxidase immobilized enzyme reactors. This electrode exhibited a more rapid and selective response to hydrogen peroxide compared with other permselective film-coated electrodes. The proposed FIA system was successfully applied to the simultaneous assay of glucose, urate and cholesterol in blood serum, without any interferences from electroactive species and proteins present in the serum.

2. Experimental

2.1. Reagents

Glucose oxidase (EC 1.1.3.4, 250 U mg^{-1} protein, from *Aspegillus niger*) was obtained from Sigma (St. Louis, MO), and uricase (EC 1.7.3.3, 2.1 U mg^{-1} protein, from yeast) and cholesterol oxidase (EC 1.1.3.6, 11.2 U mg^{-1} protein, from *Nocardia sp.*) were from Oriental Yeast (Tokyo). They were used as received. Cholesterol standard (200 mg dl^{-1}), glutaraldehyde (20% solution), D-glucose, uric acid, L-ascorbic acid, Triton X-100, and 1,2-diaminobenzene were obtained from Wako (Osaka). Control human sera were obtained from Wako and Ortho Diagnostic Systems. All other chemicals were of analytical reagent grade.

2.2. Preparation of the immobilized enzyme reactors

The method was similar to that described previously [16]. Controlled-pore glass (aminopropyl-CPG, pore size 585 Å, particle size 200–400 mesh), obtained from CPG Inc. (Fairfield, NJ), was packed into three glass columns (18 mm × 3 mm i.d.). Glutaraldehyde solution (4%, v/v) in 0.1 M sodium hydrogen carbonate was circulated to activate the glass. After washing with 0.1 M phosphate buffer (pH 7.0), glucose oxidase (500 U) was loaded on one of the columns and cholesterol oxidase (28 U) on the another column by circulating enzyme–phosphate buffer (0.1 M, pH 7.0) solutions for 2 h at room temperature. Uricase (5 U) was loaded on the other by circulating enzyme–borate buffer (0.1 M, pH 9.0) according to the same procedure. The excess of enzymes and the residual aldehyde groups on the CPG were removed in a similar manner as described before [16]. The enzyme reactors were stored at ca. 5°C in the buffer used for the immobilization when not in use.

2.3. Construction of poly(1,2-diaminobenzene)-coated platinum electrode

An Eicom (Kyoto) thin-layer electrochemical flow-cell was used for the surface modification of

the electrode. The electrode assembly consisted of a platinum disk (3 mm in diameter) as a working electrode, a silver–silver chloride reference electrode, and a stainless-steel tube as an auxiliary electrode. The poly(1,2-diaminobenzene) film-coated platinum electrode was prepared by the similar procedure to that described by Sasso et al. [13]. Prior to the coating, the surface of the platinum disk was polished with alumina particles (Fujimi Metapolish, No. 4), rinsed with distilled water, and allowed to air-dry. The electropolymerization to coat the same surface with the thin film of poly(1,2-diaminobenzene) was carried out by holding the working electrode at 1.0 V vs. Ag/AgCl for 30 min in a flowing stream (pumped at a flow rate of 0.3 ml min^{-1}) of a solution of 1,2-diaminobenzene (20 mM) in 0.2 M, pH 5.2, sodium acetate buffer that had been deaerated with high-purity grade nitrogen before use, because 1,2-diaminobenzene was easily air oxidized. After the electropolymerization, the electrode was washed exhaustively with distilled water.

2.4. FIA system and procedures

The FIA system used is similar to the simultaneous determination FIA system proposed previously by Matsumoto et al. [17] and is outlined in Fig. 1. The immobilized enzyme reactors were positioned in each channel as shown and immersed in a water bath thermostated at 25 ± 0.2°C. The working carrier solutions used for the glucose and urate assays and for the cholesterol assay were 0.1 M phosphate buffer (pH 7.5) and 0.1 M phosphate buffer (pH 7.5) containing 0.75% (v/v) Triton X-100, respectively. Each carrier solution was pumped at 1.0 ml min^{-1} with a four-channel Sanuki (Tokyo) 4P3U pump, through a 16-way switching valve (Hitachi K-1600), an immobilized enzyme reactor, and a poly(1,2-diaminobenzene)-coated platinum electrode, and then was transported to a waste tank. The sample solutions were injected into each carrier stream simultaneously by switching the 16-way valve equipped with three sample loops in series (1.2 μl for glucose, 9.8 μl for urate and 4.9 μl for cholesterol), after three sample loops were filled

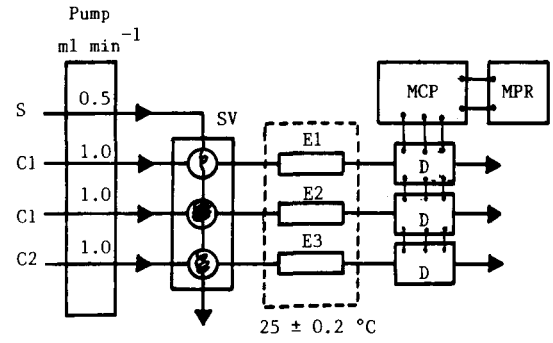

Fig. 1. FIA manifold for simultaneous assay of glucose, urate and cholesterol. Carrier solution: C1, 0.1 M phosphate buffer (pH 7.5); C2, 0.1 M phosphate buffer (pH 7.5) containing 0.75% (v/v) Triton X-100. S, sample solution; SV, 16-way switching valve with three sample loops. Enzyme immobilized reactor: E1, glucose oxidase immobilized reactor; E2, uricase immobilized reactor; E3, cholesterol oxidase immobilized reactor. D = poly(1,2-diaminobenzene)-coated platinum electrode; MCP = multichannel potentiostat, MPR = multipen recorder.

with sample solution by pumping at 0.5 ml min^{-1} for 1 min. Switching the valve was operated manually. A constant potential (0.6 V vs. Ag/AgCl) was supplied to each of the three poly(1,2-diaminobenzene)-coated flow cells with a Fuso (Kanagawa) multichannel potentiostat (HECS 966), and the signal currents were recorded simultaneously on a multipen recorder (Toadenpa PRS-5021).

3. Results and discussion

A bare platinum electrode without surface modification gave a fairly large response due to the electroactive interferences (L-ascorbic acid, uric acid, etc.) present in serum and caused a decrease in sensitivity due to electrode fouling by proteins, when serum samples were injected repeatedly in a single channel flow-injection manifold composed of a sample injector (Rheodyne 7125) and a Eicom flow-through platinum electrode. This means that the bare platinum electrode is not suitable as a detector for the FIA measurements of serum samples.

The response currents of the poly(1,2-diaminobenzene)-coated platinum electrode to hy-

Table 1
Effect of poly(1,2-diaminobenzene) film on the peak current

Platinum electrode	Response current (nA)		
	H_2O_2 (0.45 mM)	L-ascorbic acid (0.5 mM)	Uric acid (0.5 mM)
Bare	3413	3210	2971
Coated	1265	10	36

drogen peroxide, L-ascorbic acid and uric acid are shown in Table 1, compared with those of the bare electrode. Though the response current of the polymer-coated electrode for hydrogen peroxide was decreased to 38% of its previous value, the currents for L-ascorbic acid and uric acid were decreased to negligibly small values, as compared with the bare electrode. Due to such permselective characteristics of the polymer film, the access of L-ascorbic acid and uric acid, interfering species present commonly in serum, to the electrode surface is blocked. The polymer-coated electrode effectively excluded the L-ascorbic acid and uric acid below 2 mM.

The usefulness of the polymer-coated platinum electrode was evaluated by using a single channel flow-injection manifold with or without the glucose oxidase immobilized reactor. In this FIA system, 0.1 M phosphate buffer at pH 7.5 was selected as an optimum carrier solution and pumped at a constant flow-rate of 1.0 ml min^{-1}. Fig. 2 shows the effectiveness of the polymer film in decreasing the signal due to the interferents in serum to a negligible value. No evidence of electrode fouling by proteins was obtained with repeated injections of serum.

For the cholesterol assay [18], Triton X-100 should be added to the carrier solution as a detergent because of the poor solubility of cholesterol in the phosphate buffer. The poly(1,2-diaminobenzene) film was stable even in the phosphate buffer containing a concentrated detergent (1.0%), compared to the poor stability of the charge-exclusion Nafion film frequently used to enhance the selectivity of electrodes. The polymer-coated electrode could be used repeatedly for three weeks for cholesterol assays without interference with electroactive species and proteins in serum.

Three poly(1,2-diaminobenzene)-coated platinum electrodes prepared by the same procedure, were used as the detector in the simultaneous FIA system shown in Fig. 1. Glucose, uric acid and cholesterol in serum are enzymatically oxidized to produce hydrogen peroxide by the glucose oxidase, uricase and cholesterol oxidase reactors, respectively, which is amperometrically detected with the coated platinum electrode without any interferences The optimum carrier solution was 0.1 M phosphate buffer (pH 7.5) for the glucose and uric acid assays and 0.1 M phosphate buffer (pH 7.5) containing 0.75% (v/v) Triton X-100 for the cholesterol assay; the buffers were pumped at 1.0 ml min^{-1}, because this provided good sensitivity and a reasonable analytical rate. Fig. 3 shows typical calibration graphs for glucose, uric acid and cholesterol, obtained by the present FIA system. Linear relations between the signal current and the concentration of each

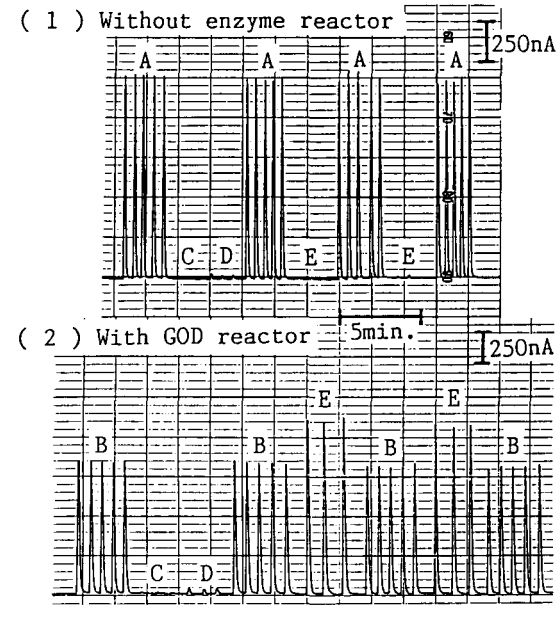

Fig. 2. Flow-injection current responses of a poly(1,2-diaminobenzene)-coated platinum electrode to 0.9 mM H_2O_2 (A), 50 mg dl^{-1} glucose (B), 0.5 mM L-ascorbic acid (C), 0.5 mM uric acid (D), and control serum (E) in a single channel flow-injection system without (1) and with (2) a glucose oxidase immobilized reactor. Carrier stream: 0.1 M phosphate buffer (pH 7.5) pumped at 1.0 ml min^{-1}. Injection volume: 5 μl.

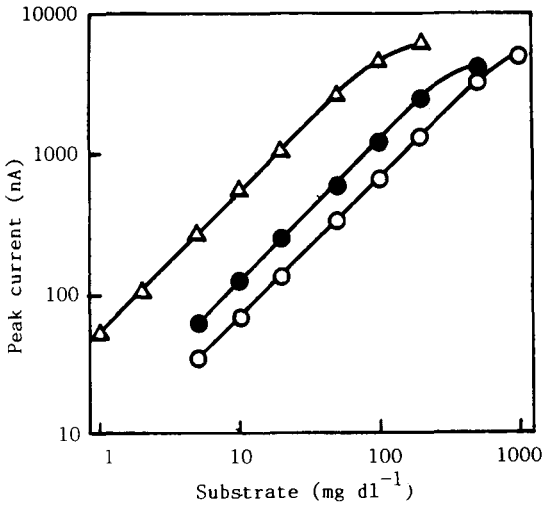

Fig. 3. Calibration graphs for glucose (○), uric acid (△) and cholesterol (●). The results were obtained under the experimenmtal conditions described in the Experimental section.

species were observed in the range 5–500 mg dl^{-1} for glucose, 1–50 mg dl^{-1} for urate and 5–200 mg dl^{-1} for cholesterol, with correlation coefficients > 0.995 for each. The lowest concentrations which could be detected by the present simultaneous assay were 1.7 mg dl^{-1} for glucose, 0.19 mg dl^{-1} for urate, and 0.88 mg dl^{-1} for cholesterol (signal-to-noise ratio = 3). Table 2 shows the results for the simultaneous assay of three substrates in human control sera. The average amounts of glucose, uric acid and cholesterol found in each control serum agreeded closely with the manufactures' data. The coefficient of variation was less than 2% for all samples. Also, up to 38 samples per hour could be assayed.

The three immobilized enzyme reactors were used repeatedly to confirm their stabilities; even after repetitive use (ca. 10 samples per day) for two months, the enzyme reactors retained over 90% of their original activities. Also, the poly-(1,2-diaminobenzene)-coated platinum electrode was stable enough to be used repeatedly for three weeks.

In conclusion, an attempt to apply the poly(1,2-diaminobenzene)-coated platinum electrode to the detection of hydrogen peroxide generated enzymatically in the enzyme reactor improved the highly selective and simultaneous assay of glucose, uric acid and cholesterol in human serum by using a multichannel flow-injection system. This FIA system can be further applied to the simultaneous assays of a variety of substrates

Table 2
Analytical results for simultaneous assay of glucose, uric acid and cholesterol in human control sera

Control serum	Glucose			Uric acid		
	Indicated value [a] (mg dl^{-1})	Analysed value (mg dl^{-1})	C.V. (%)	Indicated value [a] (mg dl^{-1})	Analysed value (mg dl^{-1})	C.V. (%)
Standard solution	80.0	80.3 ± 0.6	0.7	5.0	5.1 ± 0.08	1.6
Wako I	79 ± 10	72.2 ± 0.9	1.2	5.0 ± 0.4	4.8 ± 0.09	1.9
Wako II	255 ± 14	261.4 ± 2.3	0.9	7.7 ± 0.8	7.9 ± 0.10	1.3
Ortho normal	93 ± 7	100.6 ± 1.2	1.2	5.1 ± 0.4	5.3 ± 0.10	1.9
Ortho abnormal	296 ± 23	311.5 ± 2.1	0.7	10.5 ± 0.8	10.3 ± 0.11	1.1

Cholesterol		
Indicated value [a] (mg dl^{-1})	Analysed value (mg dl^{-1})	C.V. (%)
25.0	24.9 ± 0.3	1.2
34 ± 5	31.9 ± 0.3	0.9
14 ± 4	14.3 ± 0.2	1.4
25 ± 3	23.8 ± 0.3	1.3
43 ± 7	42.0 ± 0.5	1.2

7 Measurements on each sample
[a] Manufacturer's data. C.V. = Coefficient of variation.

in serum by using other hydrogen peroxide – producing oxidase immobilized reactors.

References

[1] T. Yao, J. Flow Injection Anal., 2 (1985) 115.
[2] T. Yao, in D.L. Wise (Ed.), Applied Biosensors, Butterworth, New York, 1989, pp. 321–348.
[3] J. Wang, Anal. Chim. Acta, 234 (1990) 41.
[4] G. Marko-Varga, Electroanalysis, 5 (1993) 403.
[5] G. Sittampalam and G.S. Wilson, Anal. Chem., 55 (1983) 1608.
[6] H. Ji and E. Wang, J. Chromatogr., 410 (1987) 111.
[7] J. Wang and T. Golden, Anal. Chem., 61 (1989) 1597.
[8] J. Wang, P. Tuzhi and T. Golden, Anal. Chim. Acta, 194 (1987) 129.
[9] G. Nagy, G.A. Gerhardt, A.F. Oke, M.E. Rice, R.N. Adams, R.B. Moore, M.N. Szentirmay and C.R. Martin, J. Electroanal. Chem., 188 (1985) 85.
[10] D.J. Harrison, R.F.B. Turner and H.P. Baltes, Anal. Chem., 60 (1988) 2002.
[11] T. Yao, Anal. Chim. Acta, 281 (1993) 323.
[12] J. Wang, S.P. Chen and M.S. Lin, J. Electroanal. Chem., 273 (1989) 231.
[13] S.V. Sasso, R.J. Pierce, R. Walla and A.M. Yacynych, Anal. Chem., 62 (1990) 1111.
[14] C. Malitesta, F. Palmisano, L. Torsi and P.G. Zambonin, Anal. Chem., 62 (1990) 2735.
[15] T. Ohsaka, K. Taguchi, S. Ikeda and N. Oyama, Denki Kagaku, 58 (1990) 1136.
[16] T. Yao and T. Wasa, Electroanalysis, 5 (1993) 887.
[17] K. Matsumoto, H. Matsubara, M. Hamada, H. Ukeda and Y. Osajima, J. Biotechnol., 14 (1990) 115.
[18] T. Yao and T. Wasa, Anal. Chim. Acta, 207 (1988) 319.

ELSEVIER

Analytica Chimica Acta 296 (1994) 277–284

ANALYTICA CHIMICA ACTA

Adsorptive stripping voltammetry of lumichrome in sea water at the static mercury drop electrode

Gioacchino Scarano *, Elisabetta Morelli

Istituto di Biofisica, Consiglio Nazionale delle Ricerche, Via S. Lorenzo 26, 56127 Pisa, Italy

Received 9 February 1994; revised manuscript received 29 April 1994

Abstract

The adsorptive voltammetric behaviour of lumichrome (7,8-dimethylalloxazine), the main product of riboflavin photolysis, was investigated in sea water. The effect of experimental parameters such as preconcentration time and potential, pH of solution and mass transport conditions on the stripping response are discussed. Sensitive measurements can be achieved after controlled adsorption followed by square wave voltammetry. The stripping peak current was found to be proportional to the bulk concentration of lumichrome. The sensitivity was 5×10^{-2} nA nM^{-1} s^{-1}, the reproducibility was 6% at a concentration of 3.6×10^{-9} M lumichrome and the detection limit was 100 pM. Using an accumulation time of 600 s at -0.4 V, this technique allows the direct determination of lumichrome naturally present in raw sea water samples. The value found was about 200 pM. The concentration of lumichrome was also determined in the same samples using liquid chromatography after a solid-phase preconcentration step. Good correlations between voltammetric and chromatographic results were found.

Keywords: Stripping voltammetry; Chromatography; Lumichrome; Sea water; Waters

1. Introduction

Flavins are biologically important trace components released in sea water by many species of phytoplankton and marine bacteria during their growth [1]. Chemically, they are known to be good photosensitizers of photochemical reactions in sea water [2]. In sea water riboflavin is irreversibly decomposed by light yielding photochemically persistent lumiflavin (4%) and lumichrome (96%) [3,4].

Quantitative measurements of flavins in sea water have been performed using solid-phase extraction coupled with liquid chromatography (LC) [5,6]. The method is sensitive at picomolar levels and it has been used to investigate the distribution of flavins in the water column.

The polarographic behaviour of flavin compounds, together with their adsorption characteristics on the mercury electrode, has been extensively reviewed [7,8]. In spite of their advantageous redox characteristics, no electrochemical approach has been exploited to measure these compounds directly in sea water.

Wang [9] first reported the use of adsorptive stripping voltammetry (AdSV) for the measure-

* Corresponding author.

SSDI 0003-2670(94)00221-7

ment of riboflavin and flavin analogues at the static mercury electrode, with a detection limit of 2.5×10^{-11} M in 0.001 M NaOH.

AdSV involves a non-electrolytic preconcentration step by adsorbing the compound on the electrode surface, followed by the voltammetric measurement of the surface-bound species.

Controlled adsorptive accumulation on the static mercury electrode was applied as an effective preconcentration step for the determination, at nanomolar level, of many other organic compounds [10–15]. By using sensitive differential pulse or square wave voltammetry, AdSV shows good precision and selectivity.

In this work AdSV of lumichrome in sea water is reported and the parameters affecting the stripping current were examined. A direct voltammetric procedure suitable to measure subnanomolar levels of lumichrome in sea water is presented. The methodology was applied to raw sea water samples and natural levels of lumichrome were found to be detected after a 600 s preconcentration time. The results compare favourably with solid-phase extraction followed by reversed-phase LC.

2. Experimental

Voltammetric measurements were carried out with a Metrohm 646 VA processor in conjunction with a 647 VA stand equipped with a Metrohm multimode electrode (MME).

A conventional three-electrode arrangement was utilized: the MME was used in the hanging mercury drop mode (HMDE), a Ag/AgCl/KCl (3 M) electrode with double junction was used as reference and a glassy-carbon rod as auxiliary electrode. The measurement cell was equipped with a vertical rod stirrer operating under computer control.

Adsorptive stripping (AdS) voltammetric measurements were performed in stirred solutions after a preconcentration step in which the mercury drop was kept at a constant potential (−0.4 V) for a selected accumulation time. After a rest period of 15 s the potential was scanned in the negative direction and the cathodic voltammogram was recorded. Each measurement was carried out on a fresh drop. Unless otherwise stated, a drop area of 0.6 mm^2 was used.

The measuring mode was square wave (SW) voltammetry; five square wave oscillations (frequency 125 Hz) were applied to a staircase voltage ramp during the last 40 ms of the step width. The parameters of the voltage ramp were: step height 6 mV, step width 0.5 s, oscillation amplitude 25 mV.

Liquid chromatography was performed on a liquid chromatograph consisting of two LKB 2150 pumps, an LKB 2152 gradient controller, a Rheodyne Model 7125 injection valve and an Alltech 250×4.6 mm i.d. column packed with Spherisorb reversed-phase ODS-2, 5 μm. The system was equipped with an UV detector (Uvicord SD, Pharmacia-LKB) set at 254 nm. The mobile phase was 30:70 (v/v) acetonitrile–50 mM sodium acetate buffer (pH 5.6). The elution was performed in the isocratic mode at a flow rate of 1 ml min^{-1}. The injection loop was 250 μl. The dead volume was 2 ml. The chromatograms were recorded on a Hewlett Packard Model 3396 computing integrator.

Solid phase extraction was performed using reversed-phase trifunctional Sep-Pak t-C18 cartridges (Waters). The method involves the passage of a selected (50–250 ml) sample volume through a precleaned (10 ml of methanol and 20 ml of Milli-Q purified water) Sep-Pak cartridge at a flow rate of 10 ml min^{-1}. After rinsing, the cartridge was eluted with 10 ml of methanol, the eluate was vacuum dried and the residue was dissolved in water to obtain the desired concentration factor.

Sea water samples were collected in the Tyrrhenian Sea (close to the Tuscan Archipelago) at 0.5 m depth. Samples were filtered through 0.45-μm membrane filters (Sartorius) and stored in the dark at +4°C in preconditioned polyethylene containers. Organic-free sea water was obtained by exposing a previously charcoal- and Sep-Pak-processed sea water sample to a 1 kW UV lamp for 8 h.

Cellular exudates were obtained from batch cultures of the marine diatom *Phaeodactylum tricornutum*, Bohlin 1897, grown in a ther-

mostated room at 23°C under continuous illumination at 3000 ± 500 lux. After cells separation (by 0.2 μm membrane filter), the solution was stored 48 h under illumination to obtain photochemical decomposition of riboflavin before use.

Stock solutions of lumichrome (7,8-dimethylalloxazine, Sigma), lumiflavin (7,8,10-trimethylisoalloxazine, Fluka) and riboflavin (Fluka) were prepared by dissolving the calculated amounts in water to obtain concentrations of 6×10^{-6} M, 7×10^{-5} M and 1×10^{-4} M, respectively. Riboflavin was always handled in the dark.

Acetonitrile and methanol were HPLC-grade (Baker), sodium acetate and acetic acid were analytical-grade (Carlo Erba), HCl was suprapur-grade (Merck).

All solutions were prepared with water purified with a Milli-Q purification system (Millipore).

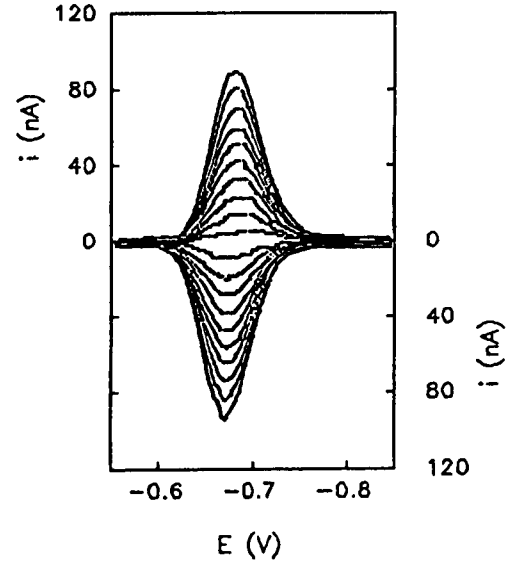

Fig. 1. Repetitive square wave cyclic voltammograms for 2.4×10^{-8} M lumichrome in sea water. The potentials of the triangular ramp were −0.55, −0.85 and −0.55 V. $E_{p(forward)} = -0.68$ V; $E_{p(reverse)} = -0.67$ V. Experimental conditions: HMDE, unstirred solution, scan rate 12 mV s^{-1}, step height 6 mV, step width 0.5 s, oscillation amplitude 25 mV, frequency 125 Hz, drop area 0.6 mm^2.

3. Results and discussion

The adsorptive voltammetric behaviour of lumichrome and parameters affecting the stripping response were investigated in sea water at pH 8.2.

The square wave voltammetric response was found to be very sensitive to the adsorption of lumichrome on the mercury drop surface.

Fig. 1 shows the SW cyclic voltammograms recorded after dipping the hanging mercury drop electrode (HMDE) in a quiescent sea water solution made 2.4×10^{-8} M in lumichrome. When repetitive cathodic and anodic scans were performed on a single mercury drop, the currents gradually increase. Thus, after ten cyclic scans, the anodic and cathodic peak currents were about 14 times higher than the corresponding peak currents of the first cyclic scan. The increase of current is due to progressive accumulation during the time of the voltage ramps and indicates that lumichrome remains adsorbed in the entire region of the examined potentials. The potential peak (E_p) values were −0.68 V and −0.67 V for the cathodic (from −0.55 to −0.85 V) and anodic (from −0.85 to −0.55 V) scan respectively, in agreement with the behaviour of an electrochemically reversible reaction.

When a single square wave cathodic scan was performed, the peak current increased with the delay time before starting the scan and it was affected by the mass transport conditions during the preconcentration step. By using a built-in vertical rod stirrer rotating at 1200 rpm with a preconcentration time (t_a) of 300 s at −0.4 V, the peak current for a solution of 2.4×10^{-8} M lumichrome was 3.6 times higher than the corresponding peak obtained with a quiescent solution. Under convective mass transport conditions the rate of stirring affected the magnitude of the stripping current (i_p). At the rotating speed of 1200, 1900 and 2600 rpm, i_p was 245, 290 and 370 nA respectively. So, assuming the adsorption process to be fast, the mass transport was the rate-limiting factor in the overall adsorption process of lumichrome in sea water. The last i_p value was about 40 times higher than that of solution specie alone, as estimated by a voltammetric scan with

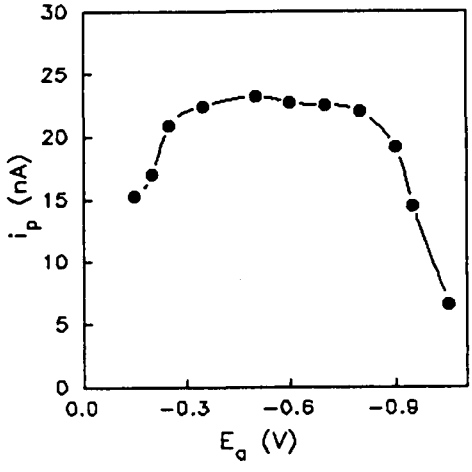

Fig. 2. Dependence of the stripping peak current of lumichrome on the preconcentration potential. 1.2×10^{-8} M in sea water; stirring rate 2600 rpm; $t_a = 60$ s; cathodic scan from −0.55 V; other conditions as in Fig. 1.

$t_a = 0$. This enhancement factor shows that controlled adsorptive accumulation can be utilized as an effective preconcentration step in the analytical determination of lumichrome in this electrolyte.

Differential pulse (DP) vs. SW voltammetry was briefly investigated on a stirred (2600 rpm) solution of 1.2×10^{-8} M lumichrome ($t_a = 60$ s; $E_a = -0.4$ V). The i_p value increased as the amplitude (ΔE) of the pulse and oscillation were varied from 25 to 100 mV and from 5 to 25 mV, respectively. With $\Delta E = 25$ mV the square wave response was 4 times higher than using differential pulse mode with $\Delta E = 100$ mV.

As expected, i_p increases as the mercury drop area (A) increases. For a 7.2×10^{-8} M lumichrome solution ($t_a = 60$ s; $E_a = -0.4$ V) the i_p increases with a slope of 37 nA/mm^2 in the range 0.15 to 0.6 mm^2.

Fig. 2 shows the dependence of the SW stripping peak current of lumichrome upon the accumulation potential (E_a) in the range −0.1 to −1.0 V (1.2×10^{-8} M; $t_a = 60$ s; stir = 2600 rpm). The i_p value was unaffected by changes of E_a in the range −0.3 to −0.8 V, for which the rate of adsorption appears to be fairly constant. At more cathodic E_a values a decrease in peak current was observed. An hypothesis to explain this behaviour could be that lumichrome is no longer strongly absorbed at potentials where the mercury drop becomes negatively charged with respect to the zero charge potential. Alternatively, if adsorption occurs, the adsorbed molecule could not retain its electrochemical characteristics when very cathodic potentials are applied during the accumulation step.

The effect of pH on E_p and i_p was investigated in the pH range from 9 to 4 (2.4×10^{-8} M; $t_a = 60$ s; $E_a = -0.4$ V). As expected for a reaction in which hydrogen ions take part in the electrochemical process, the E_p was pH dependent. It moved towards more anodic potentials as the pH was lowered. The slope of the plot, calculated in the pH range of 9.0 to 7.7, was 57 mV/pH unit, in agreement with the reported pH dependence of the polarographic half-wave potential ($E_{\frac{1}{2}}$) [8]. The i_p value was unaffected in the pH range from 9.0 to 8.0, then a 21, 75 and 87% suppression occurred at pH 7.7, 5.8 and 4.1, respectively. This behaviour of the peak current can be explained by the protonation occurring for the ionized forms of lumichrome ($pK_a = 7.2$) in the pH range 7.7–5.8 and it suggests an higher rate of adsorption when the deprotonated form predominates in solution.

The rate of surface coverage of the mercury electrode was measured as a function of accumulation time in stirred solutions of lumichrome in sea water. Fig. 3 shows a plot of the peak current observed for four concentrations in the range 6×10^{-9} M to 4.8×10^{-8} M. The peak current increases with increasing preconcentration times and the growth is faster as the concentration of the bulk solution increases. The plot for 6×10^{-9} M solution is linear in the entire range of the accumulation times tested, whereas deviations occur at higher concentrations. A least squares fit for the initial linear portion of the plots gives correlation factors $r^2 > 0.998$ and slopes of 17.5, 35.0, 71.5 and 150.3 nA min^{-1} for 6, 12, 24 and 48×10^{-9} M, respectively. The mean value for the ratio $i_p/C\cdot t_a$ was $(5.0\pm0.2)\times10^{-2}$ nA nM^{-1} s^{-1}. The finding that the peak current is proportional to the first power of adsorption time is expected for a system with convective mass transport control in which a fixed Nernstian dif-

fusion layer is established [10]. For concentrations of lumichrome higher than 6×10^{-9} M, the deviation from linearity occurs at shorter times as the concentration increases. The deviation starts when the product $C \cdot t_a$ exceeds the value 2×10^4 nM s and the covered surface approaches to 60%.

This behaviour is consistent with a process that is limited by adsorption of the reactant on the electrode surface; with longer accumulation times, the electrode surface became saturated and the peak current reaches a constant value.

Fig. 4 shows the calibration plots of i_p vs. concentration of lumichrome obtained in the range 1.2×10^{-9} to 1.2×10^{-8} M ($t_a = 300$ s) and 2.4×10^{-10} to 2.0×10^{-9} M ($t_a = 600$ s), each addition resulting in a 1.2×10^{-9} M and a 2.4×10^{-10} M increase in concentration, respectively. Organic-free sea water was used. The linearity was found for both concentration ranges; a least squares analysis of the standard addition data yields a slope of 15.8 and 28.7 nA nM^{-1} with a correlation coefficient of 0.999 and 0.998, respectively. The sensitivity measured as $i_p/C \cdot t_a$ was 5.2×10^{-2} and 4.8×10^{-2} nA nM^{-1} s^{-1}, in good agreement with the value previously calculated

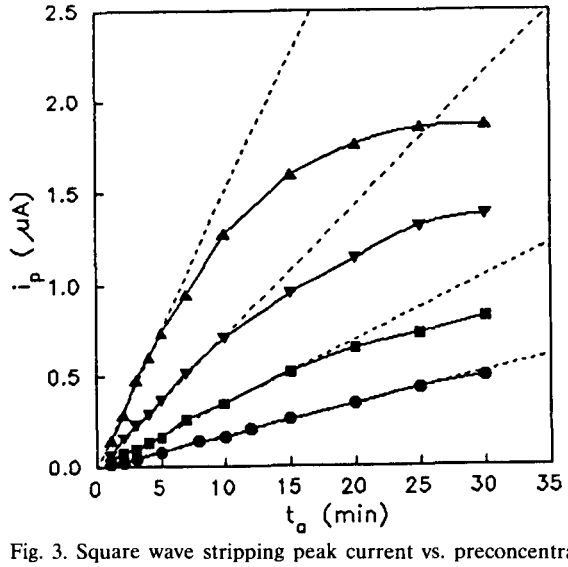

Fig. 3. Square wave stripping peak current vs. preconcentration time at different lumichrome concentrations. (●) 6; (■) 12; (▼) 24; (▲) 48 nM. Dashed lines correspond to a linear fit to the first portion of each curve. Stirred solution. $E_a = -0.4$ V.

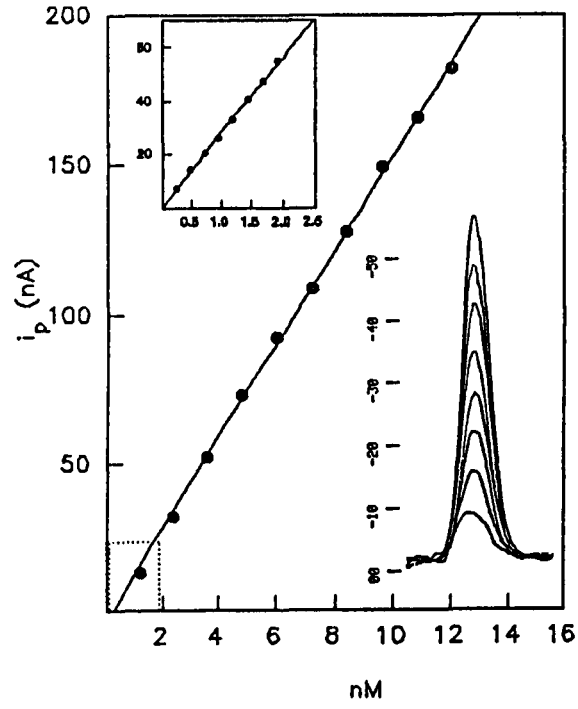

Fig. 4. Calibration plots of lumichrome in organic-free sea water. $E_a = -0.4$ V. $t_a = 300$ s for the range 1.2×10^{-9}–1.2×10^{-8} M. $t_a = 600$ s for the range 2.4×10^{-10}–2.0×10^{-9} M. The voltammograms refer to spikes of 2.4×10^{-10} M. $E_p = -0.68$ V.

from the linear portions of the i_p vs. t_a relationship.

Using a preconcentration time of 300 s, the linearity i_p vs. C was extended with the same slope until 7×10^{-8} M, then the expected deviation at $C \cdot t_a > 2 \times 10^4$ nM s was found. In terms of current this occurs when $i_p > 1.3$ μA mm^{-2} (here 0.8 μA with a 0.6 mm^2 drop area).

The reproducibility was estimated by ten successive measurements on a 3.6×10^{-9} M lumichrome solution ($t_a = 300$ s). The mean value of i_p was 55 nA, with a range of 51–58 nA and a relative standard deviation of 6%. Fig. 4 also shows the well defined SW voltammograms obtained with subsequent spikes of 2.4×10^{-10} M. E_p was -0.68 ± 0.02 V and the half-height width was 57 ± 3 mV.

In sea water at pH 8.2, the stripping peak potential was found to be independent of the preconcentration potential, the accumulation time

and the concentration of lumichrome and was similar to that observed in solution-phase SW polarography (drop time 1 s).

Riboflavin and lumiflavin also adsorb on the mercury electrode surface and they give adsorptive stripping peaks after a preconcentration step at −0.4 V. The separated effects of riboflavin and lumiflavin on the stripping response of lumichrome for a solution containing 6×10^{-9} M lumichrome and 6×10^{-8} M riboflavin or lumiflavin are shown in Fig. 5. In sea water at pH 8.2, these compounds give stripping peaks at more positive potentials (−0.56 and −0.54 V, respectively) than lumichrome, following the polarographic behaviour of isoalloxazine towards alloxazine derivatives [7]. The other flavins did not mask the stripping peak of lumichrome, this last being reduced about 100 mV more negatively. However, the stripping response obtained in a 10 fold excess of riboflavin or lumiflavin was 80% and 90% of its original value, respectively. This effect is due to the competition for the adsorption sites during the pre-electrolysis time.

The high sensitivity and reproducibility of the square wave adsorptive voltammetry of lumichrome in sea water solution, makes this technique a significant analytical method for detecting natural levels in raw sea water.

Using an accumulation time of 600 s, a measurable peak ($i_p = 4.8 \pm 1.2$ nA) at $E_p = -0.68 \pm 0.02$ V was obtained. This peak was attributed to the lumichrome naturally occurring in sea water

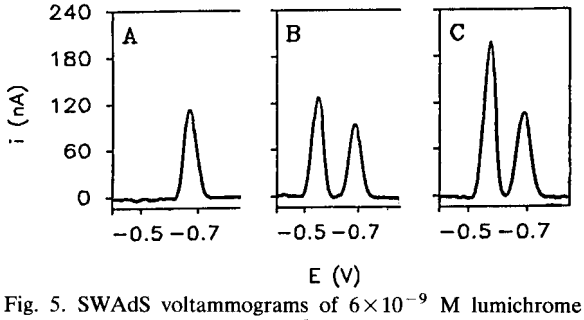

Fig. 5. SWAdS voltammograms of 6×10^{-9} M lumichrome (A) in the presence of 6×10^{-8} M riboflavin (B) and lumiflavin (C). $E_a = -0.4$ V; $t_a = 300$ s. E_p (lumichrome) = −0.68 V; E_p(riboflavin) = −0.56 V; E_p(lumiflavin) = −0.54 V.

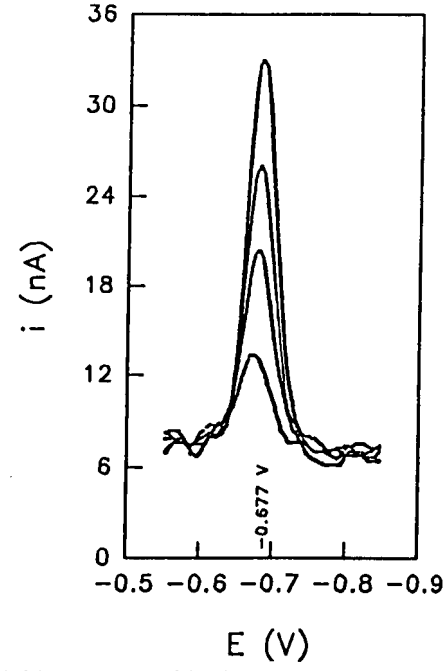

Fig. 6. Measurement of lumichrome in natural sea water by the standard addition method (three spikes of 2.4×10^{-10} M). $t_a = 600$ s; $E_a = -0.4$ V; $E_p = -0.68$ V.

and can be quantified using the standard addition method.

Ten samples of natural sea water were analysed by adding three spikes of standard lumichrome each effecting a 2.4×10^{-10} M increase in concentration (Fig. 6). The calculated concentration was $2.1 \pm 0.4 \times 10^{-10}$ M.

In order to confirm that the above quantified peak at $E_p = -0.67$ V was really due to the adsorbed lumichrome, a separate non-voltammetric measurement of this component in sea water was needed.

LC can be used to detect flavins and their degradation products in sea water after a previous preconcentration step on reversed-phase C_{18} Sep-Pak cartridges [5,6].

The extraction efficiency of Sep-Pak cartridges was previously tested by using sea water spiked with lumichrome to obtain concentrations ranging from 1.2 to 8.7×10^{-8} M. The Sep-Pak procedure resulted in a concentration factor of 10 and the extracts were analyzed by LC (direct injection) and by adsorptive SW stripping voltam-

metry (after 1:50 dilution). The average percent recovery was $106 \pm 8\%$ (Table 1) indicating that the C_{18} Sep-Pak cartridges supply a simple and efficient solid-phase extraction of lumichrome from sea water solutions.

We checked the adsorptive voltammetric response by reversed-phase LC after treating six separated 250-ml samples of natural sea water with Sep-Pak cartridges to obtain a 10^3 concentration factor. The chromatographic method allows the separation of lumichrome from the other unknown compounds retained on Sep-Pak (Fig. 7). The retention time of lumichrome was 6.5 min. With a 250-μl injection volume, solutions with concentrations of lumichrome higher than 1×10^{-8} M can be easily detected. The method shows good reproducibility; the relative standard deviation based on six injections of a 1×10^{-7} M standard was 7%. A calibration plot in the range 0.6 to 3.6×10^{-7} M was linear with a slope of 312 ± 21 arbitrary units of peak area $\times$ nM^{-1} ($r^2 = 0.995$).

The extraction method was also tested with the aim to increase the original signal of lumichrome when the adsorptive stripping voltammetric method was used. A 5 times higher concentration was found adequate to obtain a well defined peak with $t_a \leq 300$ s. All the voltammetric and chromatographic results are compared in Table 2 and show a good correlation.

The mean value of about 200 pM calculated in our samples was in the concentration range found in coastal sea water by other authors by using liquid chromatography after a preconcentration step [5,6]. The lowest concentration that can be estimated using the adsorptive square wave stripping voltammetry was 100 pM. When the signal is too low, the sample can be easily concentrated on a C_{18} Sep-Pak cartridge in order to obtain a more confident result.

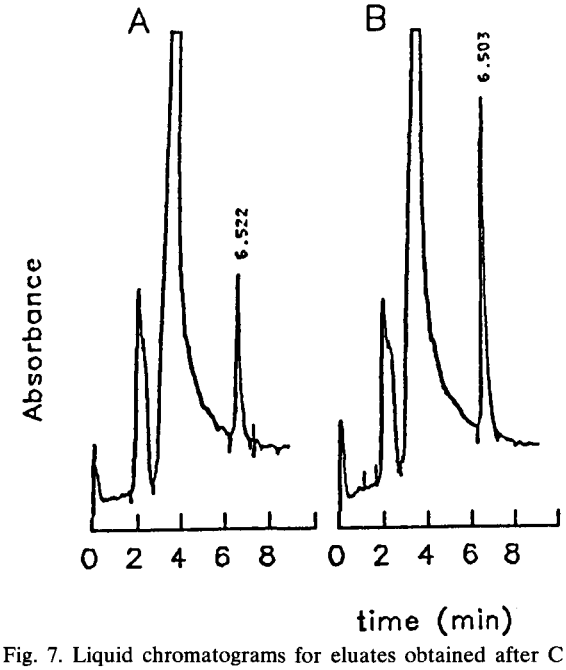

Fig. 7. Liquid chromatograms for eluates obtained after C_{18} Sep-Pak treatment of natural sea water samples. (A) Eluate. (B) Eluate spiked with 2.4×10^{-7} M lumichrome. Retention time of lumichrome, 6.5 min. Conditions: mobile phase, 30:70 (v/v) acetonitrile–50 mM sodium acetate buffer (pH 5.6); isocratic elution; flow rate, 1 ml min^{-1}; volume injected, 250 μl; UV detection at 254 nm.

Table 1
Sep-Pak extraction efficiency

LC			SWAdSV		
Expected [a], 10^{-7} M	Found, 10^{-7} M	Recovery, %	Expected [b], 10^{-9} M	Found, 10^{-9} M	Recovery, %
1.2	1.3	108	2.4	2.7	112
2.4	2.9	120	4.8	5.5	114
3.6	3.3	92	7.2	7.0	97
4.8	5.0	104	9.6	11.0	114
6.0	6.4	107	12.0	12.6	105
8.4	8.5	101	16.8	17.2	102

[a] In the Sep-Pak eluates.
[b] After 1:50 dilution of Sep-Pak eluates in organic-free sea water.

Table 2
Voltammetric and chromatographic assays of lumichrome in natural sea water samples

Technique	Treatment	Lumichrome (nM)	±S.D.	*n*
AdSV	none	0.21	0.04	10
AdSV	Sep-Pak	0.19	0.02	6
LC	Sep-Pak	0.23	0.07	6

Dissolved organic substances naturally occurring in sea water do not interfere with the direct voltammetric measurement of lumichrome in raw sea water. This is proved by the strict similarity between the slope of the standard additions performed during the measurements in natural sea water (28.6 ± 2.2 nA nM^{-1}) with the slope obtained from the calibration plot in organic-free sea water (28.7 nA nM^{-1}).

Lumichrome was also measured in sea water samples spiked with the cellular exudates of the marine alga *Phaeodactylum tricornutum*. This compound is expected to accumulate in the culture medium due to photochemical decomposition of riboflavin released during the cell growth. In our culture the concentration of lumichrome was $(8.1 \pm 0.4) \times 10^{-8}$ M as measured by direct LC. Three sea water samples were spiked with cellular exudates to obtain an expected concentration of 8.1×10^{-9} M. It is well known that, in addition to the flavins, many others biogenic compounds are produced by living cells. The theory of AdSV predicts that the presence of surface-active substances can interfere with the accumulation rate of the analyte [16]. Well shaped voltammetric peaks were obtained and the concentration of lumichrome was found to be $(7.8 \pm 0.6) \times 10^{-9}$ M, so indicating that the added organic compounds do not hinder the correct voltammetric measurement.

4. Conclusions

This work has shown that lumichrome strongly adsorbs on the mercury electrode and that accurate quantitation of this compound can be achieved by controlling its adsorptive accumulation.

When directly applied to natural sea water samples, the SWAdSV exhibits adequate sensitivity for the measurement at sub-nanomolar concentrations.

Compared to liquid chromatography, the voltammetric technique is simpler, faster and can be performed without any preliminary preconcentration step at concentrations as low as 200 pM.

This methodology can be useful for studying, at trace levels, the kinetics of the photochemical decomposition of riboflavin to lumichrome in controlled systems, as well as the rate of production of these metabolic products in laboratory cultures of phytoplankton or bacteria.

References

[1] A. Momzikoff, Cah. Biol. Mar., 10 (1969) 429.
[2] A. Momzikoff and G. Gondry-Chennebault, C.R. Acad. C., Ser. III, (1989) 527.
[3] W.C. Dunlap and M. Susic, Mar. Chem., 19 (1986) 99.
[4] A. Momzikoff, R. Santus and M. Giraud, Mar. Chem., 12 (1983) 1.
[5] W.C. Dunlap and M. Susic, Mar. Chem., 17 (1985) 185.
[6] S.E. Vastano, P.J. Milne, W.L. Stahovec and K. Mopper, Anal. Chim. Acta, 201 (1987) 127.
[7] E. Knobloch, Methods Enzymol., 18 (1971) 305.
[8] G. Dryhust, Electrochemistry of Biological Molecules, Academic Press, New York, 1977, Chap. 7.
[9] J. Wang, D. Luo, P.A.M. Farias and J.S. Mahmoud, Anal. Chem., 57 (1985) 158.
[10] C.F. Kolpin and H.S. Swofford, Jr., Anal. Chem., 50 (1978) 916.
[11] A. Webber, M. Shah and J. Osteryoung, Anal. Chim. Acta, 154 (1983) 105.
[12] J.M. Fernández Alvarez, A. Costa García, A.J. Miranda Ordieres and P. Tuñon Blanco, J. Electroanal. Chem. Interfacial Electrochem., 225 (1987) 241.
[13] A.J. Ribes and J. Osteryoung, Anal. Chem., 62 (1990) 2632.
[14] W. Jin, X. Zhao, C. Ding, F. Wang and Z. Gao, Anal. Chim. Acta, 268 (1992) 185.
[15] M.J.F. Villamil, A.J. Miranda Ordieres, A. Costa García and P. Tuñon Blanco, Anal. Chim. Acta, 273 (1993) 377.
[16] J. Wang, Stripping Analysis, Principles, Instrumentation and Applications, VCH, Deerfield Beach, FL, 1985.

ELSEVIER

Analytica Chimica Acta 296 (1994) 285–294

ANALYTICA CHIMICA ACTA

Effect of the nature of the solvent on the limit of detection in thermal lens spectrometry

Y. Martín-Biosca, M.J. Medina-Hernández, M.C. García-Alvarez-Coque, G. Ramis-Ramos *

Departament de Química Analítica, Universitat de València, 46100 Burjassot, València, Spain

Received 14 February 1994; revised manuscript received 4 May 1994

Abstract

Owing to the thermal convection in thermal lens spectrometry the noise increases linearly with the signal. The slope, k, and the intercept of the linear noise versus signal plots depend on the nature of the solvent rather than the absorbing species. Attempts to correlate these parameters with the mechanical and thermo-optical properties of the solvent are made. When the absorbance of a blank solution increases, the limit of detection (LOD) increases proportionally to k. This decreases the differences between the LODs obtained in water and in other solvents of better thermo-optical properties, but with higher values of k.

Keywords: Thermal lens spectrometry; Limits of detection; Background noise

1. Introduction

In thermal lens spectrometry (TLS) absorption of a pump laser beam, followed by relaxation of the electronic energy gives rise to a thermal gradient. The gradient behaves as a divergent lens in defocusing a probe laser beam. The change of intensity in the probe beam centre at the far field is proportional to the concentration of the absorbing species. This absorptiometric technique has been shown to provide superior sensitivity and improved spatial resolution when compared to conventional spectrophotometry. Consequently, many procedures for the TLS determination of ultra-traces of highly absorbing species have been described [1–11]. Several reviews have been published [12–16].

Following the parabolic model [17,18], and introducing the correction coefficients of Dovichi [13] and Carter and Harris [19], the TLS signal is given by:

$$\frac{\Delta I}{I} = \frac{I(0) - I(\infty)}{I(\infty)} = 0.52\theta + 0.13\theta^2 \qquad (1)$$

where:

$$\theta = \frac{2.303P(-\mathrm{d}n/\mathrm{d}T)A}{\lambda_{\mathrm{pr}}\kappa} \qquad (2)$$

$\Delta I/I$ is the relative change of intensity at the probe beam centre, P is the pump power, $(\mathrm{d}n/\mathrm{d}T)$ is the temperature coefficient of the refrac-

* Corresponding author.

SSDI 0003-2670(94)00219-C

tive index, A is the absorbance, λ_{pr} is the wavelength of the probe laser, and κ is the thermal conductivity of the medium.

As deduced from Eq. 2, a high sensitivity is obtained with large powers, highly absorbing species and solvents with good thermo-optical properties, that is, with large values of the $|dn/dT|/\kappa$ ratio. For organic solvents, this ratio ranges from 1.9×10^{-4} mW^{-1} cm (methanol) to 5.9×10^{-4} mW^{-1} cm (carbon tetrachloride). Water exhibits a very low value, only 0.14×10^{-4} mW^{-1} cm (at 20°C) [13]. When a polar solvent is required, alcohols or water–alcohol and water–acetone mixtures have been recommended ($|dn/dT|/\kappa = 2.4 \times 10^{-4}$ and 2.9×10^{-4} mW^{-1} cm, for ethanol and acetone, respectively).

In an analytical procedure, however, the limit of detection (LOD) depends on the signal-to-noise ratio and not only on the sensitivity. The LOD is usually defined as the analyte concentration giving a signal of value $S_{bl} + 3\sigma_{bl}$, where S_{bl} and σ_{bl} are the signal of the blank and the associated noise (as the absolute value of the standard deviation), respectively. Since the LOD depends on σ_{bl}, and not only on the sensitivity, to select a solvent in TLS, both $|dn/dT|/\kappa$ and the noise characteristics of the solvent should be considered.

When lasers of adequate stability are used, the predominant source of noise in TLS with liquid samples is thermal convection within the sample solutions [20,21]. Thermal convection produces local changes in the refractive index, which originates profile deformations and changes in the direction of the probe beam. The convective noise is always present when TLS measurements are performed and, as shown in this work, it increases linearly with the TLS signal. Therefore, the expected value of S_{bl}, which can be higher than the TLS signal given by the pure solvent, S_0, should also be considered.

All chemical species present in the blank solution, including the solvent, the matrix of the sample, the reagents and the impurities contribute to the signal and, therefore, to the convective noise. Signal contributions within the UV–visible region are due to both the presence of species having electronic absorption bands at a relatively small distance from the pump radiation wavelength, and to high order overtones of vibrational transitions of the solvent. The latter are not negligible in TLS. Carbon tetrachloride, which has excellent thermo-optical properties, is also an extremely transparent solvent, with vibrational overtones of very low intensity within the UV–visible region.

In this work, a study of the noise as a function of the TLS signal in different solvents is performed, and the influence of several parameters on the LODs is discussed. A better understanding of the factors involved is necessary for the development of TLS as a routine analytical tool. The composition of the solvent cannot be altered in some instances. In many other cases, a miscible alcohol or acetone can be added to the aqueous solutions to enhance the sensitivity, or the analytes can be extracted into a variety of solvents. Several mixtures of different solvents have the same eluent strength and are almost equivalent in liquid chromatography and, therefore, the mixture giving the best LODs should be selected for TLS detection. In these cases, criteria to select the solvent leading to the best LOD should be applied.

2. Experimental

2.1. Apparatus

A thermal lens setup pumped by a 4-W Ar^+ laser (Spectra-Physics, Model 2016, Mountain View, CA) and probed with a 5 mW He–Ne laser (Spectra-Physics, Model 105) in a coaxial configuration was used. The 514.5 nm line of the Ar^+ laser (100 mW at the laser head and about 80 mW at the cell location) was modulated at 4 Hz with a chopper (Stanford, Model SR540, Sunnyvale, CA). A PC/AT computer, provided with a DAS-8 interface (Metrabyte, Taunton, MA) was used to acquire and treat the data. The TLS signals were measured as ΔI, the absolute difference between the voltage values generated by the maximum and minimum radiation intensities at the probe beam centre. A TLS measurement

every 2 s was generated. Other details have been described elsewhere [21,22].

A 5-ml standard quartz cell, an 18-μl flow cell (Hellma, Mülheim-Baden) and an 8-μl HPLC cell (Hewlett-Packard, Palo Alto, CA), all of them of 1 cm optical pathlength, were used. A Minipuls 3 peristaltic pump (Gilson, Middleton, WI) and PTFE tubes of 0.8 mm i.d. were also used.

2.2. Reagents

The following HPLC-grade solvents were used: acetone, methanol, ethanol, *n*-butanol, chloroform and carbon tetrachloride (Panreac, Barcelona). Analytical grade solvents were: *n*-pentanol (Merck, Darmstadt), *n*-propanol and chloroform (Panreac). Stock solutions were: 1.2×10^{-3} M $K_2Cr_2O_7$ (Panreac) in water, 5.0×10^{-2} M $CoCl_2 \cdot 6H_2O$ (Panreac) in water; 4.5×10^{-6} M methyl red (Scharlau, Barcelona) in water, methanol, ethanol, *n*-butanol, *n*-pentanol and acetone; 2.0×10^{-6} M eriochrome black T (EBT) (Probus, Barcelona) in methanol, ethanol and *n*-pentanol; 6×10^{-6} M 1-(2′-pyridylazo)-2-naphthol (PAN) (Scharlau) in methanol, ethanol, *n*-pentanol, chloroform and carbon tetrachloride, and 2.9×10^{-6} M iodine resublimed (D'Hemio, Madrid) in chloroform and carbon tetrachloride. All these reagents were of analytical grade, except iodine, which was pure. Dilutions of the stock solutions were made with the same solvent. Nanopure deionized water (Barnstead deionizer, Sybron, Boston, MA) was also used.

2.3. Procedures

The experiments were performed in a small closed inner room with an almost constant temperature of ca. 22°C, where the setup was installed. To achieve the thermal equilibrium with the environment, the solutions were introduced into the room at least 30 min before performing the measurements. Also, the cells were kept closed several minutes before and during the measurements.

Unless otherwise stated, the experimental procedure used to measure the TLS signal and the associated noise was the following: about 3 ml of the test solution was introduced into the 5-ml cell, 30 measurements were made and the mean value of the signal and its standard deviation were calculated. This was done three to five times, renewing the solution in the cell for every set of 30 measurements. The mean of the thermal lens signal, S, and the corresponding standard deviation, σ, was obtained.

The data obtained in the absence of any species other than the solvent, $S_0 \pm \sigma_0$, were compared with the data obtained with the same solvents in the presence of increasing concentrations of different organic and inorganic dyes, $S \pm \sigma$. Only data achieved within the same working session were compared. The values of σ were plotted against the corresponding values of $(S - S_0)$, at increasing concentrations of the absorbing compound, and least-squares regression analysis was applied to the data. The intercept of the fitted curve, σ_0^*, was considered as a more reliable value of the noise associated to S_0.

Calibration graphs were obtained in the following methyl red concentration ranges: 2.2×10^{-8}–6.7×10^{-8} M in water, 2.4×10^{-7}–1.5×10^{-6} M in methanol, 3.0×10^{-7}–1.5×10^{-6} M in ethanol, $1.9 \times 10^{-7} - 1.3 \times 10^{-6}$ M in *n*-butanol, 1.6×10^{-8}–6.6×10^{-8} M in *n*-pentanol, 3.6×10^{-8}–2.4×10^{-7} M in acetone, and 8.2×10^{-8}–2.0×10^{-7} M in water–glycerine mixtures. For PAN the concentration ranges were 1.9×10^{-8}–3.5×10^{-7} M in methanol, 4.3×10^{-8}–4.6×10^{-7} M in ethanol, 4.3×10^{-8}–2.2×10^{-7} M in chloroform, and 4.1×10^{-8}–2.5×10^{-7} M in carbon tetrachloride. For EBT they were 5.0×10^{-9}–9.5×10^{-8} M in methanol and 1.3×10^{-8}–1.4×10^{-7} M in ethanol, and for iodine 1.4×10^{-7}–8.5×10^{-7} M and 1.3×10^{-7}–7.2×10^{-7} M in chloroform and carbon tetrachloride, respectively.

3. Results and discussion

3.1. The relationship between signal and noise in TLS

In all cases, when the values of σ were plotted versus $(S - S_0)$, at increasing concentrations of the absorbing compound, a linear graph was

achieved (Figs. 1 and 2). The equation of the straight line is:

$$\sigma = \sigma_0^* + k(S - S_0) \quad (3)$$

The σ_0^* and k values obtained with several dyes and for a series of pure and mixed solvents are given in Table 1. As shown also in Fig. 2, σ_0^* and k depend on the nature of the solvent rather than on the nature of the absorbing species.

Instrumental and thermal convection contributions are included in σ_0^*. Instead, it is reasonable to assume that the linear increase of the noise that was produced when the signal increased was mainly due to the increase in thermal convection rather than to instrumental causes. Evidence for this is the rather different values of k obtained in some cases for different solvents, for the same signal range and within the same working session.

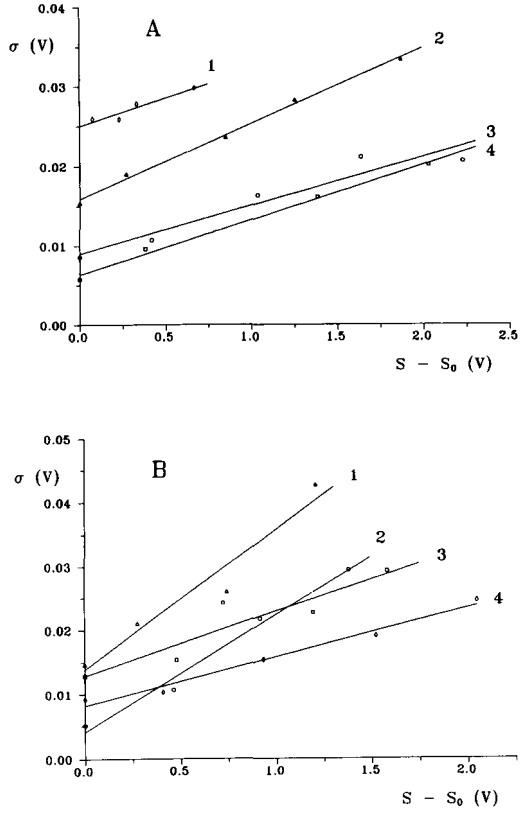

Fig. 1. Dependence of the noise on the signal at increasing concentrations of an absorbing compound in different solvents. Part A, methyl red in: (1) *n*-pentanol; (2) *n*-butanol; (3) methanol; (4) ethanol. Part B: (1) acetone (methyl red); (2) carbon tetrachloride (PAN); (3) chloroform (PAN); (4) water (potassium dichromate).

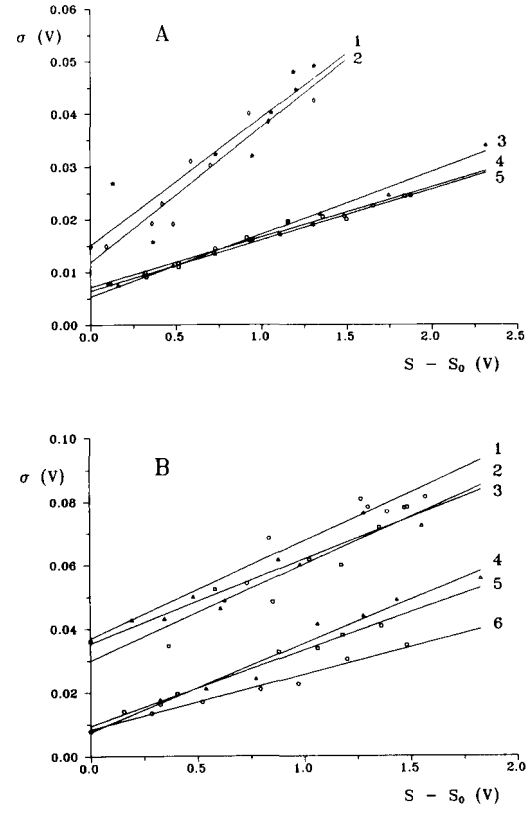

Fig. 2. Dependence of the noise on the signal at increasing concentrations of several absorbing compounds in the same solvent. Part A: (1) PAN and (2) EBT in methanol; (3) potassium dichromate, (4) methyl red and (5) cobalt(II) in water. Part B: (1) methyl red, (2) PAN and (3) EBT in *n*-pentanol; (4) PAN, (5) EBT and (6) methyl red in ethanol.

From Eq. 3, the signal-to-noise ratio can be expressed as a function of the signal as follows:

$$\frac{S}{\sigma} = \frac{1}{\dfrac{\sigma_0^* - kS_0}{S} + k} \quad (4)$$

which indicates that when the signal increases, the signal-to-noise ratio approaches asymptotically to $1/k$. Therefore, in TLS the convective noise severely limits the signal-to-noise ratio that can be reached with each solvent. The variation of S/σ at increasing values of the signal for several absorbing species in different solvents is

represented in Fig. 3. The data agree with the shape of the curves predicted by Eq. 4.

3.2. Correlation between σ_0^*, k and the nature of the solvent

Average values of S_0, σ_0^* and k, together with some physical properties of the solvents, are given in Table 2. The values of S_0 and σ_0^* should depend on the molar absorptivity of the solvent, and the instrumental noise should also contribute to σ_0^*. The solvent showing the lowest noise in the absence of a dye was carbon tetrachloride. The S_0, σ_0 and σ_0^* values increased in the order water < methanol ≈ ethanol < *n*-butanol < *n*-pentanol. The values of these parameters also increased for water–methanol, water–propanol and water–glycerine mixtures when the amount of alcohol in the mixture increased. This agrees with the expected increase in the molar absorptivity of the solvents.

An attempt to correlate k with some physical and mechanical properties of the solvents is made in Table 2. Since k has been defined as the increase of noise divided by the increase of the TLS signal (Eq. 3), and not as that divided by the

Table 1
Values of S_0, σ_0^* and k obtained in different days for several solvents and absorbing compounds

Compound	Solvent	Day	$S_0 \pm \sigma_0$ (mV)	σ_0^* (mV)	$k \times 10^3$	r [c]
$K_2Cr_2O_7$	Water	1	100 ± 1	4.9 ± 0.9	8.4 ± 0.6	0.995
		2	104 ± 2	3.2 ± 0.7	9.0 ± 0.5	0.997
		3	89 ± 2	3.8 ± 1.9	10.4 ± 1.3	0.98
		7	103 ± 5	4.6 ± 0.4	9.7 ± 0.3	0.96
		8	98 ± 4	2.7 ± 1.0	9.6 ± 0.7	0.995
		9	117 ± 3	3.0 ± 0.7	7.3 ± 0.6	0.994
		10	112 ± 2	2.7 ± 0.9	5.8 ± 0.7	0.98
		13	101 ± 5	4.9 ± 1.4	8.0 ± 2.0	0.97
		13 [a]	126 ± 4	3.9 ± 0.5	3.8 ± 0.7	0.96
		13 [b]	83 ± 4	3.9 ± 0.3	4.7 ± 0.5	0.99
Methyl red	Water	11	96 ± 3	5.9 ± 1.5	5.3 ± 1.2	0.98
		12	117 ± 3	–	–	–
Methyl red	Acetone	1	174 ± 7	10.0 ± 3.0	22.0 ± 4.0	0.97
Methyl red	Methanol	2	231 ± 8	5.4 ± 1.1	16.9 ± 0.9	0.997
		3	233 ± 20	8.9 ± 1.2	14.0 ± 0.7	0.997
		4	226 ± 6	6.7 ± 1.3	5.8 ± 0.9	0.93
		7	272 ± 3	8.5 ± 0.3	17.9 ± 0.7	0.98
Methyl red	Ethanol	4	223 ± 5	5.1 ± 0.1	6.4 ± 0.1	0.999
		13	214 ± 7	7.5 ± 0.3	13.1 ± 0.5	0.999
		13 [a]	–	7.0 ± 1.4	8.0 ± 2.0	0.97
		13 [b]	228 ± 9	9.8 ± 1.4	8.8 ± 1.4	0.96
Methyl red	*n*-Butanol	2	231 ± 1	9.5 ± 4.0	14.9 ± 3.0	0.96
		3	228 ± 7	18.4 ± 0.6	15.8 ± 0.6	0.999
		4	237 ± 4	11.5 ± 0.5	9.1 ± 0.4	0.998
	n-Pentanol	4	356 ± 10	17.7 ± 0.6	6.7 ± 1.5	0.96
Methyl red	Water–glycerine, 1:1	11	588 ± 20	26.0 ± 1.3	13.5 ± 1.5	0.994
Methyl red	Water–glycerine, 1:3	11	633 ± 50	36.3 ± 2.0	83.7 ± 4.0	0.999
Methyl red	Water–methanol, 1:4	12	235 ± 5	–	–	–
Methyl red	Water–propanol, 1:4	12	232 ± 6	–	–	–
PAN	Carbon tetrachloride	5	187 ± 10	2.8 ± 2.0	18.0 ± 2.0	0.994
		6	209 ± 10	3.4 ± 2.0	18.2 ± 3.0	0.98
PAN	Chloroform	5	272 ± 16	9.2 ± 5.0	10.0 ± 4.0	0.855
		6	301 ± 15	9.0 ± 1.3	14.3 ± 1.3	0.990

[a] Data obtained with the 18 μl cell.
[b] Data obtained with the 8 μl cell.
[c] From the regression lines, 5–10 points.

Table 2
Average values of S_0, σ_0^* and k compared to some thermo-optical and mechanical properties of the solvents [a]

Solvent	S_0 (mV)	σ_0^* (mV)	$k \times 10^3$	n	$-dn/dT \times 10^4$ ($°C^{-1}$)	$(-dn/dT)/\kappa$ (cm mW^{-1})	η (cP)	$(-d\eta/dT) \times 10^3$ (cP $°C^{-1}$)	ρ (g ml^{-1})	$(-d\rho/dT) \times 10^3$ (g ml^{-1} $°C^{-1}$)
Water	102	3.9	9.2	1.334	0.81	0.136	0.89	20	1.00	0.28
Methanol	241	7.4	13.7	1.342	3.94	1.950	0.55	8.7	0.81	0.93
Ethanol	–	6.3	9.8	1.359	4.0	2.395	1.10	20	0.79	0.86
n-Butanol	232	13.1	13.3	1.397	–	–	2.62	65	0.82	0.70
n-Pentanol	–	–	–	1.408	–	–	3.54	110	0.80	0.70
Glycerine	–	–	–	1.474	–	–	954	86,000	1.27	0.55
Acetone	–	–	–	1.357	5.42	2.853	0.136	2.8	0.81	1.11
Chloroform	287	9.1	12.2	1.444	6.03	5.154	0.54	6.6	1.53	1.86
Carbon tetrachloride	198	3.1	18.1	1.459	6.12	5.942	0.91	13	1.63	1.91

[a] Data for 25°C; dn/dT and κ data are from reference 13; $d\rho/dT$ data are from Ref. [23]; other data are from Ref. [24].

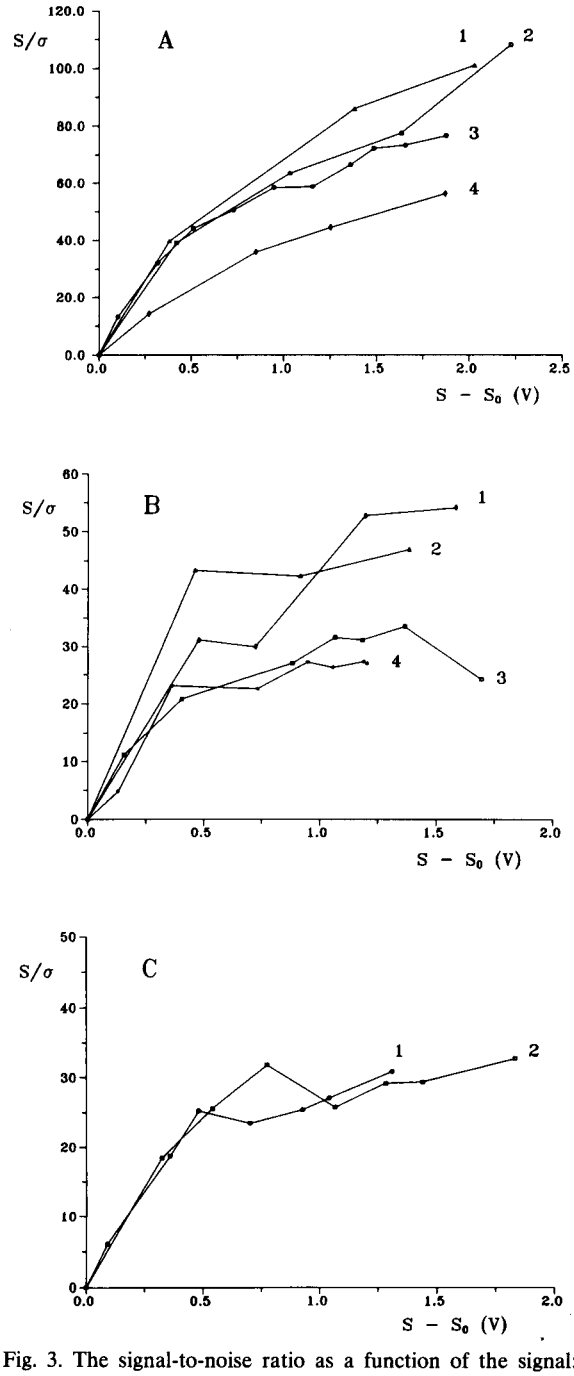

Fig. 3. The signal-to-noise ratio as a function of the signal: Part A, methyl red in: (1) ethanol; (2) methanol; (3) water; (4) n-butanol. Part B, PAN in: (1) chloroform; (2) carbon tetrachloride; (3) ethanol; (4) methanol. Part C, EBT in: (1) methanol; (2) ethanol.

increase of the absorbance, it should not depend on $|dn/dT|/\kappa$. Convection is produced by the differences of density in a gravitational field, therefore, k should increase when the thermal coefficient of the density, $d\rho/dT$, increases. Since the temperature differences generated by the thermal lens effect are very small, i.e., of the order of 0.1 K [13], the density gradient should be also very small. However, a strong convective stream can be visually observed with a magnifying lens in the presence of suspended particles.

Other physical properties are inter-correlated with $d\rho/dT$ and k, which makes interpretation difficult. Thus, convection is controlled by the viscosity and, therefore, the speed of the convective stream which crosses through the thermal gradient should decrease as the viscosity increases. Owing to the small thermal gradient, the viscosity gradient should also be very small. However, since $d\eta/dT$ is larger than $d\rho/dT$ and convection is produced by the latter, probably the effects of the viscosity gradient on convection cannot be neglected.

The convective stream is more intense in the central region of the thermal gradient, where the temperature is higher and the viscosity is lower than in the surroundings. The absolute value of the thermal coefficient of the viscosity increases with the viscosity of the solvent. Therefore, in viscous solvents the speed of the convective stream in the central part of the gradient can be much higher than in the surroundings. This could also make turbulences higher than in less viscous solvents. In this case, the effects associated to η and $d\eta/dT$ would be inversely correlated, whereas these solvent properties are directly correlated, which would partially compensate or cancel their possible influence on k.

3.3. *Influence of several experimental conditions on σ_0^* and k*

Aqueous solutions of potassium dichromate were used to study the influence of the optical alignment on σ_0^* and k. The beams were made coaxial in the cell region, and the alignment was refined until an almost perfectly symmetrical image was obtained on the detector entrance. Then,

the probe beam was both horizontally and vertically displaced with respect to its normal position, and data were taken. It was observed that the noise increased slightly when the probe beam was not perfectly coaxial with the pump beam.

The influence of the volume and shape of the measurement cell was also studied. The 18 μl and 8 μl flow cells were filled up from a peristaltic pump, and the pump was stopped at least 30 s before taking the measurements. The results obtained with aqueous potassium dichromate solutions and methyl red solutions in ethanol are also given in Table 1. The σ_0^* values were similar to those obtained with a 5-ml cell, but the k values were reduced in a 35–50% with the 18- and the 8-μl cells. Therefore, the narrow channel cells effectively slowed down the increase of the convective noise with increasing signal.

A very large value of σ_0 was obtained when reagent grade chloroform was used ($\sigma_0 = 350$ mV). It was presumed that the large amount of noise was due to the presence of particles in the solvent. After forcing the solutions through a 0.22-μm pore size filter, the value of σ_0 was reduced to 10.6 ± 0.7 mV. When HPLC grade chloroform was used instead, the noise was similar before and after filtering the solutions, with $\sigma_0 = 6 \pm 4$ and 9.0 ± 0.9 mV, respectively. Thus, the use of solvents of HPLC-grade is recommended. When solvents of a lower quality are only available, the noise may be decreased by filtering the solutions.

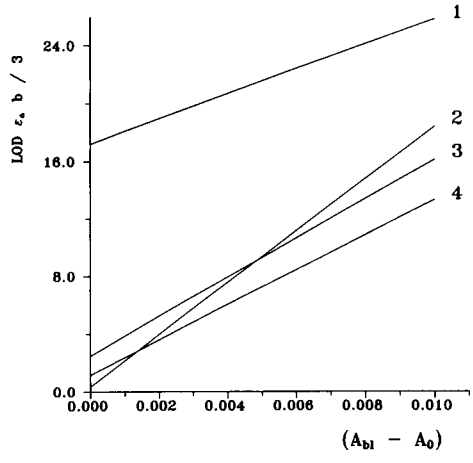

Fig. 4. Representation of Eq. 7 for several solvents at increasing values of $(A_{bl} - A_0)$: (1) water; (2) carbon tetrachloride; (3) methanol; (4) chloroform. The values $P = 100$ mW and $\lambda_{pr} = 633$ nm were used to calculate m.

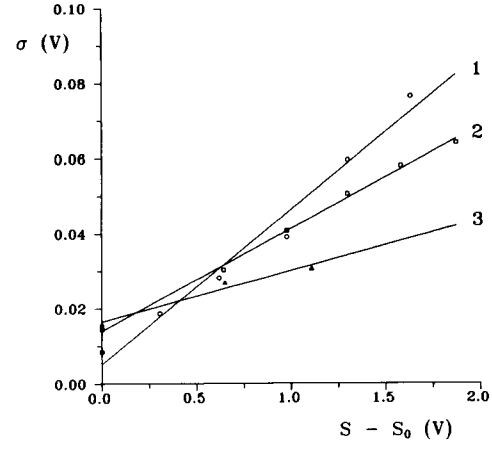

Fig. 5. Dependence of the noise on the signal at increasing concentrations of potassium dichromate in water, and at various pump frequencies: (1) 4 Hz; (2) 8 Hz; (3) 16 Hz.

3.4. Reproducibility of σ_0^* and k

The reproducibility of the σ_0^* and k values was studied with solutions of potassium dichromate in water, and methyl red in methanol and n-butanol, performing the TLS measurements in different days (see Table 1). Higher values of the corresponding coefficient of variation (C.V.) should be expected at increasing values of the noise parameters, σ_0^* or k. However, the C.V. values obtained are useful to estimate the reliability of the σ_0^* and k values. The inter-day reproducibility of σ_0^* was C.V. = 26, 22 and 35% for water, methanol and n-butanol, respectively. Similarly, the inter-day reproducibility of k was 18, 40 and 27%, respectively. In spite of the large C.V. values, almost in all cases the values of σ_0^* and k obtained in different days maintained the order water < methanol < n-butanol, and water < methanol ≈ n-butanol, respectively.

3.5. Dependence of the LOD on the absorbance of the blank

Both σ_0^* and k can be used to characterize solvents in terms of the convective noise, and to

establish how the LOD increases with the absorbance of the blank. For a given value of the signal of the blank solution, S_{bl}, the LOD (in concentration units) is given by

$$\mathrm{LOD} = \frac{3\sigma_{bl}}{m\varepsilon_a b} = \frac{3}{m\varepsilon_a b}\left[\sigma_0^* + k(S_{bl} - S_0)\right] \quad (5)$$

where ε_a is the molar absorptivity of the analyte, b is the optical pathlength, and $(m\varepsilon_a b)$ is the sensitivity. From Eqs. 1 and 2 we have

$$m = 0.52\frac{2.303P(-\mathrm{d}n/\mathrm{d}T)}{\lambda_{pr}\kappa} \quad (6)$$

where the quadratic term has been neglected. If A_{bl} and A_0 are the absorbance of the blank and solvent, respectively, we have $(S_{bl} - S_0) = m(A_{bl} - A_0)$, and

$$\mathrm{LOD} = \frac{3}{\varepsilon_a b}\left[\frac{\sigma_0^*}{m} + k(A_{bl} - A_0)\right] \quad (7)$$

Therefore, when A_{bl} increases, the LOD increases with a slope proportional to k and to $1/\varepsilon_a$, which does not depend on the thermo-optical properties of the medium. A plot of Eq. 7 for several solvents at increasing values of $(A_{bl} - A_0)$ is shown in Fig. 4.

In the absence of an absorbing species in the blank solution, other than the solvent, the second term in Eqs. 5 and 7 is zero, and the LODs of the solvents follow the order of the $|\mathrm{d}n/\mathrm{d}T|/\kappa$ values, i.e., carbon tetrachloride < chloroform < methanol < water. Instead, at large values of A_{bl}, the LOD will depend mainly on k, rather than on $|\mathrm{d}n/\mathrm{d}T|/\kappa$, and a solvent with a lower value of k can be better than other solvents with better thermo-optical properties, but with larger values of k.

In the literature, water is not considered as a good solvent for TLS because of the very low value of $|\mathrm{d}n/\mathrm{d}T|/\kappa$, which leads to a low sensitivity. Therefore, the use of water–ethanol or water–acetone mixtures has been recommended. However, very low values of S_0 and σ_0^* are achieved in water, which partially compensates for the poor thermo-optical properties. Water has also a low value of k, which decreases the differences between water and other solvents of better thermo-optical properties, at large values of A_{bl}.

Finally, the influence of the pump frequency was studied. The σ vs. $(S - S_0)$ straight lines obtained with series of potassium dichromate aqueous solutions at 4, 8 and 16 Hz are shown in Fig. 5. When the pump frequency increased, σ_0^* also increased (5×10^{-3} at 4 Hz and 16×10^{-3} at 16 Hz), and k decreased (41×10^{-3} at 4 Hz and 14×10^{-3} at 16 Hz). However, owing to the lower sensitivity, the LOD as calculated with Eq. 5 increased with a factor of 6× and 16× at 8 and 16 Hz, respectively.

Acknowledgments

This work was supported by the DGICYT of Spain, Project PB90/425. Y. Martín Biosca thanks the Consellería de Cultura, Educació i Ciència de la Generalitat Valenciana for the FPI grant.

References

[1] M. Miyaishi, T. Imasaka and N. Ishibashi, Anal. Chim. Acta, 124 (1981) 381.
[2] R.A. Leach and J.M. Harris, J. Chromatogr., 218 (1981) 15.
[3] K. Fujiwara, W. Lei, H. Uchiki, F. Shimokoshi, K. Fuwa and T. Kobayashi, Anal. Chem., 54 (1982) 2026.
[4] K. Fujiwara, H. Uchiki, F. Shimokoshi, K. Tsunoda, K. Fuwa and T. Kobayashi, Appl. Spectrosc., 36 (1982) 157.
[5] K. Fujiwara, K. Kishibe, H. Uchiki, F. Shimokoshi, K. Fuwa and T. Kobayashi, Anal. Biochem., 127 (1982) 164.
[6] T.G. Nolan, B.K. Hart and N.J. Dovichi, Anal. Chem., 57 (1985) 2703.
[7] J.A. Alfheim and C.H. Langford, Anal. Chem., 57 (1985) 861.
[8] T. Berthoud and N. Delorme, Appl. Spectrosc., 41 (1987) 15.
[9] G. Bidoglio, G. Tanet, P. Cavalli and N. Omenetto, Inorg. Chim. Acta, 140 (1987) 293.
[10] G. Ramis Ramos, M.C. García Alvarez-Coque, B.W. Smith, N. Omenetto and J.D. Winefordner, Appl. Spectrosc., 42 (1988) 341.
[11] J.M. Sanchis Mallols, R.M. Villanueva Camañas and G. Ramis Ramos, Chromatographia, 38 (1994) 365.
[12] M.D. Morris and K. Peck, Anal. Chem., 58 (1986) 811A.
[13] N.J. Dovichi, CRC Crit. Rev. Anal. Chem., 17 (1987) 357.
[14] J. Georges and J.M. Mermet, Analusis, 16 (1988) 203.

[15] V.I. Grishko and I.G. Yudelevich, Zh. Anal. Khim., 44 (1989) 1753.
[16] G. Ramis Ramos, Anal. Chim. Acta, 283 (1993) 623.
[17] J.P. Gordon, R.C.C. Leite, R.S. Moore, S.P.S. Porto and J.R. Whinnery, J. Appl. Phys., 36 (1965) 3.
[18] C. Hu and J.R. Whinnery, Appl. Optics, 12 (1973) 72.
[19] C.A. Carter and J.M. Harris, Appl. Optics, 23 (1984) 476.
[20] L.E. Buffet and M.D. Morris, Appl. Spectrosc., 37 (1983) 455.
[21] E.F. Simó Alfonso, M.A. Rius Revert, M.C. García Alvarez-Coque and G. Ramis Ramos, Appl. Spectrosc., 44 (1990) 1501.
[22] E.F. Simó Alfonso, M.C. García Alvarez-Coque, G. Ramis Ramos, A. Cladera Forteza, M. Estela Ripoll and V. Cerdá Martín, Anal. Lett., 25 (1992) 573.
[23] E.W. Washburn (Ed.), International Critical Tables of Numerical Data, Physics, Chemistry and Technology, Vol. 3, National Research Council, New York, 1928.
[24] R.C. Weast and M.J. Astle, CRC Handbook of Chemistry and Physics, 60th edn, Boca Raton, FL, 1980.

ELSEVIER

Analytica Chimica Acta 296 (1994) 295–304

ANALYTICA CHIMICA ACTA

Determination of gold at the ultratrace level in natural waters

R. Cidu [a,*], L. Fanfani [a], P. Shand [b], W.M. Edmunds [b], L. Van't dack [c], R. Gijbels [c]

[a] *University of Cagliari, Department of Earth Sciences, Via Trentino 51, I-09127 Cagliari, Italy*

[b] *British Geological Survey, Hydrogeology Research Group, Maclean Building, Crowmarsh Gifford, Wallingford OX10 8BB, UK*

[c] *University of Antwerp (UIA), Department of Chemistry, B-2610 Antwerp-Wilrijk, Belgium*

Received 23 September 1993; revised manuscript received 29 April 1994

Abstract

Several methods for the preconcentration of dissolved gold in natural waters were evaluated for use with graphite furnace atomic absorption spectroscopy (GFAAS) or inductively coupled plasma mass spectrometry (ICP-MS). An anion exchange method prior to GFAAS, and a solvent extraction method prior to ICP-MS both proved to have similar recoveries, low limits of detection (0.4 and 0.2 ng l^{-1}, respectively, for a 2-l sample) and good reproducibility. Parallel analyses of particulate gold were also carried out by instrumental neutron activation analysis (INAA) with detection limits between 0.04 and 0.5 ng l^{-1} depending on the volume of filtered water, to provide a complete evaluation of transported gold. These methods were subsequently tested on stream, spring and adit water samples, to check the accuracy of methods for natural waters. Results obtained by ICP-MS and GFAAS on natural water samples were comparable. The maximum dissolved gold concentration was 3 ng l^{-1}, and particulate gold formed less than 50% of the total amount of gold transported. No significant variation was found in the dissolved gold content of one spring water sample monitored monthly over a one year period.

Keywords: Atomic absorption spectrometry; Inductively coupled plasma mass spectrometry; Gold; Preconcentration; Waters

1. Introduction

Geochemical exploration for gold has been focused largely on the determination of gold in rock, stream sediment and soil samples. Until recently, hydrogeochemical prospecting for gold has not been considered to be a particularly promising method [1], due to the low concentrations of gold in natural waters at ambient conditions of redox potential (Eh), pH and temperature. Nevertheless, recent work [2–9] has shown that gold anomalies in solution, up to several tens or even hundreds of nanogrammes per litre (ng l^{-1}), occur in association with different gold deposits. These results suggest that gold may be transported in solution in natural waters, confirming field evidence, e.g., dendritic gold and nugget formation, that remobilisation of gold does occur in certain environments [10].

Few techniques are suitable for gold analysis in waters because high sensitivity is required. The techniques most commonly used are instrumental

* Corresponding author.

SSDI 0003-2670(94)00215-8

neutron activation analysis (INAA) and graphite furnace atomic absorption spectroscopy (GFAAS). More recently, inductively coupled plasma mass spectrometry (ICP-MS) has been used effectively for both stream [9] and sea waters [11]. Concentrations of dissolved gold at the ng l^{-1} level are too low for the direct application of the above mentioned analytical techniques; hence, a preconcentration stage is required prior to analysis.

Various types and combinations of preconcentration methods have been described, including evaporation, use of activated charcoal, anion exchange and solvent extraction. Hamilton et al. [12] noted that, although evaporation methods are potentially the most accurate, the process is lengthy. Although evaporation has been used independently [13], it has been more successful when used with other methods, including solvent extraction [14] and anion exchange [11]. The preconcentration of ionic and colloidal gold onto activated charcoal has been described by Chernyayev et al. [15] and Hamilton et al. [12]: the activated charcoal is filtered and the residue analysed by INAA. Hall et al. [16] also proposed activated charcoal for concentration but extracted the gold into 4-methylpentan-2-one (methyl isobutyl ketone, MIBK) prior to analysis by GFAAS, however, pH adjustment and intense mixing of the sample were prerequisites to the complete adsorption of gold. Another possible preconcentration method is freeze-drying prior to INAA [17], although this method has not been specifically used for dissolved gold analysis.

Chao [18] and Gosling et al. [1] used anion exchange onto AG 1 resin as a preconcentration method for fresh waters, evaluating the method using a standard gold ionic solution. McHugh [19] also reported a method to concentrate Au by batch extraction using AG 1-X8 resin from which the Au could be eluted with an acetone–nitric acid solution, making ashing of the resin unnecessary. This method, however, takes as long as evaporation. Hamilton et al. [12] evaluated the use of ion exchange resins and concluded, in agreement with Schiller and Cook [20], that they were inefficient collectors of colloidal gold. A field method was developed by Hou [21] to preconcentrate dissolved gold onto pretreated polyurethane foam. The use of resins for the concentration of dissolved gold from sea water has been extensively used [11,12,22]. Solvent extraction into MIBK has been commonly used [9,23], frequently in combination with other methods, e.g., anion exchange [3,18] or adsorption onto activated charcoal [16]. The MIBK may be analysed directly by GFAAS [19] or evaporated and collected in dilute aqua regia prior to analysis by ICP-MS [9].

In this paper, some of the available analytical approaches for the analysis of soluble gold were adapted for use with GFAAS or ICP-MS, in order to obtain lower detection limits and less time-consuming analytical procedures (Fig. 1). The selected methods are critically reviewed and the analytical techniques compared using different natural water samples.

Most studies on hydrogeochemical prospecting for gold have been aimed at the dissolved fraction using membrane filter pore sizes in the range of 0.1 to 1.2 μm. Correlation of dissolved with particulate gold in areas of known gold occurrence is, however, not generally observed [1,2]. As stated by Hamilton et al. [2], the apparent scatter of particulate gold contents is probably due to the

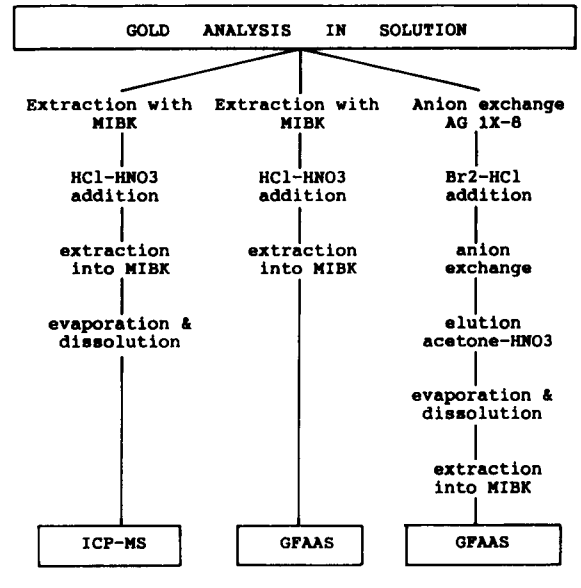

Fig. 1. Flow chart of the analytical procedures for the dissolved gold analysis.

variability, both in time and space, of the suspended matter load. In this paper, the total amount of transported gold was also studied by the analysis of the particulate fraction retained on a membrane filter.

2. Experimental

2.1. Reagents

Reagents used were: BDH Aristar HNO_3 and HCl; BDH Spectrosol 4-methylpentan-2-one (methyl isobutyl ketone, MIBK); Aldrich bromine, hydrobromic acid, and spectrophotometric grade acetone; Bio-Rad AG 1-X8 resin (100–200 mesh, chloride form); BDH Spectrosol 1000 mg l^{-1} gold standard solution in 0.5 mol l^{-1} HCl; high purity water by the Millipore purification system Milli-Q.

2.2. Sampling

Natural water samples were collected and filtered in situ using an all-plastic filtration system. A 0.4 μm pore-size polycarbonate membrane filter (47 mm diameter, Nuclepore type 111130) was used in order to separate the particulate gold. The filtration system was copiously rinsed with water sample before use. Filtered samples were collected in polyethylene bottles, pre-cleaned with a mixture of 2% HNO_3 and 6% HCl (24 h storage, at least), and subsequently rinsed with Milli-Q water and filtered water sample.

2.3. Sample stabilisation

In order to prevent adsorption of gold onto the container walls and to convert the gold to an Au–chloride complex, 1-l samples for the determination of gold in solution by MIBK solvent extraction prior to GFAAS analysis, and 2-l samples for the determination of gold in solution by MIBK solvent extraction prior to ICP-MS analysis, were acidified in situ after filtration using 10 ml of HNO_3 plus 30 ml of HCl, and 20 ml of HNO_3 plus 60 ml of HCl, respectively ($\equiv$ 4% aqua regia).

In the laboratory, 20 ml of a solution containing 5% (v/v) bromine in concentrated HCl, were added to a 2-l filtered water sample for the determination of gold in solution by anion exchange prior to GFAAS analysis. This procedure liberates any gold adsorbed onto the container walls and also converts the gold present into ionic Au–bromide/chloride complexes.

2.4. GFAAS

Preconcentration by solvent extraction into MIBK

This preconcentration method uses chloride as the complexing agent for ionic gold and MIBK as the chelating agent which can then be analysed directly by GFAAS. In the laboratory, the 1-l filtered and acidified sample was transferred to a separatory funnel fitted with a PTFE cap and stopcock. 27 ml of MIBK were added and the mixture mechanically shaken for 10 min. After settling for at least 5 min, the supernatant MIBK layer (about 1 ml) was collected in a PTFE vial, ready for analysis. A preconcentration factor of about 1000 was thus obtained.

Preconcentration by anion exchange using AG 1-X8 and subsequent MIBK extraction

This preconcentration method uses bromide and chloride as complexing agents and an anion exchange resin onto which the gold complexes are selectively adsorbed, prior to elution with an acetone–HNO_3 mixture, and finally, extraction into MIBK.

In the laboratory, 5 g of AG 1-X8 anion exchange resin were added to the 2-l filtered and acidified sample and mechanically shaken for 30 min. The sample was poured through a 20 $\times$ 300 mm column fitted with a porous glass disc. Gold was eluted from the resin with 80 ml of an acetone–HNO_3–Milli-Q solution (100:5:5, v/v) into a 200-ml glass beaker at a flow-rate of about 100 ml h^{-1}. The solution was evaporated (at 60°C) to dryness and the residue dissolved in 8 ml of bromine–hydrobromic acid (0.5:100, v/v) solution and left to stand for 30 min. This was then transferred to a 50-ml separatory funnel fitted with a PTFE cap and stopcock. 2 ml of MIBK were used to rinse the beaker, in order to extract

any remaining Au and transferred into the separatory funnel; then the beaker was rinsed with 8 ml of Milli-Q water which was also poured into the separatory funnel. The mixture was shaken for 3 min and allowed to settle for 2 min. The supernatant MIBK layer was left in the funnel and 8 ml of 0.1 M hydrobromic acid saturated with MIBK were added to remove any extracted iron. This mixture was shaken for 30 s and allowed to settle for 2 min whereupon the supernatant MIBK layer (about 1 ml) was collected in a PTFE vial, ready for analysis. A preconcentration factor of about 2000 was thus obtained.

Operating conditions

The gold contained in the MIBK was analysed using a Perkin Elmer Zeeman/3030 GFAAS system equipped with an autosampler. A pyrolytically coated graphite tube with platform was used. Instrumental parameters are listed in Table 1.

Calibration

Calibration was performed using appropriate dilutions of a 1000 mg l^{-1} Au standard solution, stabilised to 4% (v/v) aqua regia, and a blank solution of 4% aqua regia in Milli-Q water; linearity was up to 25 μg l^{-1} Au. For the solvent extraction method, 1-l solutions containing 5, 10, 20 and 40 ng l^{-1} Au were prepared, while for the anion exchange method 2-l solutions containing 0.5, 1, 2 and 5 ng l^{-1} Au were prepared, in both cases using either Milli-Q or a low salinity bottled water (e.g., Evian). These were then processed to determine recoveries following the procedures described above, and linear responses were observed.

2.5. ICP-MS

Preconcentration by solvent extraction into MIBK

In the laboratory, the 2-l filtered and acidified water sample was transferred to a separatory funnel, 63 ml of MIBK added and shaken vigorously for 6 min. After settling for 4 min the supernatant MIBK layer (about 3 ml) was collected in a PTFE beaker. The separatory funnel was washed with a few ml of aqua regia to remove any MIBK still attached and this was added to the PTFE beaker. The mixture was evaporated, using infrared lamps, to about 0.5 ml followed by the addition of about 1 ml of concentrated aqua regia. This was again evaporated to about 0.25 ml and made up to volume in a 5 ml graduated flask. A preconcentration factor of 400 was thus obtained.

Operating conditions

The gold contained in the diluted aqua regia was analysed using a VG PlasmaQuad ICP-MS. Instrumental parameters are listed in Table 1.

External drift correction did not correct sufficiently well for changes in the instrument response over time, and therefore, several internal standards were tested on gold-spiked solutions. ^{115}In was found to give very poor results during the correction procedure, but isotopes of Pt (194,

Table 1
GFAAS and ICP-MS instrumental parameters for the analysis of gold in solution

GFAAS		ICP-MS	
Wavelength	242.8 nm	Forward power	1350 W
Slit	0.7 nm	Reverse power	< 5.0 W
Integration time	5.0 s	Coolant flow	13.5 l/min
Injection volume	50.0 μl	Auxiliary flow	0.5 l/min
Drying (two steps)	80–150°C	Nebulizer flow	0.73 l/min
Charing	800°C	Sample flow	0.8 ml/min
Atomization (gas stop)	2200°C	Number of repeats	5
Purge gas	Argon	Points per peak	5
Calibration mode	Peak area	DAC step	5
Background correction	Zeeman	Number peak jump scan	100
		Peak jump dwell time	10.24 ms

195 and 196 a.m.u.) and Tl (203 and 205 a.m.u.) gave both precise and accurate results. However, the isotopes of Pt were preferred as internal standards because some of the investigated water samples contained Tl which was also extracted by MIBK.

Scanning and peak hopping modes were compared in order to determine relative precision. Both modes produce similar reproducibility, but increased precision and sensitivity were obtained in the peak hopping mode. It was also observed that precision could be improved in the peak hopping mode using longer dwell times on each peak and by decreasing the number of scans with the same total analysis time.

Memory effects due to Au becoming attached to tubing, nebuliser and torch-box assembly were observed during analysis. Wash times between samples of approximately 5 min with 4% aqua regia were necessary to reduce the Au counts to background level, which was checked prior to each analysis.

Calibration

Calibration was performed using appropriate dilutions of a 1000 mg l^{-1} Au standard solution, stabilised to 4% aqua regia, and a blank solution of 4% aqua regia in Milli-Q water. 2-l solutions containing 1, 2, 5, 10 and 15 ng l^{-1} Au were prepared, using either Milli-Q or a low salinity bottled water (e.g., Evian), acidified to 4% aqua regia, and processed using the same procedure as for samples to determine recoveries.

2.6. Determination of gold in the suspended matter

In the present study, suspended matter is defined as material which does not pass through a 0.4-μm pore-size membrane filter. The particulate gold content, together with concentrations for about 50 other elements, were determined by INAA, after pelletising the membrane filter, together with a paper filter (55 mm diameter, Whatman 541). The irradiations and analysis scheme comprised three irradiations, in different irradiation channels of the "Thetis" reactor (Institute for Nuclear Sciences of the State University at Ghent, Belgium) and subsequent measurements on a high-purity germanium semiconductor detector [24]. Calibration was performed by means of spotting appropriate amounts of synthetically prepared single element standard solutions onto a Whatman filter paper.

The amount of suspended material may be related to the flow rate and turbulence and thus be variable over time and/or space. Consequently, it is advisable to normalise the suspended matter composition against an immobile component (e.g., Al). This will highlight any influence other than mechanical weathering.

3. Results and discussion

The use of activated charcoal for gold preconcentration prior GFAAS analysis, using the method reported by Hall et al. [16], proved unsuccessful due to a large variability of the atomic absorption background; this was due to the several steps necessary to complete the preconcentration procedure. In addition, relatively high amounts of gold were detected by INAA in different brands of commercially available activated charcoal (with concentrations ranging from 0.5 to 7.2 ng g^{-1}), while important variations were also observed in different batches from single brands. Due to the above problems, the attainable detection limit using a 1-l sample was of the order of 10 ng l^{-1} which proved to be too high for an investigation of natural waters.

Dissolved gold was also analysed by INAA after preconcentration by means of freeze-drying. Filtered aliquots of 100 ml are freeze-dried in pure low-density polyethylene bags (Pinky Pack) and the residue is pelletised together with the plastic bag. The freeze-drying procedure is time consuming but it concentrates all ions, including anions and major cations. As a consequence, the detection limit of gold, or for any other element, is highly dependent on the total dissolved content of the water samples due to the induced activity of the major components (mostly Na and Br). Losses of volatile elements are minimal, except for F and Cl which are lost because the water samples are preserved, after filtration in the field, with 2 ml ultrapure nitric acid [17,24].

Table 2
Blank values for day-to-day analysis: two blanks for the HCl–MIBK and AG 1-X8 preconcentration prior to GFAAS, and five blanks for the HCl–MIBK preconcentration prior to ICP-MS

	HCl–MIBK GFAAS		AG 1-X8 GFAAS		HCl–MIBK ICP-MS	
	ng/l	S.D.	ng/l	S.D.	ng/l	S.D.
	0.15	0.09	0.31	0.15	1.0	0.37
	0.22	0.13	0.52	0.11	0.76	0.16
	0.12	0.08	0.39	0.15	0.39	0.05
	0.18	0.12	0.35	0.12	0.24	0.09
	0.10	0.09	0.55	0.11	0.13	0.07
	0.63	0.51	0.25	0.09	0.56	0.14
	0.15	0.10	0.35	0.16	0.17	0.03
	0.18	0.12	0.55	0.11	0.13	0.07
	0.21	0.15	0.28	0.10	0.18	0.06
	0.15	0.10	0.32	0.15	0.17	0.08
	0.57	0.38	0.25	0.09		
	0.14	0.09	0.27	0.16		
	0.48	0.35	0.35	0.15		
	0.15	0.11	0.55	0.11		
	0.18	0.13	0.27	0.16		
Mean	0.24	0.17	0.37	0.13	0.37	0.11
S.D.	0.21	0.13	0.12	0.03	0.29	0.09
n	30		30		50	

Because of the unfavourable detection limits observed for the activated charcoal and freeze-drying preconcentration steps prior to GFAAS and INAA analysis, solvent extraction and anion exchange were further investigated as preconcentration methods for dissolved gold prior to GFAAS or ICP-MS analysis.

3.1. Blanks

Blank values for the methods depend on both the reagents used and on instrument performance, and thus can be variable (Table 2). Blanks (duplicate for the HCl–MIBK and AG 1-X8 prior to GFAAS, and five blanks for the HCl-MIBK prior to ICP-MS analysis) were extracted together with each batch of samples and analysed in order to determine detection limits (defined as three times the standard deviation on the blank). The same quality of reagents was used for the methods over time to reproduce the background response. Day-to-day differences in instrument performance, affecting sensitivity, vary more for ICP-MS than GFAAS giving rise to a wider spread in detection limits. The blank values encountered in GFAAS are dependent on the preconcentration methods used, with the bromine present in the MIBK in the anion exchange method probably responsible for an enhanced background.

Blank levels for Au in the suspended matter,

Table 3
Recoveries for individual gold concentrations using the 1-l solution for the HCl–MIBK method prior to GFAAS analysis, and the 2-l solution for the two other methods

	HCl–MIBK GFAAS				AG 1-X8 GFAAS				HCl–MIBK ICP-MS				
Au (ng/l)	5	10	20	40	0.5	1	2	5	1	2	5	10	15
Recovery (%)	58	61	60	63	81	88	83	86	84	91	84	81	84
S.D.	34	24	16	17	16	15	13	15	14	8	12	11	10
n	(13)	(13)	(11)	(7)	(15)	(15)	(15)	(7)	(3)	(3)	(13)	(11)	(4)
Mean ± S.D. (*n*)	59 ± 25 (44)				84 ± 14 (52)				83 ± 12 (34)				

Table 4
Gold concentrations in solution and suspension, and other selected parameters of natural waters

	Flow (l/s)	pH	Eh (mV)	TDS (mg/l)	HCO_3^- (mg/l)	Cl^- (mg/l)	SO_4^{2-}	Dissolved gold		Particulate gold INAA (ng/l)	
								HCl–MIBK ICP-MS (ng/l)	AG1-X8 GFAAS (ng/l)		
Wales											
HD-126	0.3	5.2	388	330	4	11	208	3.0	2.6	0.27	adit
HD-145	0.2	5.9	nd [a]	84	nd	10	47	1.1	nd	0.13	adit
HD-152	0.2	5.1	380	187	19	15	5	0.3	0.4	0.06	adit
PL-14b	100	6.0	360	14	1	5	3	0.5	0.5	< 0.04	stream
Scotland											
TY-2b	0.3	7.4	260	393	111	5	20	1.1	1.0	0.49	adit
TY-10b	1	5.7	230	18	4	5	2	< 0.3	< 0.4	0.13	stream
TY-73b	50	5.0	320	15	1	6	2	0.3	0.4	0.03	stream
Sardinia											
Os-20	0.03	7.7	405	762	344	150	50	0.8	0.7	0.72	spring
Os-39	0.03	7.2	340	990	439	202	55	0.6	0.5	< 0.06	spring
F-5	0.1	6.7	552	7800	472	2230	2600	0.9	1.0	0.32	stream
F-5	0.06	7.2	420	8200	445	2390	3100	nd	1.3 [b]	nd	stream

[a] Not determined.
[b] By standard addition (spikes: 0, 1, 2 and 5 ng/l Au).

Table 5
Dissolved and particulate gold concentrations, and other selected parameters, as a function of time for a spring water in northern Sardinia

		April 26, 1992	June 18, 1992	July 28, 1992	Sept. 1, 1992	Sept. 28, 1992
Dissolved Au, ng/l (GFAAS)		< 1 [a]	0.7	1.2	1.0	1.5
Dissolved Au, ng/l (ICP-MS)		0.6	0.8			
Particulate Au, ng/l (INAA)		0.07	0.72	0.30	0.14	0.05
Au/Al (10^{-3}) in suspension		0.02	0.13	0.05	0.02	0.01
	Flow (l/min)		pH		Eh (mV)	
Mean ± S.D. (n = 13)	1.5 ± 0.3		8.0 ± 0.2		380 ± 27	

[a] Determined in a 1-l sample.
[b] Duplicate sample (S.D. = 0.2).

as determined by INAA, were found to be 0.18 ± 0.08 ng per filter. This translates into detection limits, defined as three times the standard deviation on the blank, of between 0.04 and 0.5 ng l^{-1} respectively for 6 and 0.5 l of filtered water. These attainable detection limits will however be affected by the amount and composition of the suspended material retained on the membrane filter, due to the enhancement of the gamma-activity of the sample.

3.2. Recoveries

For the MIBK preconcentration method, as used for the GFAAS analysis, the mean recovery percentage is rather low, with, moreover, an uncertainty which deteriorates appreciably for lower gold contents (Table 3). Therefore this methodology is not suitable for the accurate determination of very low dissolved gold contents in natural waters, whilst this simple and fast method can conveniently be used for water samples draining gold deposits in particular environments for which several tens of ng l^{-1} Au in solution have been reported [2–8]. The MIBK preconcentration method, as used prior to ICP-MS analysis and the anion exchange method prior to GFAAS analysis, both have good recovery and reproducibility (Table 3). Recovery tests by standard addition, using the anion exchange method prior to GFAAS analysis, with spikes of 0, 1, 2 and 5 ng l^{-1} Au onto 2-l filtered natural waters, with total dissolved solids (TDS) up to 8 g l^{-1} (see Table 4), were carried out: the mean recovery was 82% (S.D. = 15; n = 12), and matrix effects were not observed.

At ten times the limit of detection, both of the above mentioned MIBK preconcentration methods have significantly different recovery percentage and associated relative uncertainties (Table 3). These dissimilarities are probably due to differences in the steps of the procedure, namely the proportion of organic phase collected and the subsequent direct analysis of this phase by GFAAS, whereas in the ICP-MS method the complete supernatant phase is collected and converted to a final ≡ 4% aqua regia solution for analysis.

4. Analysis of natural waters

The methods using MIBK extraction prior to ICP-MS and anion exchange prior to GFAAS, were tested on different types of surface and ground waters from areas of known gold mineralisation in Wales, Scotland and Sardinia. The waters were of widely differing character with a range in pH, Eh, chemical composition and amount of total dissolved solids.

Results for gold in solution and suspension, together with other selected parameters, are reported in Table 4. Concentrations of gold in solution are based on the analysis of 2-l samples,

Oct. 27, 1992	Nov. 27, 1992	Dec. 21, 1992	Jan. 27, 1993	Feb. 18, 1993	March 24, 1993	April 21, 1993	May 28, 1993
0.9	1.2	1.2	1.6 [b]	0.8	1.6	0.8	0.9
0.10	0.06	0.26	0.16	< 0.03	< 0.08	< 0.08	0.08
0.02	0.01	0.02	0.04				0.03
TDS (mg/l)		HCO_3^- (mg/l)		Cl^- (mg/l)		SO_4^{2-} (mg/l)	
761 ± 26		326 ± 12		148 ± 6		43 ± 4	

blank subtracted, and corrected for recovery. Concentrations of gold in solution obtained by GFAAS and ICP-MS correspond remarkably well, considering the different preconcentration methods and analytical techniques used. The dominant form of gold in these waters is either in true solution or as colloids less than 0.4 μm, with particulate gold varying from less than 10 up to 50% of the total gold.

The spring sample Os-20, draining a catchment incorporating a small gold vein in northern Sardinia, contains detectable dissolved gold, in an area where background concentration of dissolved gold is below the detection limit of 0.4 ng l^{-1}. This spring was selected for monitoring seasonal changes in gold concentration and long-term reproducibility of the methods in natural waters. The spring water was sampled monthly over a period of one year and analysis of gold in solution was carried out within 20 days of sampling. Results of gold in solution and suspension, together with other selected parameters, are shown in Table 5. Good agreement was observed for gold in solution when both the GFAAS and ICP-MS methods were used. Concentrations of dissolved gold do not show significant variation over the monitoring period (mean = 1.1 ± 0.3 ng l^{-1}, n = 12), with other parameters also indicating a substantially stable chemical composition: variations are usually less than 10%. Concentrations of gold in the suspended matter are in the range of not-detectable to 0.72 ng l^{-1}; normalising to an immobile element, e.g., aluminium, substantially reduces the variation.

5. Conclusions

Several methods were tested for their ability to extract and determine gold at the low levels typical of natural waters. Two of the methods produced consistently good recoveries and low detection limits: extraction into MIBK followed by ICP-MS; and anion exchange (AG 1-X8) followed by GFAAS analysis. Tests on natural water samples using both methods showed a remarkable agreement for dissolved gold concentrations. Gold concentrations in solution did not show significant variation in one water sample with stable chemical composition, taken monthly over a period of one year. A comparison of gold contents in solution to that in suspension indicated that the dominant form of gold is in true solution or present as colloids ≤ 0.4 μm. Detection limits using these procedures are low enough to determine the dissolved gold concentrations of waters draining gold bearing rocks. Gold contents in suspension should be normalised to an immobile element, e.g., aluminium, to take into account the effect of suspended matter load.

The different preconcentration and analytical techniques developed can be adapted to suit the needs of most analytical laboratories.

Acknowledgments

The authors wish to thank the Commission of the European Communities for financial support through contract No. MA2M-0041. We would like to thank J.M. Cook for constructive comments on an earlier draft of this manuscript. P. Shand and W.M. Edmunds publish with the approval of the Director of the British Geological Survey (NERC).

References

[1] A.W. Gosling, E.A. Jenne and T.T. Chao, Econ. Geol., 66 (1971) 309.
[2] T.W. Hamilton, J. Ellis, T.M. Florence and J.J. Fardy, Econ. Geol., 78 (1983) 1335.
[3] J.B. McHugh, J. Geochem. Explor., 30 (1988) 85.
[4] M. Bergeron and J. Choinière, J. Geochem. Explor., 31 (1989) 319.
[5] M. Benedetti and J. Boulegue, Earth Planet. Sci. Lett., 100 (1990) 108.
[6] M. Benedetti and J. Boulegue, Geochim. Cosmochim. Acta, 55 (1991) 1539.
[7] J.B. McHugh and W.R. Miller, USGS Open-File Rep. 92-303, (1992).
[8] D.J. Grimes, J.B. McHugh, W.H. Ficklin and A.L. Meier, in D.I. Fletcher (Ed.), SEG ext. abstr. Integrated Methods in Exploration and Discovery, (1993).
[9] R. Cidu and W.M. Edmunds, Trans. Inst. Min. Metall. Sect. B, Appl. Earth Sci., (1990) B153.
[10] A.W. Mann, Econ. Geol., 79 (1984) 38.
[11] K.K. Falkner and J.M. Edmond, Earth Planet. Sci. Lett., 98 (1990) 208.
[12] T.W. Hamilton, J. Ellis and T.M. Florence, Anal. Chim. Acta, 148 (1982) 225.
[13] L.D. Turner and M. Ikramuddin, in A.A. Levinson (Ed.), Precious Metals in the Northern Cordillera, Rexdale, Ontario, Association of Exploration Geochemists, 1982, p. 79.
[14] J.B. McHugh, J. Geochem. Explor., 20 (1984) 303.
[15] A.M. Chernyayev, L.E. Chernyayeva, M.N. Yermeyeva and M.I. Andreyev, Geochem. Int., 6 (1969) 348.
[16] G.E.M. Hall, J.E. Valve and S.B. Ballantyne, J. Geochem. Explor., 26 (1986) 191.
[17] S.H. Harrison, P.D. La Fleur and S.B. Zoller, Anal. Chem., 47 (1975) 1685.
[18] T.T. Chao, Econ. Geol., 64 (1969) 287.
[19] J.B. McHugh, Talanta, 33 (1986) 349.
[20] P. Schiller and G.B. Cook, Anal. Chim. Acta, 54 (1971) 364.
[21] Zh. Hou, J. Geochem. Explor., 33 (1989) 255.
[22] M. Koide, D.S. Lee and M.O. Stallard, Anal. Chem., 56 (1984) 1956.
[23] B.R. Brooks, A.K. Chaterjee and D.E. Ryan, Chem. Geol., 633 (1981) 1263.
[24] W. Blommaert, R. Vandelannoote, L. Van't dack, R. Gijbels and R. Van Grieken, J. Radioanal. Chem., 57 (1980) 383.

ELSEVIER

Analytica Chimica Acta 296 (1994) 305–313

ANALYTICA CHIMICA ACTA

Direct determination of lanthanides, yttrium and scandium in bauxites and red mud from alumina production

M. Ochsenkühn-Petropulu [a,*], Th. Lyberopulu [b], G. Parissakis [a]

[a] *Laboratory of Analytical and Inorganic Chemistry, Department of Chemical Engineering, National Technical University of Athens, Iroon Polytechniu 9, Zographu Campus, 15773 Athens, Greece*

[b] *Chemistry Department, Institute of Geological and Mineral Exploration (IGME), Messogion 70, 11527 Athens, Greece*

Received 8 March 1994; revised manuscript received 6 May 1994

Abstract

An analytical procedure for the rapid, accurate and reproducible determination of lanthanides, yttrium and scandium in iron–aluminium rich matrices as bauxites and red mud from alumina production was developed. After a suitable dissolution, the samples were directly analysed for these elements by inductively coupled plasma atomic emission spectroscopy (ICP-AES), without using any separation or preconcentration step. Some of the investigated elements were also directly determined in the solid samples by x-ray fluorescence analysis (XRF). The optimum conditions and analytical wavelengths were selected by both methods for each investigated element, after detailed studying of the spectral interferences from the major elements from the matrix and the interlanthanide-interferences. In the unique reference bauxitic material BX-N, for which only some proposed values exist, the concentration of nearly all lanthanides, yttrium and scandium Sc could be determined. The precision and accuracy of the described ICP-AES and XRF methods for these elements were tested on the geological standard materials SY-2, SY-3 (Canadian syenites) and the proposed values of BX-N. In this study the enrichment factor of the above mentioned elements in red mud were also determined in comparison to the feed bauxites and the constancy of the concentration level in productions samples, followed up over three years. The obtained results for the lanthanides were evaluated on the basis of chondrite normalized distribution patterns.

Keywords: Atomic emission spectrometry; Inductively coupled plasma spectrometry; X-Ray fluorescence spectrometry; Lanthanides; Yttrium; Scandium; Bauxites; Red mud

1. Introduction

In some bauxite deposits of the main Greek bauxite reserves in the Parnassos-Ghiona mountains, a strong enrichment of the lanthanides and yttrium was found, especially in the lowermost parts of the deposits with concentrations up to 0.5% [1,2]. The lanthanides, along with yttrium and scandium, have an increasing world demand for new technology applications, such as in advanced ceramics, alloys, lasers, fuel cells, superconductors and supermagnets, etc. [3]. Taking this into consideration, as well as that the total bauxite reserves of Greece, estimated to 500 million tons are the biggest in Europe [4], it is of great interest to investigate the distribution of

* Corresponding author.

SSDI 0003-2670(94)00223-9

these elements in bauxites. More important, a systematic study has to be carried out to investigate the concentration level, its constancy and the enrichment of the above mentioned elements in red mud, the waste product from the alumina production by the Bayer process [5], for which up to now only a few data have been published, referring to the determination of some lanthanides in single red mud samples [6–8]. Several modern multielement instrumental methods are used for the determination of lanthanides in geological materials, such as inductively coupled plasma atomic emission spectrometry (ICP-AES) [9–11], inductively coupled plasma mass spectrometry (ICP-MS) [2,12–14], instrumental neutron activation analysis (INAA) [15], x-ray fluorescence analysis (XRF) [16,17]. Among them, the analytical techniques of ICP-AES and XRF were applied in this study for the direct determination of yttrium, scandium and the lanthanides in bauxite and red mud samples, coming from the alumina production. Most of these methods use a preconcentration or a separation step of these elements from the matrix, prior to their analysis [18–20], making the whole procedure time consuming. The present work deals with the development of analytical procedures which by the rationalization of both the sample preparation and the follow-up of the concentration of these elements in production samples, will allow their rapid, accurate and reproducible determination in iron rich matrices. For this purpose a detail study for the several interferences from the main elements of the matrix and of the interlanthanides interferences was performed and the optimum conditions for the determination of each of the investigated elements were chosen. The accuracy of both analytical techniques used, was checked with appropriate international geological reference materials.

2. Experimental

2.1. Instrumentation

The ICP-AES measurements were performed with a Jobin Yvon, Model JY 38, ICP atomic emission spectrometer in the sequential mode. The instrumental specifications and operating conditions are listed in Table 1. For the XRF analysis a Philips PW 1410 x-ray spectrometer was used. The experimental conditions chosen are given in Table 2.

2.2. Reagents

High purity single element solutions of lanthanides, yttrium and scandium of 1000 mg l^{-1} in 1% (v/v) HNO_3 each, supplied by Alfa Products, Thiokol Ventron, were used as stock standard solutions. As a blank a synthetic bauxite matrix was prepared according to the mean concentration of the main components of the Greek bauxites [21], as Al_2O_3 (57.2%), Fe_2O_3 (21.2%), SiO_2 (3.7%), TiO_2 (2.4%) and CaO (1.5%). The blank spiked with appropriate volumes of the stock

Table 1
Specifications and operating conditions of the ICP-AES spectrometer

Spectrometer	Jobin-Yvon 38, nitrogen flushed spectrometer
Grating	Holographic, 3600 grooves/mm, 120×140 mm, utile 110×136 mm, blazed for 1st order
Wavelength range	165–500 nm, step scanning 0.002 nm
HF-generator	55.5–56.6 MHz, maximum power 2.2 kW
Torch	Type DURR-JY with three concentric tubes, aluminium injector
Spray chamber	Glass, Scott-type
Nebulizer	Meinhard type
Peristaltic pump	Ismatec
Reference wavelength	C 193.026 nm
Power input	1 kW
Frequency	50 MHz
Outer gas flow rate	15 l/min
Nebulizer gas flow rate	1.2 l/min
Sample uptake rate	2 ml/min
Observation high	16 mm above load coil
Integration time	5 s
Measurement time	0.4–0.6 s per data point
Slit width	Entrance 15 μm, exit 20 μm

Table 2
Instrumental parameters for the direct XRF analysis of lanthanides, Y and Sc in bauxites and red mud

X-ray spectrometer	Philips PW 1410
X-ray tubes	W or Cr
Power	60 kV, 30 mA
Analysing crystalls	LiF(200), LiF(220)
Collimator	Fine
Detector	Flow proportional with P10 gas
Counting	40 s
Pulse height selection	Base 200 window 250 div.

solutions, was used as a synthetic multi-element standard solution. Three reference materials, the bauxite BX-N from ANRT (Association Nationale de la Recherche Technique, France) and the syenites SY-2 and SY-3 from CCRMP (Canadian Certified Reference Material Project) were used to check the accuracy of the methods.

2.3. Analytical procedure

The analysed bauxite and red mud samples were delivered from the Greek alumina production over a period of about 3 years. The bauxite samples were mixtures of different bauxite deposits from the main bauxitic area in Greece, the Parnassos Ghiona mountains and they had a wide grain size distribution from 3.36 to 0.075 mm. Prior to analysis the samples were crushed and powdered in an agate mortar to a grain size of less than 75 μm (-200 mesh). The corresponding red mud samples coming from the last washing tower from the Bayer process, had a pH value of about 10 (20% aqueous suspension) and the grains were extremely fine (80% were -200 mesh). For the ICP-AES analysis a suitable dissolution procedure of the bauxite and red mud samples has been developed. Specifically 0.5 g of the dry, powdered and homogenized samples were fused with 3 g $NaKCO_3$–$Na_2B_4O_7$ (1:1) in a platinum crucible at 1100°C for about 20 min, then the flux was dissolved in conc. HCl–H_2O (1:1) and was transferred into a volumetric flask filled up to 100 ml.

According to this procedure a total dissolution of the investigated samples was easily achieved. The obtained solutions were directly aspirated into the flame of the ICP spectrometer, without using any preconcentration or separation step. By the same procedure the reference bauxite BX-N, as well as the syenites SY-2, SY-3 were analysed. Each sample was dissolved three times separately and for each solution three replicate measurements of all investigated elements were carried out, by using seven points for the peak measurement and subtracting the background signal. For the qualitative XRF analysis of bauxites a spectral scan between 20° till 100° for LiF 200 and 60° till 140° for LiF 220 with a scan speed of 1°/min was chosen for the investigated elements. The major elements of the samples were also determined by XRF. For the quantitative XRF measurements the step by step method for each 0.02° was used, to obtain the peak maximum and the background left and right of the peak.

The quantitative XRF analysis was carried out by comparing the peak high of the sample with that of the BX-N standard or by using the standard addition method. For the second method, three aqueous slurries were produced, each containing 6 g of the powdered and homogenized bauxite or red mud sample and appropriate amounts of the stock standard solutions of the investigated elements. After homogenization, the slurries were dried at 110°C till constant weight and were ground in an agate mortar with 2.5 g starch, pressing finally the mixtures to pellets of 4 cm diameter and about 3 mm thickness.

3. Results and discussion

The average chemical composition of the investigated bauxite samples, referring to the main elements was similar to those described earlier elsewhere [21], while for the major compounds of the corresponding red mud the following mean composition resulted: Fe_2O_3 (42.5%), CaO (19.7%), Al_2O_3 (15.6%), SiO_2 (9.2%), TiO_2 (5.9%) and Na_2O (2.4%). For the selection of the suitable analytical lines for the ICP-AES determination of all lanthanides, yttrium and scandium directly in the obtained bauxite and red mud solutions, all wavelength proposed [2,9,18,22–24] were checked for their sensitivity, as well as for

Table 3
Analytical lines used for the analysis of lanthanides, Y and Sc in bauxites and red mud by the ICP-AES technique and their limits of detection

Element	Wavelength (nm)	Limit of detection ($\mu g/g$)
La	398.852	1.2
Ce	418.660	5.4
Pr	422.298	3.0
Nd	430.357	4.8
Sm	442.434	3.0
Eu	381.967	0.024
Gd	303.284	0.3
Tb	384.875	
Dy	340.780	0.42
Ho	345.600	0.42
Er	369.265	0.72
Tm	313,126	
Yb	328.937	0.024
Lu	261.542	
Y	321.668	
Sc	363.074	

their interferences with the main elements of the matrix and for interlanthanide's interferences. Profiles for each initially selected line were obtained by spectral scanning (0.002 nm steps) using single element solutions for all elements of interest. In Table 3 the most undisturbed wavelengths of sufficient sensitivity, selected in this study for the investigated samples, are listed together with the obtained detection limit. The corresponding background measurement position was +0.016 nm. The limits of detection represent the corresponding concentrations to the analytical signals, which are three times the standard deviation of the background in the vicinity of the signal. Table 4 shows the interferences found for some of these selected analytical lines from the main elements of the bauxite matrix and from other lanthanides. These spectral interferences are expressed as interferent equivalent concentration IEC (mg/l) and were obtained by using 1000 mg/l of each of the main element of the matrix and 1 mg/l of each lanthanide, respectively. For all other selected wavelengths, not mentioned in this table, the IEC was lower than 0.01 mg/l. Taking into account the concentration of the main elements of the bauxite matrix, the expected concentration of the investigated elements [2] and the one obtained from Table 4 IEC values, it was found that the most severe interference was that of Fe at Lu, since the iron concentrations in the bauxite and red mud solutions were about 750 and 1500 mg/l, respectively, while those of Lu were only a few ppm. The interferences of Ti on Sm and of Ca on Sc are negligible at the actual concentrations. Among the lanthanide interferences only Sm disturbs the determination of Tb. Furthermore it was not possible to analyse the element Tm, due to its low concentration in the investigated samples. Therefore the lanthanides Tb, Tm and Lu were not determined in this study by ICP-AES, although for Lu a correction could be performed in relation to the actual iron concentration of the sample. For the XRF analysis of lanthanides in the bauxites and red mud samples the Lα1 lines were used, while for the determination of Y and Sc the Kα lines, working with the LiF 200 and LiF 220 analysators. Wherever possible an interference free analytical line was chosen for each element. In Table 5 the selected analytical lines for the direct XRF determination and their limits of detection are listed. By the XRF analysis La, Ce, Pr, Nd and Sm from the light rare earth elements, only Lu from the heavy rare earth elements and Y, Sc could be analysed, due to the large spectral interferences of the iron rich matrix and to the other interelement interferences. In particular the Lα1 lines of Tb and Dy were covered by the FeKα band and the Lα1 lines of Ho, Er and Tm from the FeKβ band. EuLα1 was covered by the MnKα and the CrKβ lines and YbLα1 by the NiKα line. The interferences of the CeLβ2 line on the SmLα1 could be eliminated using a correction method, which was based on the measurement of the ratio of CeLα1 to CeLβ2′ (peak maximum at SmLα1) in a synthetic bauxite matrix and in the sample and subtracting the calculated Ce contribution from the measured SmLα1 peak in the sample. The accuracy and the precision obtained by ICP-AES and XRF for the direct determination procedure described for lanthanides, Y and Sc were tested with the reference material bauxite BX-N, for which only some proposed values exist [25] and with the syenites SY-2 and SY-3 (Table 6). A

Table 4
Interfering elements by the ICP-AES determination of lanthanides, yttrium and scandium at the selected wavelengths (IEC = interferent equivalent concentration)

Element	Wavelength (nm)	IEC (mg/l)	Interfering element	Concentration (mg/l)	Interfering wavelength (nm)
Nd	430.357	0.020	Pr	1.000	430.359
Sm	442.434	0.400	Ti	1000.000	442.439
Tb	384.875	0.600	Sm	1.000	384.881
Lu	261.542	0.030	Fe	1000.000	261.542
Sc	363.074	0.260	Ca	1000.000	363.075

mean deviation of +1.7% of the proposed values (accuracy) resulted for BX-N by ICP-AES and −3.9% by XRF. The deviations for SY-2 and SY-3 were +3% and +4.5%, respectively. The precision of the determinations was on the average ±6% for ICP-AES and ±9% for XRF.

An additional assessment of analytical accuracy may be obtained by normalizing the REE (rare earth elements or lanthanides) concentrations to chondrite and plotting the results against the atomic number of each individual REE [26]. In Fig. 1 the chondrite normalized plots for the ANRT bauxite BX-N is shown. A smooth curve for all REE resulted, except for Eu, showing a negative anomaly.

In Table 7 the yttrium, scandium and lanthanide concentration of the feed bauxites and the corresponding red mud from the Greek aluminium production in samples, followed-up over three years are listed. In Table 8 the average concentration of the investigated samples and the corresponding enrichment factors of the individual lanthanides in the red mud are presented. It results that the total average concentration of Y, Sc and the investigated lanthanides (ΣREE + Y + Sc) is about 560 μg/g in the bauxites and 1040 μg/g in red mud. The production feed is quite uniform for the period of investigation with a relative standard deviation for the investigated elements of about ±20%. The enrichment factor for each of the above mentioned elements in the red mud, in comparison to the original ore, is about two, following those for iron, proving in that way that all lanthanides, Y and Sc pass quantitatively into the red mud during the alumina processing. The chondrite normalizing plots for the average values of the investigated bauxites (Fig. 1) show a small positive Ce anomaly [27]. The investigated bauxites and red mud are also enriched in light lanthanides, ΣLREE (La–Eu) towards the heavy ones, ΣHREE (Gd–Lu), having an average ratio of ΣLREE/ΣHREE of about 10. This ratio is usually found in alkaline rocks or carbonatites and is characteristic for the higher mobility of the LREE during weathering processes leading to bauxite formation.

Taking into consideration the annual production of 5×10^5 tons [28] of the by-product red mud and its lanthanide, Y and Sc content, the potential use of the red mud as another source of these elements might arise. Nowadays the commercial resources of Sc contain up to 100 μg/g Sc [3,8], and the presence of thorium in monazite – one of the main sources of lanthanides – causes environmental problems due to the radioactivity of its processing residues. The relatively high

Table 5
Interference free analytical lines used for the direct XRF determination of lanthanides, yttrium and scandium in bauxite and red mud and their limits of detection

Element	Line	2 θ (degrees)		Limit of detection (μg/g)
		LiF 200	LiF 220	
La	Lα1	82.91	138.78	9
Ce	Lα1	79.01	128.17	8
Ce	Lβ1	71.62		7
Pr	Lα1	75.42	119.73	2
Nd	Lα1		112.68	5.5
Nd	Lβ1		99.08	10
Sm	Lα1	66.23	101.14	4.5
Lu	Lα1	47.43	69.31	0.54
Y	Kα	23.80		5.5
Y	Kβ1	21.38		5
Sc	Kα	97.70		

Table 6
REE, Y and Sc results for ARNT bauxite BX-N obtained by ICP-AES and XRF and for CCRMP syenites SY-2 and SY-3, obtained by ICP-AES

Element	BX-N					SY-2		SY-3			
	This study		Proposed value [25]	Dev. from prop. value [%]		This study ICP-AES	Proposed value [25]	This study ICP-AES	Proposed value [25]	Dev. from prop. value (%)	
	ICP-AES	XRF		ICP-AES	XRF					SY-2	SY-3
La	377 ±15	380 ±19	370	1.90	2.70	70 ±10	*75*	1265 ±50	*1340*	−6.70	−5.60
Ce	547 ±30	550 ±20	520	5.20	5.80	162 ±15	175	2190 ±40	*2230*	−7.40	−1.80
Pr	58 ± 3					19.6± 2	*18.8*	220 ±10	*223*	4.40	−1.30
Nd	171 ±10	154 ±12	160	6.90	−3.80	74 ± 4	73	710 ±15	670	4.20	5.60
Sm	23.8± 1.5	19 ± 1.5	22	8.20	−13.60	15.8± 0.6	*16.1*	110 ± 4	109	1.40	0.90
Eu	4.0± 0.3		4	0.00		2.8± 0.3	2.4	21.5± 0.5	17	−1.80	26.50
Gd	19.9± 1.5		18			16.8± 1	*17*	120 ±10	105	16.60	14.30
Dy	12.8± 1.3					18.7± 1	18	121 ±10	118	−1.10	2.50
Ho	3.0± 0.5					4.2± 0.2	3.8	27.5± 3	*29.5*	3.90	−6.80
Er	10.8± 0.6					13 ± 0.5	12.4	78 ± 2	68	10.50	14.70
Yb	11.2± 0.3		11	1.80		16.5± 0.2	17	68 ± 1	62	4.80	9.70
Lu		1.5± 0.4	1.7	−12.30	−11.80		2.7		7.9	2.90	−3.50
Y	100 ± 6	116 ± 4.8	114		1.80	124.2± 5	128	693 ±20	718	−3.00	−3.50
Sc	56.2± 3	55 ± 5	*60* [a]	−6.30	−8.30	7.9± 0.9	*7*	7.6± 0.8	6.8	12.80	11.70
mean R.S.D.	±7.0%	±9.2%				±7.0%		±4.9%			
mean dev. from prop. value				1.7%	−3.9%					3%	4.5%

[a] Data in italics are recommended values

Table 7
Lanthanides, Y and Sc abundances in bauxite and red mud samples from the Greek alumina production followed up over three years (all values in $\mu g/g$)

Element	Bauxite 1		Bauxite 2		Bauxite 3		Bauxite 4	Bauxite 5	Bauxite 6	Bauxite 7	Bauxite 8	Bauxite 9	
	ICP-AES	XRF	ICP-AES	XRF	ICP-AES	XRF						ICP-AES	XRF
La	91	90.20	81	65.00	88.4		82.5	72	124.2	62.8	118.2	65.4	
Ce	216	224.00	229	236.00	234.3		222.8	216.6	213.8	177.2	247.5	250	
Pr	17	20.00	14.7	14.30	15.1		11	7.3	10.7	5.7	18.9	17.8	
Nd	70	71.50	59	49.00	67.2		60.2	52.9	68.2	44.8	96	47.8	
Sm	16	13.50	14.1	14.70	13.4		11.4	10	13	8.5	17.4	13.2	
Eu	3.4		2.9		2.5		2.6	1.8	2.6	1.5	3.2	2	
Gd	16.6		14.5		13.8		13.8	10.2	11.8	9.1	13.9	11.2	
Dy	10.6		8.1		6.6		6.8	7.7	6.1	5.8	5.7	5.6	
Ho	2.8		1.95		2.1		2.2	1.6	1.8	1.2	2.9	1.6	
Er	9.3		6.05		8.1		7.6	7.9	10.1	10.4	7.2	6	
Yb	10.4		8.7		8.8		8.1	7	7.7	6.5	7.7	7.4	
Lu		1.38		1.22		1.54							
Y	70	71.50	43	58.00	54	49.00	60	41	62	54	62	53	49
Sc	57		55		58		62	57	66	62	62	56	55
ΣREE + Y + Sc	590.1		539.20		573.80		551	493	598	449.5	662.6	537	

Elements	Red mud 1		Red mud 2		Red mud 3		4	5	6	7	8	Red mud 9	
	ICP-AES	XRF	ICP-AES	XRF	ICP-AES	XRF						ICP-AES	XRF
La	117	123	157	102	227.2		138.3	180	127.7	114.9	203.6	148.2	
Ce	390	450	416.7	353	459.8		398.0	431.7	399.7	334.4	440.3	524	
Pr	24	28	29.6	25	40.2		24	24.4	17.8	17.0	20.2	33.4	
Nd	93	91	110	86	161.8		114.0	123.2	103.8	95.7	122.8	163.8	
Sm	26.6	24	28.1	29	37.0		28.6	29	25	23.0	26.5	38.0	
Eu	4.4		5.4		7.0		4.9	5.1	4.0	4.1	5.2	4.6	
Gd	22.6		27.5		26.8		23.5	22.2	21.1	18.1	21.0	26.6	
Dy	13.7		16.1		16.7		14.2	14.9	12.0	11.0	14.8	16.6	
Ho	3.6		3.9		6.6		3.9	4.4	3.5	3.9	5.4	3.8	
Er	12.7		14.7		18.9		15.6	19.3	17.9	18.9	22.4	14.4	
Yb	15.2		16.8		19.4		15.6	15.3	13.6	12.9	16.0	15.6	
Lu		2.6		2.3		2.36							
Y	89	98.8	71	85.0	122	68.0	102	80	86	77	100	111	96
Sc	113.4		126		132.3		113.4	134.1	139.5	105.3	126	133.7	156
ΣREE + Y + Sc	925.2		1022.8		1275.7		996	1083.6	971.6	836.2	1124.2	1233.7	

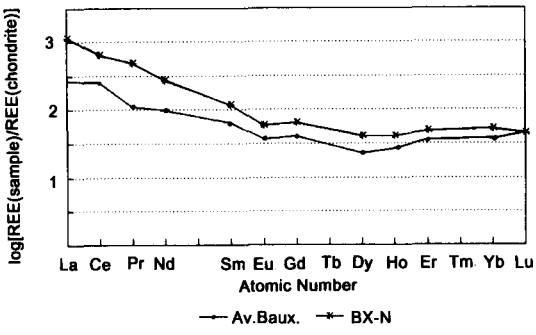

Fig. 1. Chondrite normalized REE patterns of the reference bauxite BX-N from ANRT and of the average bauxite feed from the alumina production.

concentration of lanthanides, Y and Sc is due to the presence of discrete REE minerals in bauxites, especially bastnaesite [1,29] and Sc is notably fixed in titanium minerals present in the bauxites. The minerals hosting the lanthanides, Y and Sc in the bauxites of this region are under further investigation.

4. Conclusions

The comparison of ICP-AES and XRF shows that with ICP-AES nearly all lanthanides except Tb and Tm could be determined directly in the iron rich bauxites, while with XRF the direct determination is possible only for the light rare earth elements, except Eu, and from the heavy REEs only for Lu. For Y and Sc both techniques give satisfactory results. The precision, accuracy and the detection limits are better for ICP-AES than for XRF; the differences are not very significant, however. Whereas XRF is a non-destructive technique the samples have to be dissolved for ICP-AES.

By the developed analytical procedure the possibility of a rapid, accurate and reproducible determination of lanthanides, yttrium and scandium in samples from the alumina production is demonstrated.

Acknowledgments

The authors are grateful to the company "Aluminium of Greece S.A." for supplying the bauxite and red mud samples from their alumina production. This work is supported by a grant, PENED 91 ED 123 from the Greek Ministry of Science and Technology.

Table 8
Average concentration of lanthanides, yttrium and scandium in bauxites and red mud samples from the alumina production and corresponding enrichment factors (all concentrations in $\mu g/g$).

Element	Average concentration				Average Enrichment Factor	
	Bauxite	R.S.D. %	Red mud	R.S.D.%	Red mud/bauxite	R.S.D.%
La	87.2 ± 21.9	25.10	149.0 ± 40.0	26.80	1.78 ± 0.59	33.10
Ce	224.3 ± 21.7	9.70	418.0 ± 52.9	12.70	1.87 ± 0.17	9.10
Pr	13.9 ± 4.8	34.50	25.8 ± 7.5	29.10	2.13 ± 0.67	31.40
Nd	62.4 ± 15.6	25.00	115.0 ± 27.0	23.50	1.99 ± 0.63	31.70
Sm	13.2 ± 2.6	19.70	28.9 ± 5.2	17.90	2.30 ± 0.49	21.30
Eu	2.5 ± 0.63	25.20	5.0 ± 0.9	18.00	1.89 ± 0.58	30.70
Gd	12.8 ± 2.3	17.90	23.3 ± 3.2	13.70	1.86 ± 0.27	14.50
Dy	7.0 ± 1.6	22.80	12.8 ± 1.9	14.80	2.15 ± 0.46	21.40
Ho	2.0 ± 0.56	28.00	4.3 ± 1.0	23.20	2.15 ± 0.63	29.30
Er	8.1 ± 1.6	19.70	17.2 ± 3.1	18.00	2.15	
Yb	8.0 ± 1.2	15.00	15.6 ± 1.9	12.20	1.99 ± 0.24	12.10
Y	55.9 ± 9.3	16.6	9.12 ± 15.7	17.2	1.68 ± 0.47	22.80
Lu	1.38 ± 0.37	26.80	2.4 ± 0.32	13.3	1.76 ± 0.37	27.90
Sc	59.0 ± 3.7	6.30	127.9 ± 14.7	11.5	2.17 ± 0.27	11.40
Mean					1.99 ± 0.25	12.60
ΣLREE/HREE	10.30		9.80			

References

[1] Z. Maksimovic and E. Roaldset, Travaux ICSOBA, 13 (1979) 199.
[2] M. Ochsenkühn-Petropulu, K.M. Ochsenkühn and J. Luck, Spectrochim. Acta, 46 (1991) 51.
[3] S. Vijayan, A.J. Melnyk, R.D. Singh and K. Nutall, Miner. Eng., 41 (1989) 13.
[4] G. Bardossy, Erzmetall, 42 (1989) 172.
[5] H.H. Emons, G. Bräutigam, P. Hellmold, H. Holldorf, R. Kümmel and H. Martens, in Grundlagen der Anorganischen Chemie, Salle and Sauerländer, Frankfurt, 1983, p. 331
[6] G. Bardossy, G. Panto and G. Varhegyi, Travaux ICSOBA, 13 (1976) 221.
[7] V.G. Logomerac, ICSOBA, 3 (1971) 383.
[8] A.S. Wagh and W.R. Pinnock, Econ. Geol., 82 (1987) 757.
[9] J.G. Crock and F.E. Lichte, Anal. Chem., 54 (1982) 1329.
[10] M.I. Rucandio, Anal. Chim. Acta, 264 (1992) 333.
[11] I. Roelandts and A. Deblond, Chem. Geol., 95 (1992) 167.
[12] K.E. Jarvis, Chem. Geol., 68 (1988) 31.
[13] F.E. Lichte, A.L. Meier and J.G. Crock, Anal. Chem., 59 (1987) 1150.
[14] M. Ochsenkühn and J. Luck, Proceedings of the 11th International Mass Spectrometry Conference, Bordeaux, Adv. Mass Spectrom., 11 B (1990) 1662.
[15] P. Vucotic, J. Radioanal. Chem., 78 (1983) 105.
[16] V.P. Bellary, S.S. Deshpande, R.M. Dixit and A.V. Sankaran, Fresenius' Z. Anal. Chem., 309 (1981) 380.
[17] P. Robinson, N.C. Higgins and G.A. Jenner, Chem. Geol., 55 (1986) 121.
[18] K. Iwasaki and H. Haraguchi, Anal. Chim. Acta, 208 (1988) 163.
[19] C.J. Kantipuly and A.D. Westland, Talanta, 35 (1988) 1.
[20] D.W. Zachmann, Anal. Chem., 60 (1988) 420.
[21] K.M. Ochsenkühn and G. Parissakis, Mikrochim. Acta, I (1977) 447.
[22] J.N. Walsh, F. Buckley and J. Barker, Chem. Geol., 33 (1981) 141.
[23] K.H. Lieser and W. Fey, Fresenius' Z. Anal. Chem., 331 (1988) 330.
[24] P.W.J.M. Boumans, Line Coincidence Tables for Inductively Coupled Plasma Atomic Emission Spectrometry, Pergamon, Oxford, 1981.
[25] K. Govindaraju, Geost. Newslett. 13 (1989) 1.
[26] P. Henderson, Rare Earth Element Geochemistry, Elsevier, Amsterdam, 1984.
[27] K.M. Ochsenkühn and M. Ochsenkühn-Petropulu, Proceedings of the 3rd International Symposium of Analytical Chemistry in the Exploration, Mining and Processing of Materials, IUPAC, Johannesburg, 1992, p. 75.
[28] Hellenic Alumina Industry Team, Extended summary on the Greek alumina plant, Mineral Wealth, 76 (1992) 51.
[29] Z. Maksimovic and G. Panto, Travaux, 13 (1983) 191.

ELSEVIER

Analytica Chimica Acta 296 (1994) 315–323

ANALYTICA CHIMICA ACTA

Spectrometric determination of gold, platinum and palladium in geological materials by d.c. arc plasma

M. Tripković [a,*], M. Todorović [b], I. Holclajtner-Antunović [c]

[a] *Institute of Physics, P.O. Box 57, 11001 Belgrade, Yugoslavia*
[b] *Faculty of Chemistry, University of Belgrade, 11001 Belgrade, Yugoslavia*
[c] *Faculty of Physical Chemistry, University of Belgrade, 11001 Belgrade, Yugoslavia*

Received 19 November 1993; revised manuscript received 23 February 1994

Abstract

A method for the separation and determination of Pt, Au and Pd in various geological materials by coprecipitation with tellurium and applying two spectrometric methods was considered in detail. Particular attention was paid to the influence of matrix elements on the determination of these metals. In one instance the metals were determined in solution by applying a U-shaped arc stabilized by an argon vortex and in the other in the solid sample by applying a vertical arc burning in a stream of argon–oxygen. The accuracy of the method was verified using the international reference standard SARM-7, and the results achieved were compared with published data.

Keywords: Atomic emission spectrometry; Arc excitation; D.c. arc plasma; Geological materials; Gold; Palladium; Platinum

1. Introduction

Great attention is paid to the problem of the determination of platinum metals (PMs) [1]. The choice of the method used depends on the matrix in which the PMs occur, their concentration, the sensitivity and precision required and economy and speed of determination. It is well known that in geological (and other natural) samples, these elements are inhomogeneously distributed and usually present in a low absolute amount, which is the main limitation to the application of direct methods. Therefore, the determination of PMs in geological samples involves primarily the preparation of a representative sample and separation of the analyte from the ore matrix simultaneously with preconcentration. In the second step, the analyte concentration is measured by an appropriate method.

Several chemical methods for the separation and preconcentration of PMs from geological samples have been developed and are continuously being refined, e.g., fire assay [2–5], extraction with various extracting agents [6–8], separation with ion-exchange resins [9–11] and copre-

* Corresponding author.

DI 0003-2670(94)00212-5

cipitation with tellurium [12–16] and mercury [17,18]. Many instrumental techniques have been used in conjunction with the different chemical procedures, e.g., atomic absorption [11,19] and emission spectrometry [7,8,20], x-ray fluorescence spectrometry [21], mass spectrometry [15,22] and neutron activation analysis [23].

The choice of the method is a compromise between all the requirements of the complete procedure. It is worth mentioning that modern, very precise and accurate methods such as furnace atomic non-thermal excitation spectrometry (FANES) and inductively coupled plasma mass spectrometry (ICP-MS), demanding extremely small amounts of samples, are very expensive. With geological samples, which owing to their nature need large amounts of natural sample at the start (at least 1 g), it is possible to analyse the prepared samples very successfully by simpler and cheaper methods. Hence the use of very small amounts is irrelevant.

In order to find the most suitable carrier during the precipitation of PMs, some tests with mercury and tellurium had already been done. Tellurium was chosen as more suitable because it can be used efficiently in a small amount and it is less environmentally dangerous than mercury. The separation method with tellurium as a carrier was applied and improved in this work.

The prepared samples were analysed by two types of arc discharges. In one instance, a solution of Pt, Pd and Au was evaporated on graphite powder after separation and these mixtures were analysed using a vertical d.c. arc stabilized with a stream of argon and oxygen mixture. As a more suitable spectrochemical source for the determination of PMs in solution, a low-current, U-shaped arc stabilized by an argon vortex was used. This source is characterized by great stability and high powers of detection and it is highly economical.

It is shown that by applying a relatively simple procedure of separation in conjunction with the simple and economic method of atomic emission spectrometry, it is possible to attain very precise and accurate results. Special attention was paid to the influence of matrix elements on the determination of PMs by use of the U-shaped arc.

2. Experimental

2.1. Previous investigations

The first papers on the coprecipitation of PMs by means of tellurium [12,13] recommended 0.2 mg of tellurium for 1–25 μg of gold. The same is valid for platinum [12]. Recent papers [14,15] recommend various amounts, even up to 5 mg of Te. We therefore investigated the effect of different amounts of tellurium on a degree of coprecipitation of the PMs studied.

In order to simplify this and other investigations with artificial samples, a solution simulating the composition of the matrix of an average silicate specimen after removal of SiO_2 and the dissolution of matrix elements was prepared. An average silicate sample has the following composition (according to international geochemical standards): 52.0% SiO_2, 3.8% Fe_2O_3, 7.5% FeO, 13.1% Al_2O_3, 7.9% MgO, 5.9% CaO, 5.4% K_2O and 2.4% Na_2O. If 50 g of solid sample were taken and SiO_2 was removed, after dissolution in the solution there would be 4.3 g of Fe, 3.5 g of Al, 2.6 g of Mg, 2.1 g of Ca, 2.3 g of K and 0.9 g of Na. The aforementioned amounts of elements (in the form of appropriate compounds) corresponding to 0.1 g ml^{-1} of starting solid sample were measured out and used to prepare 500 ml of solution in a volumetric flask.

In order to investigate the influence of different amounts of Te, five aliquots of 20 ml (corresponding to 2 g of solid sample) were taken and to each of these solutions the same concentrations of Pt, Pd and Au were added.

Coprecipitation was performed with various amounts (0.2, 0.5, 1.0, 2.0 and 5.0 mg) of tellurium. All samples were prepared in duplicate and the separation procedure was carried out. The spectral line intensities of the PMs were measured and the mean values of these intensities corrected for the background emission are given in Table 1. It can be seen that 0.5 mg of Te provides satisfactory results. A larger amount of Te increases the amount of tin(II) chloride needed for reduction, so 0.5 mg of Te was adopted.

The effect of the amount of the sample on the conditions of coprecipitation was also investi-

Table 1
Dependence of relative spectral line intensities (ΔI_{rel}) of Pt, Pd and Au on the amount of Te

Te (mg)	ΔI_{rel} [a]		
	Au 267.6 nm	Pt 265.9 nm	Pd 340.4 nm
0.2	44.5	9.0	45.0
0.5	55.0	14.1	63.1
1.0	54.1	13.2	63.2
2.0	54.0	14.1	63.5
5.0	55.0	14.0	63.0

[a] ΔI_{rel} represents the difference in relative emitted intensities of spectral lines of elements in solution and of the background at the position of the corresponding line in the blank solution (0.5% KCl).

gated, as the separation procedure developed for both methods of determining PMs requires different amounts of sample. The influence of the amount of sample in the same volume of solution on the precipitation of tellurium and PMs was investigated. Three artificial mixtures corresponding to contents of 0.5, 1.0 and 2.0 g of the solid sample in 150 ml of 1.5 M HCl were made and to each of them the same amount of PMs and 0.5 mg of Te were added. The results obtained are presented in Table 2. It is obvious that changes in the amount of sample do not affect the relative intensities of the spectral lines of the PMs, i.e., the determination of their concentrations.

2.2. Standards and reagents

Standards of Pt, Pd and Au were prepared by dissolving the metals in aqua regia and converting them into chlorides by several treatments with concentrated HCl. The concentration of each element in the standard solutions was 1 mg ml^{-1}. The same volumes of standard solutions of each element were used and a stock standard solution was prepared with a concentration of 100 μg ml^{-1} of the particular element. These solutions and solutions of lower concentrations of PMs were kept in 1 M HCl in plastic bottles. In order to make a solid standard, a synthetic mixture corresponding to the average content of a silicate rock was previously made from spectrochemically pure substances. The corresponding amounts of PM solution were placed over this mixture in order to obtain a set of standards from 0.1 to 5.0 μg g^{-1}. These standards were dried under an IR lamp and were homogenized, and were then ready for separation.

A 1 mg ml^{-1} Te solution in 1 M HCl was prepared from the spectrochemically pure metal, dissolved in aqua regia and treated several times with concentrated HCl.

Table 2
Dependence of relative spectral line intensities (ΔI_{rel}) of Pt, Pd and Au on the amount of sample

Sample weight (g)	Volume (ml)	ΔI_{rel}		
		Pt 265.9 nm	Pd 340.4 nm	Au 267.6 nm
0.5	150	16.5	56.0	69.9
1.0	150	16.4	55.5	70.1
2.0	150	16.6	56.1	69.6

2.3. Equipment

Depending on the requirements for accuracy and speed, two independent procedures of determination with almost the same sensitivity can be applied. The first procedure involves the analysis of the separated solution using by a U-shaped argon-stabilized arc (Fig. 1). This source was developed over 10 years ago [24] and subsequently

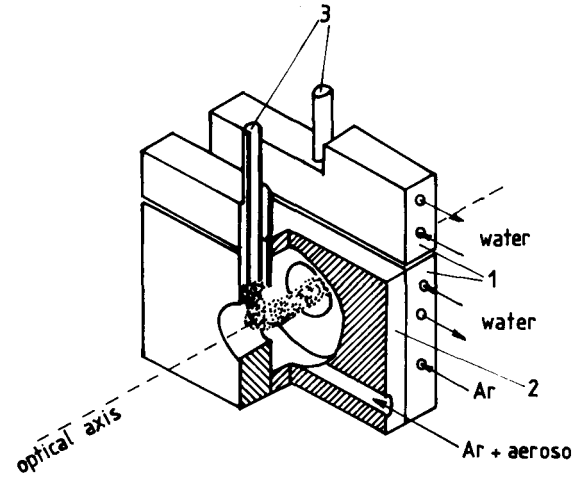

Fig. 1. Stabilized arc device. 1 = Water-cooled metal segments; 2 = central PTFE segment; 3 = graphite electrodes.

improved [25]. Its main characteristics are high stability and, owing to the relatively long horizontal column from which the radiation is taken, its detection limits for many elements are comparable to those with ICP atomic emission spectrometry (AES). The advantages of this source compared with ICP-AES are that it is much cheaper and also the argon consumption in the analysis is at least ten times less. Also, it is simpler to handle. Any laboratory spectrometer can be used as a dispersion system, but a good-quality grating is needed.

The second procedure consists in the analysis of the graphite mixture in a d.c. vertical arc stabilized by a stream of gas mixture consisting of argon and oxygen from a plasma jet.

The experimental equipment and operating conditions are given in Table 3.

2.4. Decomposition and separation procedure

In order to accelerate the separation procedure, a sample of 4 g was divided into two equal portions and each was separately and simultaneously treated with the following procedure. Decomposition is done in such a way that 4.0 g of NH_4F (mixed with the sample) and 2.5 ml of HF are added and then heated until HF evaporates. The procedure of addition and evaporation of HF is repeated four times and in this way SiO_2 is removed. Aqua regia is then added and evaporated several times in order to remove HF entirely and to convert the salts into a solution. The whole decomposition process takes about 6 h. The solution is evaporated to a small volume and then treated several times with concentrated HCl. Each time the solution is evaporated close to dryness, but care should be taken that it is not entirely dry. The solution in concentrated HCl is finally reduced to a volume of 1–2 ml. An amount of 0.5 mg of Te is added to these solutions. The solution is filtrated through a Schleicher & Schuell white ribbon No. 300110 filter-paper in order to separate it from insoluble particles of organic substances (frequently carbon) which are not oxidized in the procedure. If a noticeable precipitate occurs, it should be fused with five times the amount of Na_2O_2 and dissolved into warm, concentrated HCl. The neutralized solution should be combined with the main solution. If there is no precipitate, the filter is rinsed with a mixture of concentrated HCl and a volume of water such as to make the entire solution of 150 ml from 1 to 1.5 M with respect to HCl. It is important to point out that the solution molarity must be retained strictly within the quoted limits. Below an HCl concentration of 1 M the Te carrier of PMs is not precipitated and above 1.5 M it starts to dissolve.

This solution is heated to boiling and 5 ml of a 20% solution of tin(II) chloride, freshly made in 1 M HCl, is added. Under these conditions the reduction of other components (such as iron and copper) is primarily achieved and then Te and the PMs are reduced to the elements; this is why attention should be paid to the amount of tin(II) chloride added, which must be sufficient for the entire reduction. When small amounts of matrix elements are present, 5 ml of tin(II) chloride are necessary for reduction; if necessary a second

Table 3
Experimental equipment and operating conditions

Excitation source	U-shaped arc		D.c. vertical arc
Spectrograph		PGS-2	
Grating	Bausch & Lomb cut at 56.58°		600 grooves mm^{-1} blazed at 320 nm
Detector	Hamamatsu R-212 photomultiplier		Kodak SA-1 plate
Arc current (A)	7.5		10
Flow-rate of Ar (l min^{-1})	0.2		5
Flow-rate of O_2 (l min^{-1})			1.25
Nebulizer	Meinhard TR-50-C_1		
Liquid uptake (ml min^{-1})	1.1		
Exposure time (s)			30

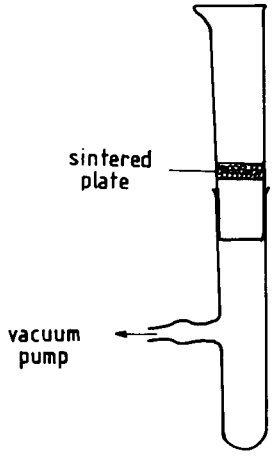

Fig. 2. The sintered-glass crucible.

portion of tin(II) chloride can be added to ensure complete reduction. After boiling the solution for about 5 min and then leaving it for about 20 min, the almost invisible black precipitate becomes larger. Filtration is performed through a sintered glass crucible of porosity G-4, of size about 1 cm^2. The shape of this crucible is shown in Fig. 2. In this way, fast and efficient filtration is achieved.

The precipitate is rinsed with 0.5 M HCl, then dissolved in aqua regia and placed in a 50-ml glass beaker. Evaporation to a small volume is again carried out and several treatments with concentrated HCl are applied in order to convert the PMs into chlorides, followed by evaporation to a small volume and transfer of solutions of both portions of samples into a 10-ml beaker and, after evaporating, into a 5-ml volumetric flask. A solution of KCl (spectroscopic buffer) is added so that its content in the final solution for analysis is 0.5%. It was found previously [24] that addition of 0.5% KCl to the analyte solution improves the excitation conditions in the U-shaped arc, resulting in enhancement of spectral line intensities and suppression of matrix effects.

An identical procedure for separation is performed when determining PMs in a solid sample; 1 g of the sample for decomposition is sufficient. Small amounts shorten the decomposition time and are sufficient because a tenfold excess of Pt, Au and Pd concentration is achieved with respect

Table 4
Spectroscopic conditions used in the experiment

Element	λ (nm)	Slit (μm)	
		U-shaped arc	D.c. arc
Pt	265.9	50	30
Au	267.6	20	30
Pd	340.4	50	30

to the sample, namely the chloride solution of Te and PMs from 1 g of sample, using a small 5-ml beaker, is transferred to 100 mg of graphite powder and is evaporated under an IR lamp. The dry graphite mixture is mixed with Li_2CO_3 (spectroscopic buffer) so that its concentration in the mixture is 5%, and is then homogenized. The preparation is then completed.

2.5. Analysis of samples

For the determination of PMs the same spectral lines of the PMs were used in both methods and are presented in Table 4. As was found earlier [24], in the U-shaped d.c. arc source there is a displacement of the maximum intensity of the spectral lines of elements in a radial direction depending on their ionization potentials. The non-easily ionized elements (such as Au, Pt and Pd) are excited in the vicinity of the arc axis, which was taken into account in the course of the experiment.

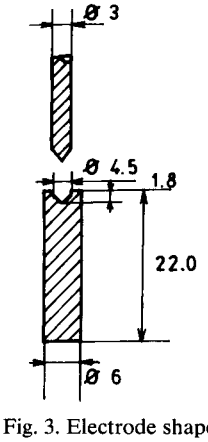

Fig. 3. Electrode shape.

Table 5
Contents of Fe, Cu and Al in geological samples before and after separation procedure

Sample No.	Fe (%)		Cu (%)		Al (%)	
	Before	After	Before	After	Before	After
1	3.3	0.0006	0.5	0.00003	2.5	0.00060
2	28.7	0.0019	10.9	0.00030	2.2	0.00030
3	3.4	0.0003	0.2	0.00001	0.4	0.00001
4	25.2	0.0015	12.9	0.00060	1.0	0.00020
5	8.1	0.0009	2.0	0.00020	6.0	0.00100
6	6.4	0.0005	16.0	0.00100	3.2	0.00070
7	3.0	0.0003	–	–	7.0	0.00150

According to the proposed method of separation and the presented conditions of excitation, it is possible to determine 0.1 μg ml^{-1}, which for the foregoing procedure means 0.12 μg g^{-1} PM in the sample.

For analysis of the graphite mixture by the d.c. arc method, the graphite electrodes (Fig. 3) are loaded with 20 mg of graphite mixture.

Under these conditions, 0.1 μg g^{-1} Au and Pd and 0.15 μg g^{-1} Pt could be determined. Naturally, the worse reproducibility is a result of the greater arc variations, the manner of radiation detection and a possibly greater error of determination owing to the smaller amount of sample used for the analysis.

3. Results and discussion

Various geological materials which contain as main components SiO_2, Al_2O_3, Fe_2O_3, CaO and MgO, in addition to copper concentrates, were analysed using the proposed separation and decomposition procedures; the matrix components such as iron, aluminium and copper, remaining after the removal of SiO_2, may vary over a large concentration range. The U-shaped arc as the excitation source is generally more sensitive to matrix effects than ICP-AES, which in this instance has the advantage over the arc. This is why an investigation was performed to establish whether there is an influence of remaining matrix elements on determination of PMs.

Out of about 300 samples that were analysed using the proposed procedure, seven representative samples with very different compositions of matrix components were selected in order to examine the influence of the amount of matrix elements on PM determination. Their amounts were determined before and after the separation procedure and the results are presented in Table 5. Obviously, if the concentration of matrix elements in the sample is greater, they remain in the solution to a great extent after the separation, which is why the rinsing of the Te and PM precipitate should then be longer. However, as it is not reasonable to determine the matrix elements in all samples, it was investigated whether the residual concentration affects the line intensities of the elements being determined. When the residual concentration of matrix elements in the volume of the solution containing Pt, Pd and Au after separation is calculated using the results in Table 5, the concentrations given in Table 6 are obtained. Artificial solutions were made as to follows: all of them contained 3 μg ml^{-1} each of Pt, Au and Pd in addition to matrix elements at concentrations from the lowest found concentrations (Table 6) multiplied by 2, 5 and 10. The

Table 6
Concentration of matrix elements determined in final solution in addition to PMs

Sample No.	Fe (μg/ml)	Cu (μ/ml)	Al (μg/ml)
1	4.6	2.1	4.5
2	13.2	1.0	2.5
3	2.0	0.25	0.9
4	11.8	4.0	1.2
5	6.0	6.0	3.0
6	11.5	10.0	5.0
7	1.9	–	8.5

Table 7
Effect of the residual concentration of Fe on the accuracy of determination of Pt, Pd and Au

Fe (μg/ml)	Pt (μg/ml)	Pd (μg/ml)	Au (μg/ml)
0	3.0	3.0	3.0
4	3.0	2.9	3.0
10	3.1	3.0	3.0
20	3.5	3.2	3.1

Table 8
Effect of the residual concentration of Cu on the accuracy of determination of Pt, Pd and Au

Cu (μg/ml)	Pt (μg/ml)	Pd (μg/ml)	Au (μg/ml)
0	3.0	3.0	3.0
4	3.0	2.9	3.0
10	2.9	3.0	2.9
20	2.8	2.7	2.8

Table 9
Effect of the residual concentration of Al on the accuracy of determination of Pt, Pd and Au

Al (μg/ml)	Pt (μg/ml)	Pd (μg/ml)	Au (μg/ml)
0	3.0	3.0	3.0
2	2.9	3.0	3.0
5	3.0	2.9	3.1
10	2.9	3.0	3.0

exception is copper, where the lowest concentration of 0.25 μg ml^{-1} is neglected and 1 μg ml^{-1} is taken as the lowest. The line intensities of Pt, Pd and Au were measured and their concentrations in the presence of various concentrations of the matrix elements were determined. The results are presented in Tables 7–9.

As could be expected, despite the various amounts of residual matrix elements present, they essentially do not affect the determination of Pt, Pd and Au. The exceptions are 20 μg ml^{-1} Fe, which increases the concentration of Pt by 17%, and 20 μg ml^{-1} Cu, which decreases the concentration of Pd by 10%. All other results remain within the limits of error. From the analysis of samples in which the presence of these two elements in the final solution could be expected, it was seen in no instance was 20 μg ml^{-1} Fe or Cu present. The recommendation can be made that in all instances when a larger amount of tin(II) chloride is used for the coprecipitation of Te and PM, the washing of the precipitate with 0.5 M HCl should be longer.

The accuracy of the method was verified in two ways: by comparing the results with those obtained by other methods, and by means of the international standard SARM-7.

Table 10 compares the results obtained by the proposed method, by fire assay (where the PMs are determined as a sum) and by extraction with methyl isobutyl ketone and determination by the ICP-AES. The results obtained are in good agreement.

Using the proposed procedure for separation and determination by means of an argon-stabilized U-shaped arc, Pt, Pd and Au were determined in the international standard SARM-7. The results obtained by the proposed method together with the standard deviations of the measurements are compared with the certified values in Table 11. The agreement for Pt and Pd is within 2%, whereas for Au, owing to its lower concentration, the relative difference is 6.5%. If these results are compared with literature data for the same reference standard and for various determination methods (ICP–mass spectrometry [26], extraction with *N,N*-diphenylthiourea and triphenylphosphine and ICP-AES [7]), then the agreement of the results achieved by the proposed method for SARM-7 is much better.

Table 10
Comparison of results obtained by the proposed and other methods (μg g^{-1})

Sample No.	Fire assay: ΣPMs	Extraction: Au	Proposed method		
			Au	Pt	Pd
1	20	–	19.0	< 0.1	< 0.1
2	14.8	–	12.4	1.2	1.3
3	–	5.6	5.7	–	–
4	–	0.4	0.5	–	–

Table 11
Verification of results obtained using U-shaped arc for SARM-7 reference material

Element	SARM-7 certified value ($\mu g\ g^{-1}$)	Proposed method [a] ($\mu g\ g^{-1}$)	Relative difference (%)
Pt	3.74	3.67 ± 0.05	−1.9
Pd	1.53	1.50 ± 0.04	−2.0
Au	0.31	0.29 ± 0.02	−6.5

[a] Mean ± S.D. ($n = 3$).

It should be added that owing to the inhomogeneous distribution of PMs in geological samples and also their property to be *forged* and *hardly grained* up, a larger amount of sample ensures higher accuracy. For this reason, the application of the proposed procedure together with fire assay preconcentration would provide not only a higher accuracy but also lower detection limits for PM determination.

As the U-shaped argon-stabilized arc for determining Pt, Pd and Au in geological materials was applied here for the first time, it was of interest to compare the limits of detection with those achieved by ICP-AES [27]. In both instances the detection limits were calculated according to Ref. [27] and are given in Table 12. As can be seen, lower detection limits are achieved using the argon U-shaped stabilized arc with the exception of Pt, whose detection limit is the same as that for ICP-AES. The limit of detection for Pt calculated by Kaiser's method [28] is even lower (50 ng ml^{-1}).

It should be pointed out that the proposed procedure of separation, i.e., decomposition twice of 2 g of each sample, shortens the time of decomposition to about 6 h, and at least halves the consumption of HF. The coprecipitation of PMs with the proposed amount of Te (2×0.5 mg) decreases the consumption of Te fivefold, and also that of tin(II) chloride, compared with data in the literature [14]. Bearing in mind that by applying the U-shaped argon-stabilized arc less (10%) argon is consumed than by ICP-AES, it can also be concluded that the proposed procedure is not only faster but considerably more economical with the same sensitivity of determination. The cost of analysis of one sample is reduced by about 30%, which is of importance when large series of samples are to be handled.

Table 12
Comparison of the detection limits (ng ml^{-1}) obtained by U-shaped arc and ICP-AES methods [27]

Element	U-shaped arc	ICP-AES
Au	18	31
Pd	31	44
Pt	80	81

4. Conclusions

The proposed procedure for the separation of Pt, Pd and Au from the matrix is relatively simple and applicable to different geological and other materials. The procedure for determination depends on the equipment available in the laboratory. The procedure may be applied with good sensitivity, as described in this paper, using a vertical d.c. arc in a stream of argon and oxygen or a U-shaped argon stabilized arc, or by ICP-AES.

The manner of decomposition of large amounts of sample enables the duration of the procedure to be shortened. In addition, the economy of the procedure is considerable and is achieved by the rational use of necessary reagents and the application of the stabilized U-shaped arc, with no decrease in accuracy.

In this work the argon-stabilized U-shaped arc was applied for the determination of PMs in geological samples for the first time. The detection limits achieved for Au and Pd are lower than and for Pt comparable to those achieved by ICP-AES.

Acknowledgement

We express our gratitude to Professor J.P. Willis of Cape Town University (South Africa) for sending us the international standard SARM-7.

References

[1] S. Kalman, Talanta, 34 (1987) 677.
[2] E.E. Bugbee, A Textbook of Fire Assaying, Wiley, New York, 1957.
[3] T.J. Bornhorst, W.I. Rose, S.P. Wolfe and E.L. Hoffman, Geostand. Newsl., 8 (1984) 1.
[4] A. Diamatatos, Analyst, 213 (1986) 111.
[5] R.V.D. Robert, E. Van Wyk and R. Palmer, N.I.M. Report 1371, Council for Mineral Technology, Randburg, South Africa, 1971, p. 14.
[6] G.P. Sighinaldi and A.M. Santos, Microchim. Acta, 2 (1976) 33.
[7] P.J.H. Severens, E.J.M. Kalassen and J.M.J. Maessen, Spectrochim. Acta, Part B, 38 (1983) 727.
[8] I.F. Seregina, G.L. Buhbinder, L.N. Shabalova, E.N. Gilbert, O.M. Petruhin and Yu.A. Zolotov, Zh. Anal. Khim., 41 (1986) 5.
[9] F.E. Beamish, Talanta, 14 (1967) 991.
[10] A.E. Pitts and F.E. Beamish, Anal. Chem., 41 (1969) 1907.
[11] A. Rivoldini and T.H. Haile, At. Spectrosc., 10 (1989) 89.
[12] S.K. Hagen, Microchimie, 15 (1936) 180.
[13] W.E. Cadwell and K.N. McLeod, Ind. Eng. Chem., Anal. Ed., 9 (1937) 530.
[14] J.G. Sen Gupta, Talanta, 36 (1989) 651.
[15] S.E. Jacson, B.J. Fryer, W. Gosse, D.C. Haeley, H.P. Longerich and D.F. Strong, Chem. Geol., 83 (1990) 119.
[16] I. Shazali, L. Van't Dack and R. Gijbels, Anal. Chim. Acta, 196 (1987) 49.
[17] A.K. Das, Indian J. Technol., 18 (1980) 477.
[18] R.K. Tewari, V.K. Tarsekar and M.B. Lokhande, At. Spectrosc., 11 (1990) 125.
[19] F.E. Beamish and J.C. Van Loon, Analysis of Noble Metals, Academic Press, New York, 1977.
[20] R.M. Barnes and A. Diallo, in L.P.R. Butler (Ed.), Analytical Chemistry in the Exploration, Mining and Processing of Materials, Blackwell, Oxford, 1986, pp. 3–13.
[21] J. Whitney, paper presented at the Eastern Analytical Symposium, New York, 1982.
[22] A.R. Date, A.E. Davies and Y.Y. Cheung, Analyst, 112 (1987) 1217.
[23] E.L. Hoffman, A.L. Naldrett, J.C. Van Loon, R.G.V. Hancock and A. Manson, Anal. Chim. Acta, 102 (1978) 157.
[24] M. Marinković and V.G. Antonijević, Spectrochim. Acta, Part B, 35 (1980) 129.
[25] M. Pavlović, N. Pavlović and M. Marinković, Spectrochim. Acta, Part B, 46 (1991) 1487.
[26] E. Denoyer, R. Ediger and J. Hager, At. Spectrosc. 10 (1987) 97.
[27] R.K. Winge, V.J. Peterson and V.A. Fassel, Appl. Spectrosc., 33 (1979) 206.
[28] H. Kaiser, Fresenius' Z. Anal. Chem., 216 (1966) 80.

ELSEVIER

Analytica Chimica Acta 296 (1994) 325–332

ANALYTICA CHIMICA ACTA

Adsorption of palladium by glycolmethacrylate chelating resins

E. Anticó [a], A. Masana [a], V. Salvadó [a], M. Hidalgo [a], M. Valiente [b,*]

[a] *Departament de Química, Universitat de Girona, Plaça Hospital 6, 17071 Girona, Spain*
[b] *Química Analítica, Universitat Autònoma de Barcelona, 08193 Bellaterra, Spain*

Received 4 January 1994; revised manuscript received 28 April 1994

Abstract

The adsorption of Pd(II) and Cu(II) on macroporous hydrophilic glycolmethacrylate gels with side chains containing 8-hydroxyquinoline (Spheron Oxine 1000), thiol (Spheron Thiol 1000) and salicyl groups (Spheron Salicyl 1000) has been investigated. Palladium is strongly adsorbed by Spheron Oxine and Spheron Thiol resins from a hydrochloric medium. The influence of pH and ionic strength has been determined. The elution of Pd(II) was carried out by using acidified thiourea or potassium thiocyanate solutions. Desorption was most effective for Spheron Oxine resin. The kinetics of metal adsorption by Spheron Oxine 1000 was also studied. The experimental data were analyzed numerically by considering both the forward and the reverse reaction, and corresponding constants are calculated for different initial metal and resin concentrations. Separation of aqueous mixtures of Pd(II) and Cu(II) by using Spheron Oxine is discussed.

Keywords: Adsorption; Copper; Glycolmethacrylate chelating agents; Palladium

1. Introduction

Several methods are available for the concentration and separation of noble metals [1]. The sorption methods are widely used and they are the most effective at very low metal concentration.

The conventional ion-exchange resins have found applications in many fields, but their use in hydrometallurgy has been limited due to a lack of selectivity.

Much work has been done in recent years on chelating resins in an attempt to improve the selectivity [2]. Because the noble metals have a greater tendency to form complexes than other metals, the complex-forming sorbents are particularly useful in this respect. Especially polymer-supported functional groups containing nitrogen and sulfur as donor atoms, which are known as effective extractants for the separation of precious metals from base metals [3,4], are suitable for the removal of platinum group metals and gold. Examples are modified polymers with dithiocarbamate groups [5], isothiouronium groups and dithizone [6–8].

Additional selectivity can also be obtained by an appropriate pH control [9,10].

* Corresponding author.

SSDI 0003-2670(94)00220-G

A chelating molecule which has received much attention is 8-hydroxyquinoline (8-HQ). It is used extensively in solvent extraction [11]. Application of chelating sorbents depends mainly on their kinetic characteristics, determined by the nature of the polymeric matrix. 8-HQ has been immobilized on different solid supports: condensation of resorcinol–formaldehyde [12], polystyrene–divinylbenzene [13], silica gel [14], Fractogel TSK (vinyl polymer agglomerate) [15]. The immobilization of 8-HQ onto polystyrene–divinylbenzene has been widely investigated and studies by Parrish and co-workers [13,16] are well known. Polystyrene sorbents are more stable than phenol–formaldehyde matrices but the reported exchange rates are normally low. Although phenol–formaldehyde resins have been superseded by polystyrene resins, the hydrophobic nature of these materials unfavourably affects the sorption process. Resins loaded with silica-bound chelating agents exhibit favourable kinetics but also a low capacity and poor pH stability. Sorbents with a fast exchange rate are those based on hydrophilic macroporous copolymers [2].

Most of the chelating ion-exchange resins commercially available have aminocarboxylic acids as functional group [17] and only one (Spheron Oxine 1000) contains the 8-HQ group. Spheron Oxine 1000 is a macroporous chelating resin in which 8-HQ is bound through an azo group and a flexible side chain as spacer to an hydrophilic copolymer of hydroxyethylmethacrylate and ethylenedimethacrylate. The sorbent Spheron Oxine was developed by Slovák et al. [18]. Spheron modified resins are distinguished by their hydrophilicity, because its side chains contain hydroxyl groups, and further by a high degree of porosity and a large internal surface. These facts contribute to a rapid metal adsorption.

Spheron Oxine 1000 and other different polymeric matrices functionalized with 8-hydroxyquinoline have been applied mainly as extractants for base metals, especially Cu(II), Fe(III), Al(III), Co(II) and Ni(II) [12,18,19], and few attention has been paid to the study of the sorption of noble metals by polymeric 8-hydroxyquinolines.

The sorption of Pt(IV) and Pd(II) by chelating resins functionalized with similar groups was studied by Myasoedova et al [20] using a polystyrene supporting thioxine moieties (included in Polyorgs sorbents) and Svec and Jehlickova [21] with a glycolmethacrylate supporting 8-aminoquinoline.

The present work includes a study on the sorption of Pd(II) by modified Spheron resins and its separation of base metals. Special emphasis was given to the palladium–Spheron Oxine system as an implementation of previous work on the solvent extraction of Pd(II) by Kelex 100 [7-(4-ethyl-1-methyloctyl)-8-quinolinol] [4]. In this respect results will provide a possible comparison of corresponding liquid–liquid and solid–liquid systems.

2. Experimental

2.1. Reagents and solutions

The Pd(II) stock solution was prepared from solid $PdCl_2$ (Spanish Society of Precious Metals) and standardized gravimetrically with dimethylglyoxime [22]. The stock solution of Cu(II) obtained from solid $CuCl_2$ (analytical-reagent grade, Panreac) was standardized volumetrically [22]. Metal concentrations of the test solutions ranging from 2.5 to 0.06 mM were obtained by dilution.

Sodium chloride (analytical-reagent grade, Panreac) was purified as previously described [23] and it was employed to adjust the ionic strength of the metal solutions.

Solutions of potassium thiocyanate and thiourea (analytical-reagent grade, Panreac) at different concentrations in the range 0.1–0.7 M were used in palladium stripping procedures.

Glycolmethacrylate supports functionalized with either 8-hydroxyquinoline (Spheron Oxine 1000), or a thiol group (Spheron Thiol 1000) or a salicyl group (Spheron Salicyl 1000) were used besides the unmodified support (Spheron 1000). All the resins were kindly supplied by Lachema (Brno) (see Fig. 1).

The particle size and the pore diameter of supported polymer were 40–63 μm and 37–50 nm, respectively, except for Spheron Thiol 1000 which has a particle size of 63–100 μm.

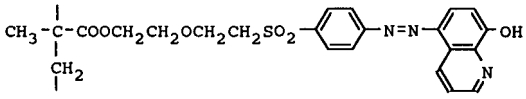

SPHERON OXINE 1000

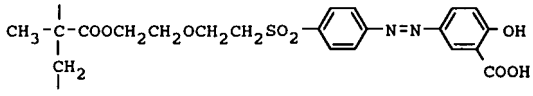

SPHERON SALICYL 1000

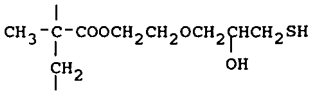

SPHERON THIOL 1000

Fig. 1. Modified Spheron resins.

2.2. Apparatus

An UV–visible Hitachi U-1100 spectrophotometer, a Varian Spectra A-300 atomic adsorption spectrophotometer and a Labinco rotary mixer have been used.

2.3. Procedures

Determination of resin capacity

Batch sorption procedures were applied. Samples of 0.1 g of dry resin were shaken mechanically in stoppered glass tubes, containing an appropriate volume of the solution of the studied metal–cation ensuring an excess of metal over the theoretical capacity of the resin. Experiments were carried out at pH 2.0 and an ionic strength of 0.1 M and some of them at pH 1.23 and an ionic strength of 0.06 M. The metal adsorbed by the resin was obtained by determining the remaining metal in the aqueous phase after the resin was filtered. Pd(II) was determined spectrophotometrically by adding an excess of thiocyanate and measuring the absorbance of the $Pd(SCN)_4^{2-}$ complex at 310 nm [24] or by atomic adsorption spectrometry. The Cu(II) concentration was determined by atomic adsorption spectrometry.

Resin capacities are expressed in mg or mmol per g of dry resin.

The theoretical capacity of Spheron resins was estimated by determining the nitrogen or sulphur content in the polymer (see Table 1), and assuming the 1:1 stoichiometry of corresponding metal complexes due to the metal excess that may prevent the combination of metal ions with more than one chelating group [13,18].

Stripping

After the adsorption process, filtered resin was washed with distilled water and then placed in a glass tube with 20 ml of stripping solution and agitated during 60 min. The metal concentration in the solution was determined afterwards.

Adsorption kinetics

Suspensions of 10 mg of the sorbent in 10 ml of a solution containing either Pd(II) or Cu(II) were shaken in a rotary mixer. The metal concentration was kept below the capacity of the resin.

The metal remaining in solution was determined as a function of the contact time. The collected values are the average of three independent experiments.

Table 1
Adsorption of palladium at 24 h on Spheron resins. Experiments were performed at pH 2.0 and $I = 0.1$ M

Resin	Metal adsorbed		Theoretical capacity, mmol per g resin
	mg Pd(II) per g resin	mmol Pd(II) per g resin	
Spheron Oxine 1000	57.02	0.536	0.68
Spheron Thiol 1000	100.94	0.949	2.01
Spheron Salicyl 1000	10.05	0.094	0.77
Spheron 1000	1.6	0.015	0.0

[a] As defined in text.

3. Results and discussion

3.1. Adsorption equilibria

The adsorption capacity data have been interpreted in terms of equilibrium reactions. Assuming the 1:1 stoichiometry of the complex formed, the following equations, including the aqueous chlorocomplexes, may represent the process of palladium adsorption:

$$HR + PdCl_4^{2-} \rightleftarrows R - PdCl_n^{-[(n+1)-2]} + (4-n)Cl^- + H^+ \quad (1)$$

$$HR + PdCl_3(H_2O)^- \rightleftarrows R - PdCl_m^{-[(m+1)-2]} + (3-m)Cl^- + H^+ + H_2O \quad (2)$$

HR represents one of the different forms of Spheron resins (Spheron Oxine 1000, Spheron Thiol 1000 or Spheron Salicyl 1000).

The time dependence of the adsorption of palladium on the modified Spheron resins is shown in Fig. 2. As seen, the rate of palladium

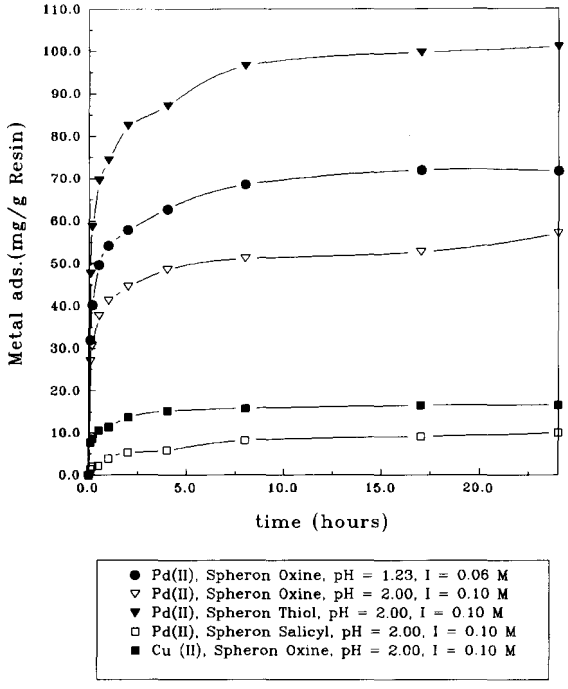

Fig. 2. Adsorption of Pd(II) and Cu(II) vs. time by the different Spheron resins.

Table 2
Influence of pH and ionic strength on the metal adsorption at $t_{1/2}$ for the system Spheron Oxine–Pd(II)

pH (I = 0.1 M)	1.5	3.2	4.5
Metal adsorbed, mg Pd(II) per g resin	31.1	31.5	30.2
I (M) (pH 1.5)	0.03	0.1	0.5
Metal adsorbed mg Pd(II) per g resin	39.5	31.1	25.2

adsorption by Spheron Oxine is affected by the chemical conditions (i.e., pH and ionic strength) of the aqueous solution. A maximum value of adsorbed Pd(II) is obtained at pH 1.23 and I = 0.06 M, which corresponds to the theoretical capacity of this resin (see Table 1). With exception of the above conditions, the obtained results at pH 2.0 and I = 0.1 M do not allow to define an equilibrium time to determine the experimental resin capacity. However, for the sake of comparison, metal adsorbed at 24 h in the different resins was measured (Table 1). As seen, the metal adsorbed for the various resins follows the order Spheron Salicyl < Spheron Oxine < Spheron Thiol. Although Spheron Thiol shows the highest metal adsorption, the metal adsorbed by Spheron Thiol is much different from the theoretical value than for Spheron Oxine. This fact may be explained by the possible 2:1 coordination (thiol: palladium), while the lower adsorption obtained for Spheron Salicyl is mainly due to the lower affinity of palladium towards the salicyl group. Also, the adsorption of Pd(II) on non-functionalized Spheron was found irrelevant (1.6 mg Pd(II) per g of resin), showing the active role of the complexing group.

The influence of pH on the adsorption of Pd(II) on Spheron Oxine was determined by measuring the metal adsorbed at $t_{1/2}$, defined as the time to occupy half of the resin sites (in this case $t_{1/2}$ = 10 min) at a given ionic strength (see Table 2). Results obtained at different ionic strength are also summarized in Table 2. As observed, the pH does not influence the metal loading in the studied range of 1.5 to 4.5. This behaviour differs from the results reported for the adsorption of base metals on polymeric 8-hydroxyquinolines, which capacities decrease sharply at pH < 5

Table 3
Elution efficiency

Eluent	% Pd(II) eluted	
	Spheron Oxine	Spheron Thiol
HCl 4 M	5	–
NaSCN 0.5 M, pH 2	31	10
Thiourea 0.5 M, pH 2	77	59
Thiourea 0.5 M, pH 5	9	20

[13,18]. This indicates the higher stability of the Pd(II)–oxine complexes [25]. On the other hand, the observed decrease of the Pd(II) adsorption with the increase of chloride concentration may be explained by the different reactivity of the aqueous chlorocomplexes of Pd(II) in reactions 1 and 2. Thus, under the experimental conditions studied $PdCl_3^-$ and $PdCl_4^{2-}$ are present at different ratios (i.e., $PdCl_4^{2-}$ is much clearly predominant at $I = 0.1$ M). $PdCl_4^{2-}$ is less reactive than $PdCl_3^-$ [26] which may explain the observed differences on the rate of adsorption of Pd(II) (see Fig. 2 and Table 2).

With respect to the stripping of the metal ion, acidic solutions and complexing agents as thiocyanate and acidified thiourea were employed. The results are represented in Table 3. As seen, the desorption process of Pd(II) is not effective using hydrochloric acid, contrary to the behaviour reported for base metals, i.e., Fe(III), Ni(II) and Pb(II) are easily eluted in acidic solution [27]. This can be explained in terms of the relative stabilities of metal–resin complexes. A selective elution could therefore be predicted. In this process, acidified thiourea is shown to be the best palladium stripping agent in all cases. The elution of adsorbed palladium is easier for the sorbent Spheron Oxine than for Spheron Thiol as a result of the different strength of the interactions which follows the hard–soft acid–base (HSAB) theory [28]. In general, a difficult desorption is reported for Spheron Thiol resins [29], also according to the expected stability of the corresponding complex.

On the other hand, a comparison of Cu(II) and Pd(II) adsorption by Spheron Oxine has been performed at pH 2 in 0.1 M chloride solution. Results of the respective adsorption processes during 24 h are represented in Fig. 2. The maxim adsorption obtained was 0.54 mmol per g of resin for Pd(II) and 0.26 mmol g per resin for Cu(II). The higher adsorption for Pd(II) in this acidic medium could be applied for a Cu(II)–Pd(II) separation. In this sense, a separate experiment was carried out to determine the separation ratio, as defined by Vernon and Nyo [30], for the palladium–copper metal pair with initial concentrations of 1 mM each, at pH 1 and $I = 0.1$ M. A value of 19.3 for the separation ratio was obtained, which predicts a possible column separation. This value may increase at higher acidic conditions. Experimental conditions for the separation of both metal ions from a solution by using a liquid chromatography column containing Spheron Oxine 1000 are now under study.

3.2. Adsorption kinetics

As stated above, the adsorption of Pd(II) by Spheron Oxine 1000 is found to be relatively rapid. This could be ascribed to the numerous hydrophilic hydroxyl groups in the polymeric matrix which facilitate the interaction of the resin with the solution (Fig. 3). For the sake of comparison, the solvent extraction of Pd(II) by Kelex 100 [7-(4-ethyl-1-methyloctyl)-8-quinolinol] is found to be slower even in presence of thiocyanate which enhances the rate of the extraction process [4]. On the other hand, the sorption of Pd(II) by polystyrene functionalized polymers containing sulfur as a donor atom [31] was found effective only with addition of thiocyanate.

This rapid uptake of Pd(II) by Spheron Oxine provides a high interest for the study of the adsorption kinetics and to a possible application

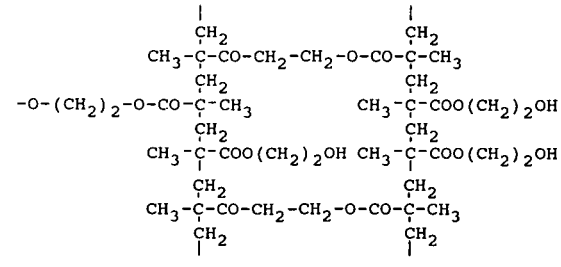

Fig. 3. Structure of the gel matrix for Spheron resins.

for separating Pd(II) from other metals based on the kinetics of the process. For such purpose separate experiments were undertaken by monitoring the metal concentration in the aqueous phase during the sorption process. In order to characterize the kinetics of the adsorption process, the data collected in the form of aqueous metal concentration vs. time were modelled by considering the equations for the extraction process (reactions 1 and 2). Thus, the general expression for the reaction rate has the form:

$$-\mathrm{d}[\mathrm{Pd(II)}]_{aq}/\mathrm{d}t = k''_f[\mathrm{Pd(II)}]^a_{aq}[\mathrm{HR}]^b - k''_r[\mathrm{Pd(II)}]^c_{Res}[\mathrm{Cl}^-]^d[\mathrm{H}^+]^e \quad (3)$$

where HR stands for Spheron Oxine, $[\mathrm{Pd(II)}]_{aq}$ is the metal remaining in solution and $[\mathrm{Pd(II)}]_{Res}$ is the metal bound to the resin.

Under the experimental conditions described in this paper we can assume that chloride and H^+ concentrations are constant. Also, values of a and c can be considered equal to 1. Eq. 3 can be therefore be rewritten

$$-\mathrm{d}[\mathrm{Pd(II)}]_{aq}/\mathrm{d}t = k'_f[\mathrm{Pd(II)}]_{aq}[\mathrm{HR}]^b - k'_r[\mathrm{Pd(II)}]_{Res} \quad (4)$$

Due to the excess of resin over metal in the initial conditions, we can also assume that the resin concentration is constant. Then,

$$-\mathrm{d}[\mathrm{Pd(II)}]_{aq}/\mathrm{d}t = k_f[\mathrm{Pd(II)}]_{aq} - k_r[\mathrm{Pd(II)}]_{Res} \quad (5)$$

Initially we have assumed a first order forward reaction. In Fig. 4, a plot of $\ln[\mathrm{Me}]/[\mathrm{Me}]_0$ vs. time for the various experiments at different initial metal concentrations is exhibited. It is observed in all cases that the experimental function is not linear as expected. As a second approach, we have considered both the forward and the reverse reactions. Fig. 5 shows that the latter model agrees with our experimental data. Theoretical values are obtained from calculations using the KILET computer program [32] which resolves corresponding equations for kinetic data. Values of k_f and k_r were determined and collected in Table 4 for experiments at different initial metal concentration (experimental data points are shown in Fig. 4).

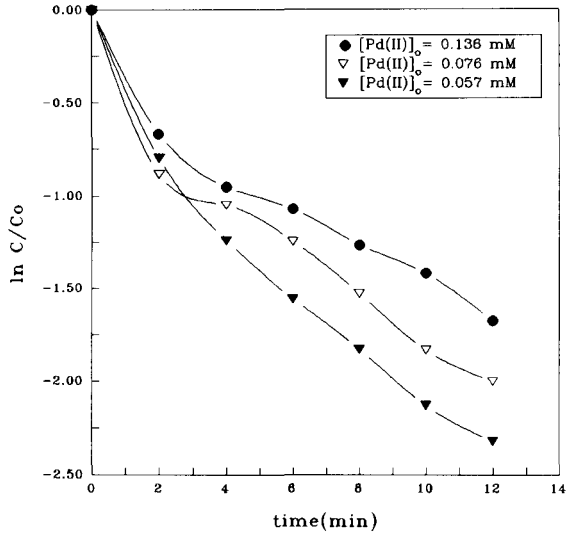

Fig. 4. Decrease of the concentration of palladium in contact with Spheron Oxine for different metal concentration. pH 2.0, $I = 0.1$ M and [Res] = 0.685 mM.

In addition, the rate of adsorption was studied

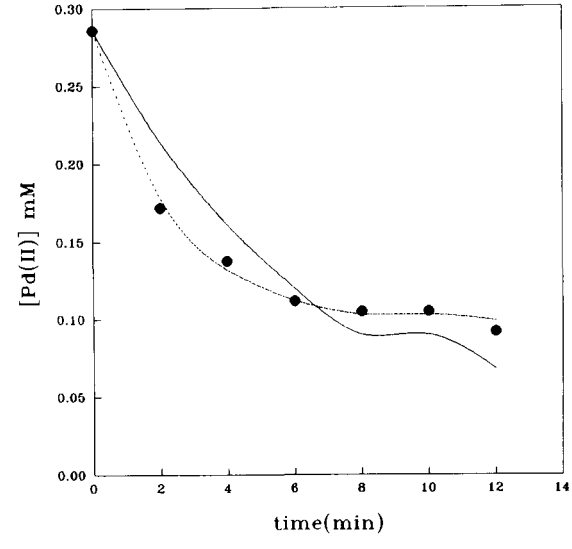

Fig. 5. Fitting for different models to the experimental data obtained for the adsorption of 0.287 mM Pd(II), pH 2.0 and $I = 0.1$ M, by 0.685 mM Spheron Oxine. ●, Experimental points; solid line, first order forward reaction; dashed line, first order forward and reverse reaction.

Table 4
Values for the constants of the forward reaction (k_f) and the reverse reaction (k_r), see reaction 5 from the text, for the adsorption of Pd(II) and Cu(II) at pH 2 and, $I = 0.1$ M by 0.685 mM Spheron Oxine

	k_f (min^{-1})	k_r (min^{-1})
[Pd(II)]$_o$ (mM)		
0.136	0.330 ± 0.101	0.103 ± 0.059
0.076	0.412 ± 0.163	0.096 ± 0.074
0.057	0.389 ± 0.058	0.054 ± 0.023
[Cu(II)]$_o$ (mM)		
0.092	0.119 ± 0.019	0.086 ± 0.033

by varying the concentration of the resin while the initial concentration of the metal was kept constant at 0.287 mM (Fig. 6). Corresponding k_f and k_r values had been calculated. Values obtained are shown in Table 5. Further, a plot of log k_f vs. log[HR] provides a linear relationship of the slope equal to 1.0, [HR] being the resin not bound to metal (values obtained under experimental conditions after 12 min of contacting time).

Taking into account the obtained kinetic relationships, we suggest the following reaction mechanism:

$$PdCl_3(H_2O)^- + HR \rightleftarrows PdCl_3^-HR + H_2O\,(slow) \quad (6)$$

$$PdCl_3^-HR \rightarrow PdCl_2R^- + Cl^- + H^+\,(fast) \quad (7)$$

Thus, reaction 6 represents the slow step, where one molecule of quinolinol from the resin

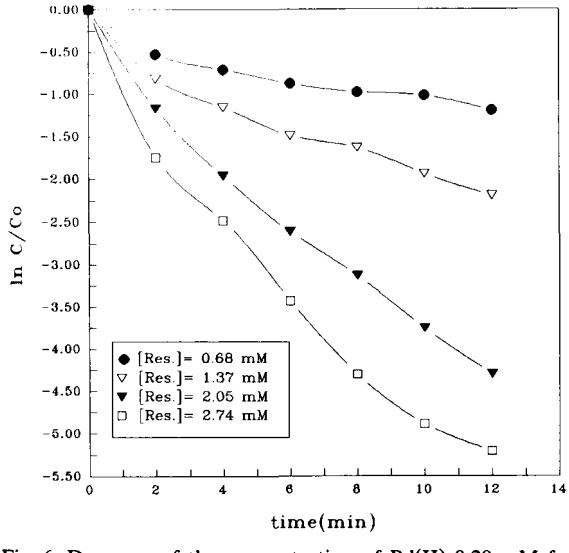

Fig. 6. Decrease of the concentration of Pd(II) 0.29 mM for different resin concentrations. pH 2.0, $I = 0.1$ M. Resin concentration calculated taking into account the theoretical capacity and the volume of the aqueous solution (10 ml).

Table 5
k_f and k_r values for the adsorption of 0.29 mM Pd(II) by Spheron Oxine at pH 2.0 and $I = 0.1$ M

[Res] (mM)	k_f (min^{-1})	k_r (min^{-1})
2.74	0.831 ± 0.109	0.015 ± 0.017
2.05	0.567 ± 0.055	0.018 ± 0.012
1.37	0.394 ± 0.097	0.070 ± 0.041
0.68	0.149 ± 0.023	0.075 ± 0.028

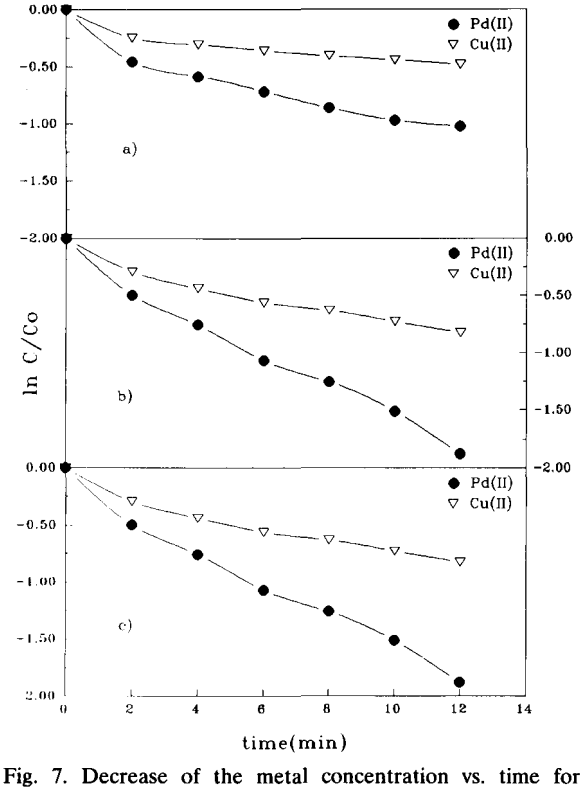

Fig. 7. Decrease of the metal concentration vs. time for mixtures of palladium and copper in contact with 0.685 mM Spheron Oxine. pH 2.0, $I = 0.1$ M. (a) 0.092 mM Cu(II) and 0.272 mM Pd(II); (b) 0.099 mM Cu(II) and 0.086 mM Pd(II); (c) 0.096 mM Cu(II) and 0.051 mM Pd(II).

coordinates the aquachlorocomplex $PdCl_3(H_2O)^-$, which is the most reactive species of Pd(II) present in solution. The second step is the corresponding release of Cl^- and H^+ to the medium.

For the adsorption of Cu(II), corresponding k_f and k_r values were obtained following the same procedure and by assuming the same model of reaction 5 (see Table 4).

Separation of Pd(II) and Cu(II) mixtures was followed as a function of contact time, similarly as for the determination of the separation ratio. The decrease of both metal concentrations during the adsorption process has been measured for three different values of the Pd(II)/Cu(II) concentration ratio. The results obtained are represented in Fig. 7 which shows that Pd(II) and Cu(II) are adsorbed by the resin at different rates. The separation of both metals increases with the solution–resin contact time. In conclusion, the different rate of adsorption of both metals could be applied for their separation. A selective stripping would be necessary to separately obtain Pd(II) and Cu(II) from a mixture.

Acknowledgments

This work has been carried out under the CEC project contract No. CI 516E. Prof. Josef Havel (Dept. of Analytical Chemistry, Masaryk University, Brno, Czech Republic) is acknowledged for his valuable help and discussion on the numerical treatment of data.

References

[1] M.J. Cleare, P. Charlesworth and D.J. Bryson, J. Chem. Technol. Biotechnol., 29 (1979) 210.
[2] G.V. Myasoedova and S.B. Savvin, CRC Crit. Rev. Anal. Chem., 17 (1986–87) 1.
[3] M. Hidalgo, A. Masana, V. Salvadó, M. Muñoz and M. Valiente, Talanta, 38 (1991) 483.
[4] E. Anticó, A. Masana, V. Salvadó, J. Havel and M. Valiente, Anal. Chim. Acta, 278 (1993) 91.
[5] K.M. Dingman, K.M. Gloss, E.A. Milano and S. Siggia, Anal. Chem., 46 (1974) 774.
[6] G. Koster and G. Schmuckler, Anal. Chim. Acta, 38 (1967) 179.
[7] A. Warshawsky, M.M.B. Fieberg, P. Mihalik, T.G. Murphy and Y.B. Ras, Sep. Purif. Methods, 9 (1980) 209.
[8] M. Grote and A. Kettrup, Anal. Chim. Acta, 172 (1985) 223.
[9] J.P. Ghosh and H.R. Das, Talanta, 28 (1981) 274.
[10] J.R. Parrish and R. Stevenson, Anal. Chim. Acta, 70 (1974) 189.
[11] E. Ma and H. Freiser, Inorg. Chem., 23 (1984) 3344.
[12] F. Vernon and H. Eccles, Anal. Chim. Acta, 63 (1973) 403.
[13] J.R. Parrish, Anal. Chem., 54 (1982) 1890.
[14] J.R. Jezorek and H. Freiser, Anal. Chem., 51 (1979) 366.
[15] W.M. Landing, C. Haraldsson and N. Paxeus, Anal. Chem., 58 (1986) 3031.
[16] P.M.M. Jonas, D.J. Eve and J.R. Parrish, Talanta, 36(10) (1989) 1021.
[17] S.J. Al-Bazi and A. Chow, Talanta, 31 (1984) 815.
[18] Z. Slovák, S. Slováková and M. Smrz, Anal. Chim. Acta, 75 (1975) 127.
[19] Z. Slovák and J. Toman, Fresenius' Z. Anal. Chem., 278 (1976) 115.
[20] G.V. Myasoedova, I.I. Antokol'skaya and S.B. Savvin, Talanta, 32 (1985) 1105.
[21] F. Svec and A. Jehlickova, Angew. Makromol. Chem., 121 (1984) 127.
[22] A.I. Vogel, Vogel's Textbook of Quantitative Inorganic Analysis, Longman, London, 1978.
[23] Some Laboratory Methods, Inorganic Chemistry, Royal Institute of Technology (KTH), Stockholm, 1959.
[24] K.S. De Haas, J. Inorg. Nucl. Chem., 35 (1973) 3231.
[25] J. Stary, Anal. Chim. Acta, 28 (1963) 132.
[26] J.V. Rund, Inorg. Chem., 13 (1974) 738.
[27] Z. Slovák and S. Slováková, Fresenius' Z. Anal. Chem., 292 (1978) 213.
[28] R.G. Pearson, J. Am. Chem. Soc., 85 (1963) 3533.
[29] Z. Slovák, M. Smrz, B. Docekal and S. Slováková, Anal. Chim. Acta, 111 (1979) 243.
[30] F. Vernon and K.M. Nyo, J. Inorg. Nucl. Chem., 40 (1978) 887.
[31] M.A. Congost, Síntesi i caracterització de nous polímers reactius portadors de grups sulfurs de fosfina i la seva aplicació en la separació de metalls preciosos, Graduate work, Universitat Autònoma de Barcelona, 1991.
[32] J. Havel and J.L. González, Scripta Fac. Sci. Nat. Univ. Purk. Bryn., 19 (1989) 183.

ELSEVIER

Analytica Chimica Acta 296 (1994) 333–341

ANALYTICA CHIMICA ACTA

Two-rate method for simultaneous determination of L-amino acid mixtures

Yun-Sheng Hsieh, S.R. Crouch *

Department of Chemistry, Michigan State University, E. Lansing, MI 48824, USA

Received 11 January 1994; revised manuscript received 11 May 1994

Abstract

A new kinetic-based method for simultaneous determination of binary mixtures is proposed that is simple, rapid, and minimizes errors arising from drift. This new method is based on the measurement of the rate at two points during the course of the enzymatic reaction and is therefore referred to as a two-rate method. The performance of the method is evaluated by the L-amino acid oxidase/Trinder reaction for the determination of binary mixtures of L-amino acids under the same conditions using air-segmented continuous flow/stopped-flow methodology. Some assumptions with this method are presented and supported by experimental data.

Keywords: Kinetic methods; Flow system; L-Amino acid mixtures; Two-rate method

1. Introduction

Multicomponent determinations are important in many areas of analytical chemistry. Kinetic methods of analysis have the potential to perform such determinations without prior separation based on differences in reaction rates with a common reagent [1–5]. Multicomponent determinations have been automated by continuous flow techniques, particularly by flow-injection methodologies [6–15].

In this work, a new reaction-rate approach for simultaneous determination of binary mixtures is proposed. This method is similar to that used in an earlier paper to minimize between-run variations in kinetic determinations due to fluctuations in experimental conditions [16] and is based upon making two-rate measurements during the course of an enzymatic reaction. The reaction response curves are monitored by using air-segmented continuous flow (ASCF)/stopped-flow methodology [17], and a linear regression procedure is used to obtain the reaction rates during the transient and steady state phases of the reaction. For substrates reacting with different rates, the calibration curves will have different regression slopes; slower reacting components will have lower slopes during both phases. The linearity of calibration curves under certain conditions is demonstrated. The assumption of additive proportional equations was made to calculate the concentrations of analytes in binary mixtures. The proposed method, unlike

* Corresponding author.

SSDI 0003-2670(94)00242-E

the previous two-rate method [16], does not compensate for errors such as between-run temperature variations. However, because it involves relative measurements and utilizes only a single reaction, it can overcome drifts and other problems in flowing systems [18].

A number of methods for quantitation of amino acids are available [2,19,20]. Of them, the use of enzyme-catalyzed reactions [20–29] is of interest because of the high selectivity of many enzymes. Enzymatic methods for amino acids are often based on a coupled enzyme reaction, in which oxidative deamination of certain L-α-amino acids is specifically catalyzed by L-amino acid oxidase to form hydrogen peroxide. The hydrogen peroxide then reacts immediately with the reduced form of a dye such as *o*-dianisidine [20,21], homovanillic acid [23], or scopoletin [24] in the presence of horseradish peroxidase to form a coloured, or fluorescent compound. After a few seconds, the concentration of the reaction product is proportional to the initial L-amino acid concentration. In this work, we employed the Trinder reaction [30] to form a coloured product and measured rates of change of the solution absorbance at 510 nm. The over-all reaction is summarized in Scheme 1.

The proposed method was evaluated by simultaneous determination of binary mixtures of L-amino acids. The reaction activities of ten essential L-amino acids in this detection system are also reported.

2. Theoretical background

Mark [31] has previously demonstrated the applicability of the method of proportional equations for simultaneous determinations of substrates of alcohol dehydrogenase. Pardue [32] has reviewed the general concepts and methodologies using regression kinetic methods for single and multicomponent determinations. In this work we have applied linear regression procedures to measure reaction rates during the transient and the steady state phases of an enzyme-catalyzed reaction for simultaneous two-component determinations of a mixture.

For an enzyme reaction following the Michaelis-Menten mechanism, the variation of the concentration of a product, χ, during the transient phase [33,34] can be expressed as

$$\chi = (1/2)k_1k_2[E]_o[S]_o t^2 \qquad (1)$$

where k_1 and k_2 are the rate constants of consecutive forward reactions, $[E]_o$ and $[S]_o$ are the

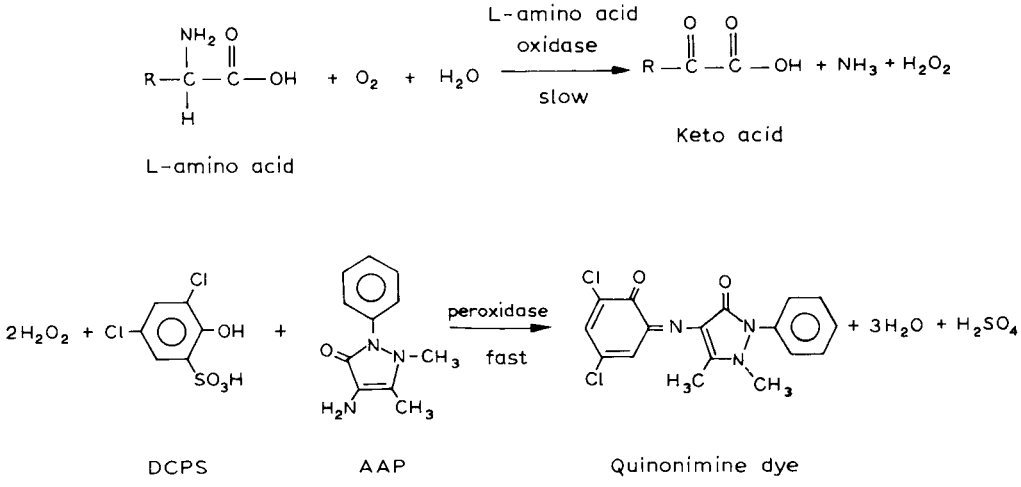

Scheme 1.

initial concentrations of enzyme and substrate, respectively, and t is the reaction time. Therefore, the rate, $R1$, during this period is equal to

$$R1 = (d\chi/dt) = k_1 k_2 [E]_o t [S]_o \cong G_a [S]_o \quad (2)$$

where $G_a = k_1 k_2 [E]_o t$ is a constant for a constant time, t, temperature and a given enzyme concentration. Under these conditions, $R1$ is directly proportional to the initial concentration of substrate, and G_a is the proportionality constant. For a mixture of n substrates reacting with a common enzyme, the individual reaction rates of each substrate are given by

$$R1,1 = G_{a,1}[S_1]_o + R1,1' \quad (3)$$

$$R1,2 = G_{a,2}[S_2]_o + R1,2' \quad (4)$$

:

$$R1,n = G_{a,n}[S_n]_o + R1,n' \quad (5)$$

where $R1,1$,..., $R1,n$ are the rates for each substrate; $G_{a,1}$,..., $G_{a,n}$ and $R1,1'$,..., $R1,n'$ are the slopes and intercepts of each calibration curve, respectively.

At steady state, the expression for the rate, $R2$, is given by

$$R2 = (R_{max}[S]_o)/(K_m + [S]_o) \approx R_{max}[S]_o/K_m = G_b[S]_0 \quad (6)$$

(If $[S]_o$ is small as compared to K_m.) Here R_{max} is the maximum attainable rate ($k_2[E]_0$), K_m is the Michaelis constant, and G_b is a constant for a given enzyme concentration equal to R_{max}/K_m. Similarly, the individual rates of each substrate are given by

$$R2,1 = G_{b,1}[S_1]_o + R2,1' \quad (7)$$

$$R2,2 = G_{b,2}[S_2]_o + R2,2' \quad (8)$$

:

$$R2,n = G_{b,n}[S_n]_o + R2,n' \quad (9)$$

For a binary mixture of substrates of concentrations $[S_1]_o$ and $[S_2]_o$, the over-all rate at time t_1, during the induction period, will be equal to

$$R1 = G_{a,1}[S_1]_o + G_{b,1}[S_2]_o + R1' \quad (10)$$

and that at time t_2, at steady state, will be equal to

$$R2 = G_{a,2}[S_1]_o + G_{b,2}[S_2]_o + R2' \quad (11)$$

The G terms for each substrate at each time and the $R1'$ and $R2'$ terms are obtained from calibration curves using solutions of known concentrations of the individual substrates. Here the individual substrates are assumed to obey Eqs. 2 and 6, and the formation of the common product is assumed to obey an additive relationship. For

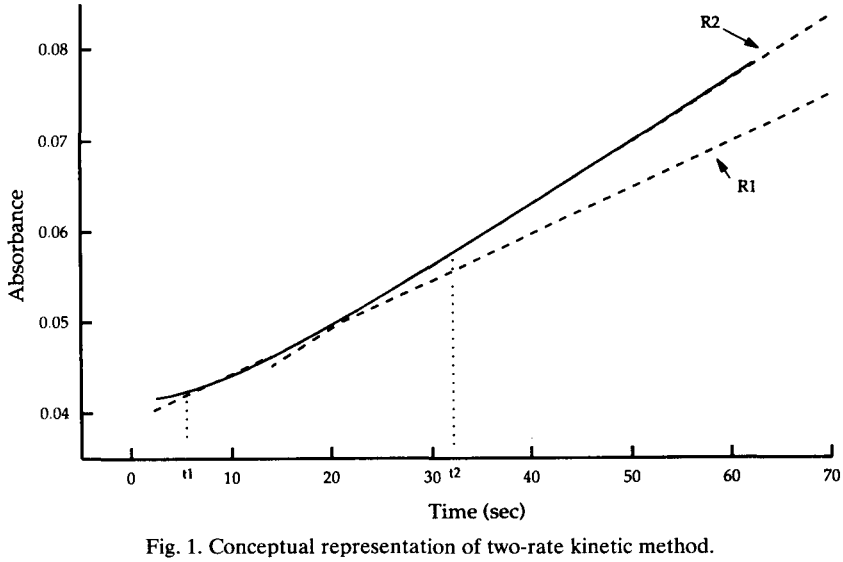

Fig. 1. Conceptual representation of two-rate kinetic method.

each sample, $R1$ and $R2$ are then obtained and Eqs. 10 and 11 are solved simultaneously for $[S_1]_o$ and $[S_2]_o$. The conceptual representation of this method is shown in Fig. 1.

3. Experimental

3.1. Reagents

All solutions were prepared in distilled, deionized water. Analytical-reagent grade chemicals were used. Stock solutions (0.01 M) of the L-amino acids were prepared by dissolving appropriate amounts of the compounds (Sigma) in water. Standard solutions were prepared from the stock solutions by dilution with 0.1 M phosphate buffer (pH 7.1) as needed. These calibration solutions were prepared just before use because of their tendency to decompose at room temperature. The composite enzyme reagent consisted of 5 ml of 4.8 mM 4-aminoantipyrine (Sigma), AAP, 5 ml of 10.7 mM 3,5-dichoro-2-hydroxyphenyl sulfonic acid (Sigma), DCPS, 0.01 M potassium chloride, about 16 mg of horseradish peroxidase (Sigma, Type II), 20 mg of L-amino acid oxidase (Sigma, Type I), and 40 ml of 0.1 M phosphate buffer mixed together in an amber bottle just before use.

3.2. Apparatus

The basic stopped-flow/ASCF components, shown in Fig. 2, were similar to those used for determining glucose [17]. A short (2 cm) reactor coil was employed to minimize the residence time, to provide mixing of solutions, and to allow as many data points to be collected during the transient phase as possible. Programs written in BASIC were used for data acquisition and analysis.

3.3. Procedures

Reactivity of L-amino acids

For investigating the reactivity of the amino acids, the appropriate L-amino acid solution,

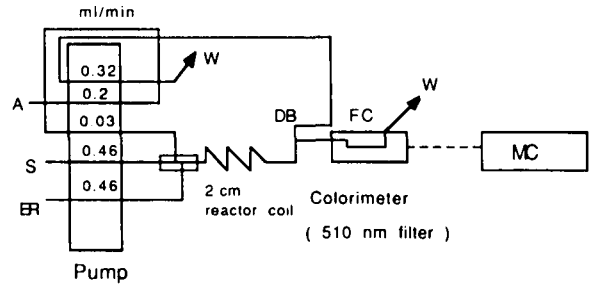

Fig. 2. Instrumentation for ASCF/stopped-flow system. A = Air, S = samples, ER = composite enzyme reagent, DB = debubbler, FC = flowcell, MC = microcomputer, W = waste.

composite enzyme reagents and air were aspirated manually through the pump into the manifold. The absorbance of the flow stream was monitored by continuously drawing a portion of the stream down through the flowcell while the air bubbles and a small amount of liquid passed into a waste container. For kinetic measurements, the stream was halted by turning off the pump manually for about 2 min after the absorbance of the products reached the plateau. The absorbance–time responses were recorded for each L-amino acid solution. At the end of the measurements, sample solution was washed out of the system with phosphate buffer solution. The reactions occurred at ambient temperature ($\sim$ 22°C).

Simultaneous determination of binary mixtures of L-amino acids

For these determinations, the calibration solutions and the binary mixtures of L-amino acids were introduced with the composite enzyme reagent. The absorbance–time responses were collected at a sampling rate of 0.3 s/data point for 1 min just after the absorbance plateau was reached. The rates of change of absorbance during the transient and steady state phases were observed and calculated with a least-squares linear regression procedure. These rates were then used to obtain the equations of the linear calibration curves from four standards in the range $0.8–2.0 \times 10^{-4}$ M for L-phenylalanine (L-Phe) and $1.0–5.0 \times 10^{-4}$ M for L-tryptophan (L-Trp), L-methionine (L-Met) and L-leucine (L-Leu). Triplicate results were obtained for each sample.

Table 1
Regression equations for two-rate kinetic determination

Mixture I				Mixture II			
	Equations	Std. error of slope	Corr. coeff.		Equations	Std. error of slope	Corr. coeff.
Rate 1	$R1$,Met = 1.51[Met] + 0.000019	0.028	0.9996	Rate 1	$R1$,Trp = 1.63[Trp] + 0.000027	0.043	0.9993
	$R1$,Leu = 1.11[Leu] + 0.0000069	0.042	0.9986		$R1$,Leu = 1.11[Leu] + 0.0000069	0.042	0.9986
Rate 2	$R2$,Met = 1.68[Met] + 0.000044	0.040	0.9994	Rate 2	$R2$,Trp = 1.76[Trp] + 0.000066	0.019	0.9998
	$R2$,Leu = 1.24[Leu] + 0.000032	0.031	0.9993		$R2$,Leu = 1.24[Leu] + 0.000039	0.031	0.9993
Eq. of mixture	$R1$ = 1.51[Met] + 1.11[Leu] + 0.000013			Eq. of mixture	$R1$ = 1.63[Trp] + 1.11[Leu] + 0.000017		
	$R2$ = 1.68[Met] + 1.24[Leu] + 0.000042				$R2$ = 1.76[Trp] + 1.24[Leu] + 0.000052		

Mixture III			
	Equations	Std. error of slope	Corr. coeff.
Rate 1	$R1$,Met = 1.51[Met] + 0.000019	0.028	0.9996
	$R1$,Phe = 3.52[Phe] + 0.000125	0.10	0.9991
Rate 2	$R2$,Met = 1.68[Met] + 0.000044	0.040	0.9994
	$R2$,Phe = 3.98[Phe] + 0.00017	0.008	0.9993
Eq. of mixture	$R1$ = 1.51[Met] + 3.52[Phe] + 0.000072		
	$R2$ = 1.68[Met] + 3.98[Phe] + 0.00011		

Thermal effect

The influence of temperature on the reactions analyzed here was studied by a conventional spectrophotometric method in which 2 ml of the L-amino acid solution were placed in a standard 1-cm cuvette. This was followed by the addition of 0.5 ml of the composite enzyme reagent. Data acquisition began about 5 s after the reagents were mixed and the cell was secured in the spectrophotometer. Absorbance values were obtained at 510 nm for 1 min. All solutions and the cell compartment were thermostated at 23 and 28°C. The reaction rates of each L-amino acid were measured and compared at the two different temperatures.

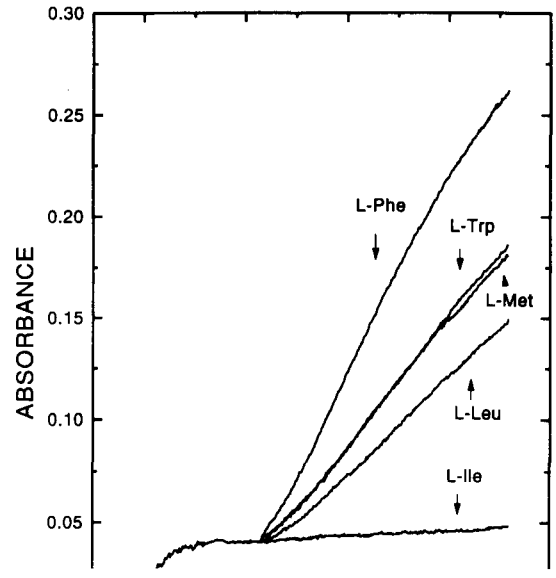

4. Results and discussion

4.1. Re

L-Al
acids; l
icant r
zymes
conditi
tivity a
a set c
alanine

Table 2
Results c

Concentr											
Added											
[Met]	[Leu]	[Met]	[Leu]	[Met]	[Ile]	[Met]	[Leu]	[Met]	[Leu]	[Met]	[Ile]
2.5	2.5	2.40	2.64	−4.0	5.6	2.5	2.5	2.31	2.77	−7.6	10.8
4.0	1.0	3.83	1.22	−4.2	22	4.0	1.0	3.84	1.22	−4.0	22
3.0	2.0	2.83	2.22	−5.7	11	3.0	2.0	2.82	2.26	−6.0	13
2.0	3.0	2.12	2.84	6.0	−5.3	2.0	3.0	1.88	3.18	−6.0	6.0
1.0	4.0	1.24	3.68	24	−8.0	1.0	4.0	0.90	4.13	−10	3.2

Concentrations of amino acids, $\times 10^4$ M					
Added		Found		%Rel. error	
[Met]	[Phe]	[Met]	[Phe]	[Met]	[Phe]
2.5	2.0	2.52	1.98	0.8	−1.0
1.5	2.8	1.71	2.97	14	6.1
2.0	2.4	2.04	2.37	2.0	−1.3
3.0	1.6	3.07	1.58	2.3	−1.3
4.0	0.8	3.68	0.95	−5.0	−5.0

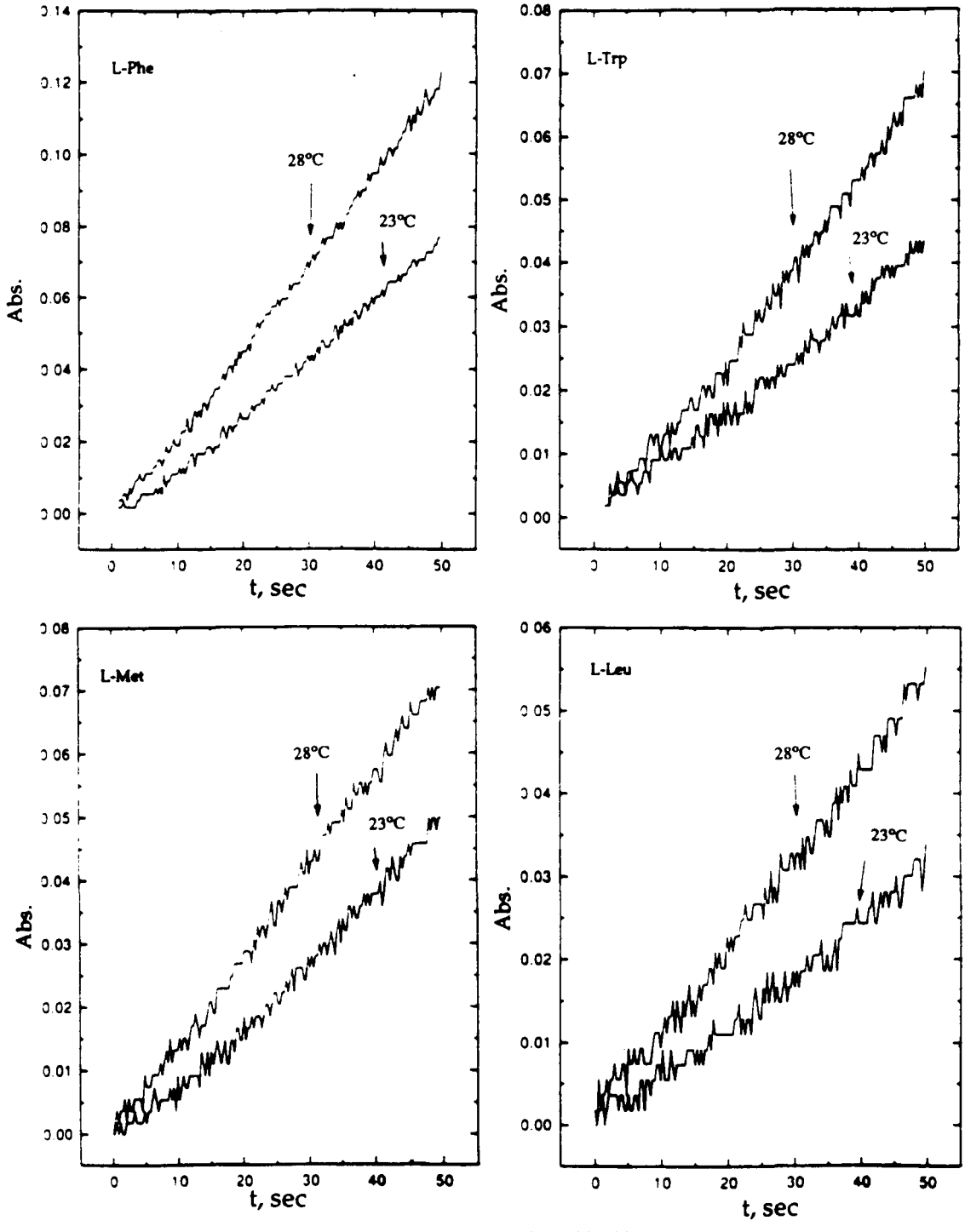

Fig. 4. Effect of temperature on L-amino acid oxidase response.

in absorbance after the flow was stopped. L-Arginine, L-histidine, L-lysine, L-valine and L-threonine gave no significant absorbance change during a 2 min interval.

4.2. Simultaneous L-amino acid determinations of binary mixtures

Three different combinations of binary mixtures of L-amino acids were chosen to demonstrate the capabilities of the proposed method. Calibration curves for each L-amino acid were plotted from rates corresponding to the transient and the steady state phases for the standard solutions. About 45 points during the transient phase were used in the linear regression analysis to determine $R1$. The magnitude and precision of the rates measured increased with the number of points used. The difference in rates between the two phases as indicated in Fig. 1 and as reported elsewhere [17] becomes indistinguishable as the number of points averaged gets large. The same number of points was used to determine $R2$ during the steady-state phase. Table 1 shows the regression equations for the standard solutions employed. The same procedures were applied for obtaining $R1$ and $R2$ with the binary unknown mixtures. The results of the analysis of these "unknown" mixtures in certain ratios, calculated from these equations, are given in Table 2. Except in two cases, relative errors are less than 10%. In this work, the background rates were always equal to $R1' + R2'$ and remained constant throughout. However, errors can arise due to the intrinsic characteristics of the chemical systems, fluctuations in temperature, instability of the detector signals, and imperfect choice of the acquired data points. If the substrate concentrations are too low or out of the dynamic ranges of the detection system, accurate rate measurements are not possible. This could limit the scope of the proposed method.

4.3. Effect of temperature

The effect of a change in temperature on the response curves is shown in Fig. 4. The ratio of the rates at the two temperatures is 0.65, 0.54, 0.65, and 0.57 for L-Leu, L-Met, L-Try, and L-Phe, respectively. A 5°C temperature increase thus causes a greater than 50% change in rate. These results are in a good agreement with those given by Guilbault and Labrano [27]. Hence, temperature should be carefully controlled in a kinetic-based determination. Fluctuations in room temperature in the studies reported here were no more than a few tenths of a degree which yielded only small errors.

5. Conclusion

The accuracy obtained here is similar to that obtained by Betteridge and Fields [9] and Fernandez et al. [10] in the resolution of the two-component mixtures by kinetic-based flow injection methods. The measurements here are based on a single reaction, however, which makes simultaneous determination simple, inexpensive, and rapid. The sample throughput is about 30 h^{-1}.

References

[1] B. Quencer and S.R. Crouch, Crit. Rev. Anal. Chem., 24 (1993) 243.
[2] P.D. Wentzell and S.R. Crouch, Anal. Chim. Acta, 224 (1989) 263.
[3] H.L. Pardue, Anal. Chim. Acta, 216 (1989) 69.
[4] H.A. Mottola, Kinetic Aspects of Analytical Chemistry, Wiley, New York, 1988.
[5] D. Perez-Bendito and M. Silva, Kinetic Methods in Analytical Chemistry, Ellis Horwood, Chichester, 1988.
[6] M.D. Luque de Castro and M.V. Cases, Analyst, 109 (1984) 413.
[7] M. Romero-Saldana, A. Rios, M.D. Luque de Castro and M. Valcarcel, Talanta, 38 (1991) 291.
[8] P. Linares, M.D. Luque de Castro and M. Valcarcel, Talanta, 33 (1986) 889.
[9] D. Betteridge and B. Fields, Fresenius' Z. Anal. Chem., 314 (1983) 386.
[10] A. Fernandez, M.D. Luque de Castro and M. Valcarcel, Anal. Chem., 56 (1984) 1146.
[11] F. Lazaro, M.D. Luque de Castro and M. Valcarcel, Anal. Chem., 59 (1987) 950.
[12] S.W. Kang, T. Sakai, N. Ohno and K. Ida, Anal. Chim. Acta, 261 (1992) 197.
[13] R. Kuroda, T. Nara and K. Oguma, Analyst, 113 (1988) 1557.
[14] D. Utley, Analyst, 115 (1990) 1239.

[15] H. Wada, T. Murakawa and G. Nakagawa, Anal. Chim. Acta, 200 (1987) 515.
[16] P.D. Wentzell and S.R. Crouch, Anal. Chem., 58 (1986) 2851.
[17] Y.S. Hsieh and S.R. Crouch, Anal. Chim. Acta, 284 (1993) 159.
[18] J.K. Foreman and P.B. Stockwell, Automatic Chemical Analysis, Ellis Horwood, Chichester, 1975, p. 131.
[19] S.A. Corcoran and S.C. Rutan, Anal. Chem., 60 (1988) 1146.
[20] H.V. Malmstadt and T.P. Hadjiioannou, Anal. Chem., 35 (1963) 14.
[21] G.G. Guilbault and E. Hrabankova, Anal. Chem., 42 (1970) 1779.
[22] K.V. Dyke and C. Szustkiewicz, Clin. Chem., 15 (1969) 155.
[23] G.G. Guilbault and J.E. Hieserman, Anal. Biochem., 26 (1968) 1.
[24] L.A. Lichtenberg and D. Wellner, Anal. Biochem., 26 (1968) 313.
[25] M. Nanjo and G.G. Guilbault, Anal. Chim. Acta, 73 (1974) 367.
[26] S. Igarashi and W.L. Hinze, Anal. Chim. Acta, 225 (1989) 147.
[27] G.G. Guilbault and G.J. Lubrano, Anal. Chim. Acta, 69 (1974) 183.
[28] G.G. Guilbault and G. Nagy, Anal. Lett., 6 (1973) 301.
[29] M. Mascini and G. Palleschi, Anal. Chim. Acta, 100 (1978) 215.
[30] D. Barham and P. Trinder, Analyst, 97 (1972) 142.
[31] H.B. Mark, Jr., Anal. Chem., 36 (1964) 1668.
[32] H.L. Pardue, Clin. Chem., 23 (1977) 2189.
[33] F.J.W. Roughton, Faraday Soc. Discuss., 17 (1954) 116.
[34] K.J. Laidler and P.S. Bunting, The Chemical Kinetics of Enzyme Action, Oxford Univ. Press, London, 2nd edn., 1973.

ELSEVIER

Analytica Chimica Acta 296 (1994) 343–345

ANALYTICA CHIMICA ACTA

Author Index

CALL FOR PAPERS

1995 International Symposium & Exhibit on PREPARATIVE CHROMATOGRAPHY

June 11-14, 1995
Washington, DC, USA

Abstract Deadline -- NOVEMBER 8, 1994

Organized by Professor Georges Guiochon
University of Tennessee and Oak Ridge National Laboratory

LECTURE & POSTER PRESENTATIONS
WORKSHOPS
SEMINARS
ROUNDTABLE DISCUSSIONS
CASE STUDIES
INSTRUMENTATION EXHIBIT

Sponsored by the Washington Chromatography Discussion Group

For more information contact: Janet Cunningham, c/o Barr Enterprises
P.O. Box 279, Walkersville, Maryland 21793 USA
(tele. 301-898-3772, fax 301-898-5596)

Sampling of Heterogeneous and Dynamic Material Systems

Theories of Heterogeneity, Sampling and Homogenizing

by **P.M. Gy**, Sampling Consultant, Cannes, France

Data Handling in Science and Technology Volume 10

Although sampling errors inevitably lead to analytical errors, the importance of sampling is often overlooked. The main purpose of this book is to enable the reader to identify every possible source of sampling error in order to derive practical rules to (a) completely suppress avoidable errors, and (b) minimise and estimate the effect of unavoidable errors. In short, the degree of representativeness of the sample can be known by applying these rules.

The scope covers the derivation of theories of probabilistic sampling and of bed-blending from a complete theory of heterogeneity which is based on an original, very thorough, qualitative and quantitative analysis of the concepts of homogeneity and heterogeneity. All sampling errors result from the existence of one form or another of heterogeneity. Sampling theory is derived from the theory of heterogeneity by application of a probabilistic operator to a material whose heterogeneity has been characterized either by a simple scalar (a variance: zero-dimensional batches) or by a function (a variogram: one-dimensional batches). A theory of bed-blending (one-dimensional homogenizing) is then easily derived from the sampling theory.

The book should be of interest to all analysts and to those dealing with quality, process control and monitoring, either for technical or for commercial purposes, and mineral processing.

Although this book is primarily aimed at graduates, large portions of it are suitable for teaching sampling theory to undergraduates as it contains many practical examples provided by the author's 30-year experience as an international consultant. The book also contains useful source material for short courses in Industry.

ELSEVIER

SCIENCE

Contents:

Foreword. First Part: General Introduction. Second Part: Heterogeneity. Third Part: General Analysis of the Concept of Sampling. Fourth Part: Achievement of Sampling Correctness. Fifth Part: One-Dimensional Sampling Model. Sixth Part: Zero-Dimensional Sampling Model. Seventh Part: Sampling by Splitting. Ninth Part: Sampling for Commercial Purposes: Specific Problems. Tenth Part: Homogenizing. Useful References. Index.

1992 xxx + 654 pages
Price: Dfl. 425.00 / US$ 243.00
ISBN 0-444-89601-5

ORDER INFORMATION

For USA and Canada
ELSEVIER SCIENCE

Judy Weislogel
P.O. Box 945
Madison Square Station,
New York, NY 10160-0757
Tel: (212) 989 5800
Fax: (212) 633 3880

In all other countries
ELSEVIER SCIENCE

P.O. Box 211
1000 AE Amsterdam
The Netherlands
Tel: (+31-20) 5803 753
Fax: (+31-20) 5803 705

US$ prices are valid only for the USA & Canada and are subject to exchange fluctuations; in all other countries the Dutch guilder price (Dfl.) is definitive. Books are sent postfree if prepaid.

711/414\143\0001-00

PUBLICATION SCHEDULE FOR 1994

	J	F	M	A	M	J	J	A	S	O	N	D
Anal. Chim. Acta	284/3 285/1–2 285/3	286/1 286/2 286/3	287/1–2 287/3 288/1–2	288/3 289/1 289/2	289/3 290/1–2 290/3	291/1–2 291/3 292/1–2	292/3 293/1–2 293/3	294/1 294/2 294/3	295/1–2 295/3 296/1	296/2 296/3 297/1–2	297/3 298/1 298/2	298/3 299/1 299/2
Vib. Spec.	6/2		6/3		7/1		7/2		7/3		8/1	

INFORMATION FOR AUTHORS

Detailed "Instructions to Authors" for *Analytica Chimica Acta* was published in Volume 289, No. 3, pp. 381–384. Free reprints of the "Instructions to Authors" of *Analytica Chimica Acta* and *Vibrational Spectroscopy* are available from the Editors or from: Elsevier Science B.V., P.O. Box 330, 1000 AH Amsterdam, The Netherlands. Telefax: (+31-20) 5862 459.

Manuscripts. The language of the journal is English. English linguistic improvement is provided as part of the normal editorial processing. Authors should submit three copies of the manuscript in clear double-spaced typing on one side of the paper only. *Vibrational Spectroscopy* also accepts papers in English only.

Rapid publication letters. *Letters* are short papers that describe innovative research. Criteria for letters are novelty, quality, significance, urgency and brevity. Submission data: max. of 2 printed pages (incl. Figs., Tables, Abstr., Refs.); short abstract (e.g., 3 lines); *no* proofs will be sent to the authors; submission on floppy disc; *no* revision will be possible.

Abstract. All papers, reviews and letters begin with an Abstract (50–250 words) which should comprise a factual account of the contents of the paper, with emphasis on new information.

Figures. Figures should be suitable for direct reproduction and as rich in contrast as possible. One original (or sharp glossy print) and two photostat (or other) copies are required. Attention should be given to line thickness, lettering (which should be kept to a minimum) and spacing on axes of graphs, to ensure suitability for reduction in size on printing. Axes of a graph should be clearly labelled, along the axes, outside the graph itself.

All figures should be numbered with Arabic numerals, and require descriptive legends which should be typed on a separate sheet of paper. Simple straight-line graphs are not acceptable, because they can readily be described in the text by means of an equation or a sentence. Claims of linearity should be supported by regression data that include slope, intercept, standard deviations of the slope and intercept, standard error and the number of data points; correlation coefficients are optional.

Photographs should be glossy prints and be as rich in contrast as possible; colour photographs cannot be accepted. Line diagrams are generally preferred to photographs of equipment. Computer outputs for reproduction as figures must be good quality on blank paper, and should preferably be submitted as glossy prints.

Nomenclature, abbreviations and symbols. In general, the recommendations of IUPAC should be followed, and attention should be given to the recommendations of the Analytical Chemistry Division in the journal *Pure and Applied Chemistry* (see also *IUPAC Compendium of Analytical Nomenclature, Definitive Rules*, 1987).

References. The references should be collected at the end of the paper, numbered in the order of their appearance in the text (*not* alphabetically) and typed on a separate sheet.

Reprints. Fifty reprints will be supplied free of charge. Additional reprints (minimum 100) can be ordered. An order form containing price quotations will be sent to the authors together with the proofs of their article.

Papers dealing with vibrational spectroscopy should be sent to: Dr J.G. Grasselli, 150 Greentree Road, Chagrin Falls, OH 44022, U.S.A. Telefax: (+1-216) 2473360 (Americas, Canada, Australia and New Zealand) or Dr J.H. van der Maas, Department of Analytical Molecular Spectrometry, Faculty of Chemistry, University of Utrecht, P.O. Box 80083, 3508 TB Utrecht, The Netherlands. Telefax: (+31-30) 518219 (all other countries).

0003-2670/94/$07.00

Essential Reading...from Wiley

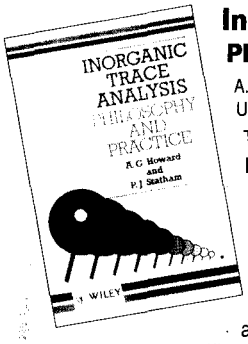

Inorganic Trace Analysis
Philosophy and Practice

A.G. HOWARD, and P.J. STATHAM, both at the University of Southampton, UK

This self-contained volume on trace analysis provides the reader with sometimes difficult to locate data and information. The work out-lines the practices often missed out in technical reports, for example the diagnosis of problems arising in trace analysis.

Whilst primarily directed towards the analyst, the philosophies, handling techniques, purification methods and information on materials which are contained in this book will also be of use of workers in other disciplines susceptible to contamination.

The authors have written a text that will not date rapidly, but will stimulate others to push forward the frontiers of trace analysis.

CONTENTS: Introduction; The Working Environment; Laboratory Materials; Storage; Reagents; The Water Supply; Working Practices; Trouble Shooting

0471941441 194pp 1993 £39.95/$63.95

Chromatography for Inorganic Chemistry

M. LEDERER, University of Lausanne, Switzerland

Our knowledge of inorganic chemistry is based in part on the use of chromatographic and electrophoretic methods over the last 50 years. Chromatography in Inorganic Chemistry provides a comprehensive account of the techniques. Extensive use of examples can be found in the book, which also gives the reader an insight into the solution chemistry of inorganic compounds and the species which exist in aqueous solution.

CONTENTS: Historical Introduction; Solvent Extraction and History of Partition Chromatography; Paper Chromatography and Thin Layer Chromatography; Electrophoresis; Gel Filtration; Ion Exchange; HPLC; Ion Chromatography; Gas Chromatography; Separation of Isotopes; Separation of Optical Isomers; Solution Chemistry of Some Elements: Boron, Condensed Phosphates, Sulphur, Halogen Acids, Rhenium and Technetium, Ruthenium, Rhodium, The Rare Earths, Chromatography at Tracer Levels.

0471942855 230pp 1994 £39.95/$63.95

Air Monitoring by Spectroscopic Techniques

Edited by M.W. SIGRIST, Institute of Quantum Electronics, Switzerland

Leading experts discuss various modern spectroscopic techniques for monitoring air pollution, and show how they can be applied to tracing and analyzing gas detection. Discusses the characteristics, advantages and future aspects of the current spectroscopic techniques used in environmental analysis. Focuses on modern methods, including state-of-the-art information and data - both laser and non-laser based - that offer advantages for air pollution and gas monitoring.

CONTENTS INCLUDE: Introduction to the subject of air pollution and the general problem of environmental sensing; Differential Optical Absorption Spectroscopy (DOAS); Light Detection and Ranging (LIDAR); Photo-acoustic Spectroscopy (PAS); Tunable Diode Laser Spectroscopy (TDLS); Fourier Transform Infrared Spectroscopy (FTIR)

Series: Chemical Analysis: A Series of Monographs on Analytical Chemistry and its Applications
0471558753 560pp 1994 £66.00/$91.95

Chemical Analysis by Nuclear Methods

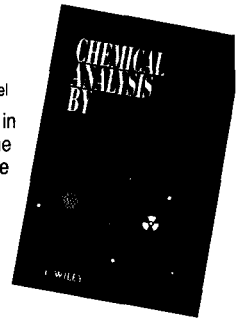

Z.B. ALFASSI, Ben Gurion University, Beer Sheva, Israel

A wide range of nuclear methods are used in chemical analysis. This volume presents the most comprehensive survey available of the most important of these methods.

This work differs from other texts in the field by being sub-divided according to the types of nuclear particles used, rather than according to applications. The first chapter gives the physical background for all nuclear methods and applications. The subsequent chapters detail the use of neutrons, charged particles and radio-isotopes in chemical analysis. The chapters are divided into a number of sections each of which has been written by an acknowledged expert in the particular analytical method being considered.

Chemical analysis by nuclear methods is written essentially for new researchers to the field, and includes all the necessary background in nuclear physics and chemistry. It will also be of interest to both materials scientists and engineers, and to biologists.

CONTENTS: Basic Background in Nuclear Physics and Chemistry Elemental Analysis with Neutron Sources; Elemental Analysis with Particle Accelerators; Use of Radioactive (Alpha, Beta and Gamma) Sources; Use of Radio Tracers

0471938343 576pp 1994 £90.00/$144.00

Biological Mass Spectrometry
Present and Future

Edited by T. MATSUO, Osaka University, Japan, R. CAPRIOLI, University of Texas Medical School, USA, M. GROSS, University of Nebraska at Lincoln, USA and Y. SEYAMA, University of Tokyo, Japan

During the 1990's rapid advances have been made in the field of Biological Mass Spectrometry, highlighted by the introduction of new techniques such as Electrospray Ionization (ESI) and Matrix-Assisted Laser Desorption (MALD).

This volume will be an essential reference work for researchers using mass spectrometry in biochemistry, protein chemistry, pharmacology, molecular biology and analytical chemistry, supplying an overview of this versatile analytical method. Biological Mass Spectrometry - Present and Future is a thorough work, presenting both the most recent applications and the expected developments in this rapidly expanding field.

CONTENTS: Introduction to Modern Biological Mass Spectrometry; New Instrumentation and Methodologies: Part A: Ionization; Part B: Mass Analysis; Part C: Structure Methods; New Applications: Part A: Peptides and Proteins; Part B: Oligosaccharides and Lipids; Part C: Nucleic Acids; Part D: Xenobiotics and Metabolites; Part E: Environmental and Endogenous Toxic Compounds; Part F: Analytical and Organic Chemistry

0471938963 688pp 1994 £120.00/$192.00

Remember for chemistry...read Wiley

Order from your Bookseller or directly from Wiley. Cheques made payable to John Wiley & Sons Ltd., marked for the attention of Nicky Douglas. For credit card orders phone +44 (0)243 770392 or Fax +44 (0)243 531712. All prices are correct at time of going to press. Please add £2.50 $5.00 to cover postage. Save money, order more than one book and postage is FREE!

John Wiley & Sons Ltd
Baffins Lane Chichester
West Sussex PO19 1UD UK

WILEY